Cholesterol als Modulator der Mikroviskosität, Migration und TRPV3-Aktivität in Keratinozyten

Dissertation
zur Erlangung des akademischen Grades
Dr. rer. med.

an der Medizinischen Fakultät
der Universität Leipzig

eingereicht von:	Anke Klein
geboren am:	30. Juni 1980 in Ludwigsburg
angefertigt am:	Rudolf-Boehm-Institut für Pharmakologie und Toxikologie Medizinische Fakultät der Universität Leipzig
Betreuer:	Prof. Dr. Michael Schaefer

Beschluss über die Verleihung des Doktorgrades vom: 24. Oktober 2017

Contents

Abbreviations

2-APB	2-aminoethoxydiphenyl borate
ABC	ATP binding cassette
CARC	inverted CRAC sequence
CFP	cyan fluorescent protein
CHO	chinese hamster ovary
CLSM	confocal laser scanning microscopy
CRAC	cholesterol recognition amino acid consensus
DRG	dorsal root ganglion
EGF	epidermal growth factor
FAST DiO	3,3-dilinoleyloxacarbocyanine perchlorate
FRAP	fluorescence redistribution after photobleaching
HaCaT	human adult low calcium high temperature
HEK293	human embryonic kidney
HEK_{mTRPV3}	HEK293 cells stably expressing mouse TRPV3
MβCD	methyl-β-cyclodextrin
NBD-PC	1-palmitoyl-2-(6-[N-(7-nitrobenz-2-oxa-1,3-diazol-4-yl)amino]caproyl)-*sn*-glycero-3-phosphocholine
PDZ	PSD-95, Dlg1, and zo-1 (this domain was first monitored in these proteins)
PTEN	phosphatase and tensin homologue
Q_{10}	temperature coefficient corresponding to a 10°C temperature increase
SHIP	Src homology 2-containing inositol 5' phosphatase
TIR	total internal reflection
TRP	transient receptor potential
TRPA	ankyrin-rich transient receptor potential
TRPC	canonical transient receptor potential
TRPM	melastatin transient receptor potential
TRPMP	mucolipidin transient receptor potential
TRPP	polycystin transient receptor potential
TRPV	vanilloid transient receptor potential

1.1 Cholesterol

Biological membranes surround cells and eukaryotic cell organelles, confer protection, and aid in controlling nutrient supply as well as cellular communication. Cellular membranes consist of a highly fluid bilayer and are composed of different lipids, which incorporate various proteins. A prominent component of animal cells is cholesterol, which was first identified in the 18th century by Poulletier de la Salle as a part of gallstones.

The structure of cholesterol is unique among membrane components (Fig. 1 A)[1,2]. It exhibits a small polar hydroxyl group, which faces the headgroups of adjacent phospholipids in bilayers, and a larger hydrophobic moiety, consisting of a bulky and stiff polycyclic structure and a flexible isooctyl hydrocarbon chain. One side of the flat ring system, known as β face, bears methyl groups, and the opposed smooth side is referred to as α face. Featuring an octanol:water partition coefficient (logP) of 7.11, cholesterol is poorly soluble in water and readily partitions into lipid membranes.

1.1.1 Functions and distribution of cholesterol

The cholesterol content varies among different cell types and organelles[1,2]. Within cells, the highest concentration of cholesterol is found in the plasma membrane (up to 50 mol%), followed by the endocytic pathway with the Golgi apparatus and the endoplasmic reticulum. Mitochondrial membranes contain vanishingly low amounts of cholesterol. Due to its small hydrophilic group, cholesterol is able to easily switch between the two membrane leaflets (flip-flop).

With regards to plasma membranes, it has been postulated that several membrane components organise themselves into microdomains that contain distinct lipids and proteins[3]. Lipid domains enriched in cholesterol and sphingolipids are called lipid rafts. Their existence, size and stability have been in discussion for a long time due to limitations of analytical methods that allow a direct examination of these domains in living cells. However, advances in microscopic and spectroscopic techniques have shed some light on the existence of fluctuating rafts in plasma membranes under physiological conditions[3].

Cholesterol participates in a plethora of physiological processes. Aside from its role as a precursor of compounds like steroid hormones and bile salts, cholesterol is also required for different vesicular transport mechanisms. Cholesterol affects the order of acyl chains of adjacent lipids and thereby modulates the physical properties of biological membranes, such as membrane fluidity and thickness[1,2]. In artificial membranes, it has been shown that cholesterol either loosens or tightens biological membranes, depending on the arrangement and saturation of neighbouring acyl side chains. In cell membranes, it mainly enhances membrane rigidity and reduces the fluidity as well as the

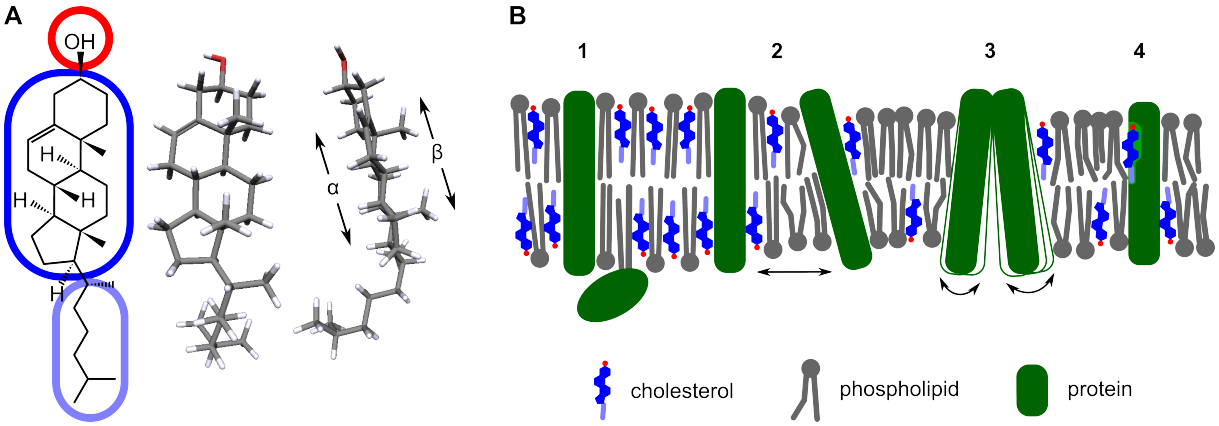

Figure 1: Structure and properties of cholesterol; **A** Structure of cholesterol. Hydrophilic (red) and hydrophobic (blue) moieties of the molecule are encircled. Stick models represent a frontal view from the β side and a side view. **B** Possible mechanisms of cholesterol-dependent regulation of protein functions. Cholesterol-rich domains can recruit signalling proteins into spatially confined signalling platforms (1). Regions of distinct cholesterol content may influence protein functions by providing different physical environments characterised by determined membrane thickness (2) or fluidity (3), thus, enabling tilted protein arrangements or protein movements. Cholesterol molecules can directly interact with hydrophobic motifs in some proteins (4).

permeability. The fact that cholesterol prevents temperature-dependent membrane phase transitions is of particular importance in living cells[1,2].

Cholesterol can initiate and modulate signal transduction processes via direct and indirect mechanisms. Certain proteins can accumulate in lipid rafts, which function as signalling platforms or hubs (Fig. 1 B1+2). Due to an increased spatial proximity of interacting partners, this condition can augment the velocity and robustness of signalling events. In contrast, the separation of molecular players in raft and non-raft regions can terminate or prevent signalling events. Cholesterol affects the physical properties of the plasma membrane (Fig. 1 B2+3) and, thus, may influence the available room for conformational mobility. Furthermore, cholesterol can regulate signal pathways by directly interacting with membrane proteins (Fig. 1 B4). Meanwhile, different cholesterol recognition domains have been identified, such as CRAC (cholesterol recognition amino acid consensus) and CARC (inverted CRAC sequence) motifs or tilted peptides[4], that facilitate cholesterol:protein interactions.

1.1.2 Some aspects of cholesterol homoeostasis and transport

In vertebrates, cholesterol is essential to maintain normal cell functions. Most of the required cholesterol can be synthesised *de novo*, and only a small fraction needs to be absorbed from the diet. All mammalian cells are able to synthesise cholesterol, but the production rates strongly vary among different cell types. The majority of *de novo*-synthesised cholesterol derives from the liver, but many other organs also produce cholesterol in considerable amounts, e.g. the intestines, adrenal glands,

reproductive organs, and epidermis.

Since cholesterol is hydrophobic, it is transported in the circulatory system within various lipoproteins. These are complex particles that contain apolipoproteins, phospholipids, cholesterol, cholesterol esters, and free fatty acids. Lipoproteins are classified according to their density, composition, and function. Cells can exchange single components with lipoproteins or absorb them entirely via receptor-mediated endocytosis. Intracellularly, cholesterol is transported via vesicles or sterol carrier proteins[5]. In order to export cholesterol from cells and to regulate the cholesterol content of the plasma membrane, cells express cholesterol transporters, including two members of the ABC (ATP-binding cassette) transporter family, namely ABCA1 and ABCG1[6].

1.2 Structure and function of the integument

The skin, as the outer physical barrier of humans and many other species, has to perform a multitude of tasks to facilitate survival. First of all, it protects the organism from harmful environmental influences, like mechanical forces, toxic substances, UV radiation, and pathogens. Furthermore, the skin is an important element of the innate immune system, and the respective functions are mediated by specific immune cells in the skin. Skin glands that secrete sweat or sebum aid in maintaining an adequate body temperature and cover the skin with a protective, antiseptic film that avoids dehydration. Sensory modalities that are implemented in the skin include hot, warm and cold temperature sensation, tactile force detection, and mechanical pain sensation.

The skin is composed of three layers (Fig. 2 A): the epidermis, dermis, and subcutis. The epidermis is the outermost layer of the skin and consists of a stratified squamous epithelium without blood vessels (detailed information in section 1.2.1 and [7,8]). A basal membrane separates the epidermis from the subjacent dermis.

The dermis consists of two layers of connective tissue with lymphatic and blood vessels, different nerve endings, skin glands, and hair follicles. The region adjacent to the epidermis, the *papillary layer*, contains loose connective tissue with a high water content and, thus, maintains the skin turgor. It forms small protrusions into the epidermis, the so-called *dermal papillae*, which strengthen the connection of epidermis and dermis. The *reticular layer* is located subjacent to the *papillary layer*. Its dense network of irregularly arranged collagenous and elastic fibres confers tear strength and elasticity of the skin.

The inner layer of the skin is the subcutis and covers muscles, tendons, and bones. Anatomically, the subcutis does not belong to the skin, but it forms an inseparable functional unit with the epidermis and dermis. The subcutis consists of loose connective tissue with many adipocytes. Hence, it serves mostly as a heat shield and energy reservoir. Similar to the dermis, lymphatic and blood vessels, mechanoreceptors and some hair follicle roots are located in the subcutaneous tissue.

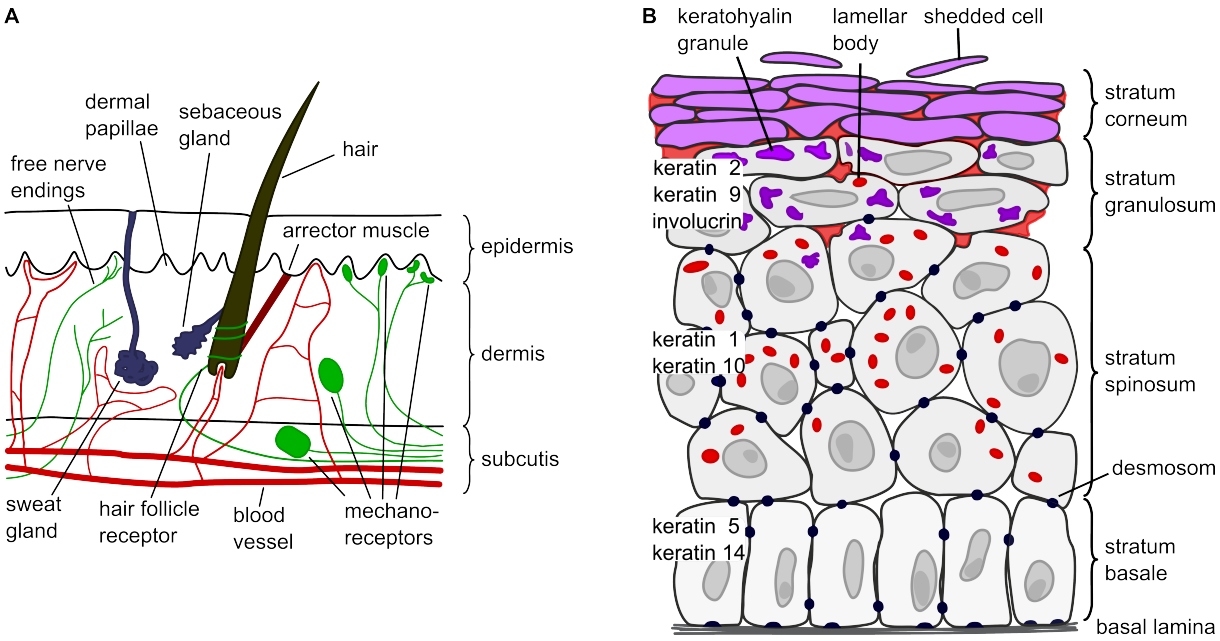

Figure 2: Structure of the skin and detailed scheme of the epidermis; **A** Three-layered organisation of the skin with skin appendages like hairs, sebaceous and sweat glands. **B** Schematic representation of the epidermis. Several keratin isoforms and involucrin are marker proteins of different stages of differentiation. Thus, they enable the distinction of the epidermal layers. For clarity, the illustration of other cell types like melanocytes or Langerhans cells has been omitted.

1.2.1 Structure of the epidermis

The major task of the epidermis is the formation of a protective barrier. Its predominant cell type is the keratinocyte, which accounts for over 90% of the cells in the epidermis. The epidermis can be morphologically and functionally divided into four distinct layers, which represent diverse levels of differentiation of keratinocytes (Fig. 2 B)[7,8]. These differentiation levels are characterised by the expression of specific proteins, such as distinct isoforms of keratin and integrins.

The innermost epidermal cell layer is the *stratum basale*. Keratinocytes in the *stratum basale* bear a strong proliferation potential and are considered epidermal stem cells. They form a cell monolayer that is attached to the basal membrane by hemidesmosomes. After several cell divisions, the keratinocytes initiate a complex differentiation programme and migrate actively towards the skin surface. In addition, melanocytes are located between the keratinocytes of the *stratum basale*. They produce and secrete melanins, which are absorbed by surrounding keratinocytes and participate in the protection from UV radiation.

In the adjacent epidermal layer, the *stratum spinosum*, keratinocytes are connected via desmosomes and they start to produce lamellar bodies (Odland bodies), which contain different lipids and proteins like hydrolytic enzymes. In this layer, Langerhans cells, specialised dendritic cells that resemble macrophages in morphology and function, mediate the initial recognition of antigens and thereby

contribute to the defence of the organism against pathogens.

On the apical side of the *stratum spinosum*, the *stratum granulosum* follows. The keratinocytes of this region adopt a flatter shape and produce keratohyalin granules, which contain precursors of proteins required for the aggregation and crosslinking of keratins. On the upper side of the *stratum granulosum*, the keratinocytes secrete the Odland bodies. Thereby, the extracellular space is enriched with different lipids[9,10] that, together with hydrophobic, crosslinked keratins, aid in establishing the skin's water impermeability. Furthermore, hydrolytic enzymes are released that later on promote the correct shedding (desquamation) of the uppermost cornified cells.

The keratinocytes of the upper *stratum granulosum* undergo apoptosis, dehydrate, and their organelles, including the nucleus, disintegrate. The remaining, still cohesive layer of cornified keratinocyte ghosts is embedded in a dense environment formed by lipids and proteins and is referred to as *stratum corneum*. These cell remnants are called corneocytes and mainly consist of different crosslinked structure proteins like keratins. Depending on the mechanical demands on the skin, the thickness of the *stratum corneum* varies. In humans, the development of keratinocytes from proliferating cells to fully cornified cells takes about two weeks. The corneocytes remain in the *stratum corneum* for another two weeks. Afterwards, desquamation, the final superficial shedding from the skin, takes place. In healthy individuals, the proliferation of keratinocytes in the *stratum basale* and the desquamation of corneocytes from the *stratum corneum* are well-balanced processes in order to maintain a even thickness of the cutis.

1.2.2 Regulation of keratinocyte differentiation

The homoeostasis of the epidermis requires a strictly regulated balance between factors that promote keratinocyte proliferation and factors that favour these cells' differentiation. A plethora of stimuli affect keratinocyte physiology, including growth factors, intercellular contacts, or temperature changes[11,12]. One of the most prominent substances influencing keratinocyte differentiation is calcium[7,8,12]. In the *stratum basale*, the extracellular calcium concentration is low; it gradually increases towards the apical layers of the epidermis and reaches its highest concentration in the *stratum granulosum*. It is not yet fully understood how keratinocytes recognise the extracellular total or ionised calcium concentration. The G protein-coupled Ca^{2+}-sensing receptor seems to play an important role in this process[12], but is most likely supported by other sensors, such as transient receptor potential channels (TRP)[12,13].

Some lipid factors, e.g. ceramides, sphingolipids, the lipid-like vitamin D3 and vitamin A, have been shown to influence keratinocyte physiology[14]. Steroids like cholesterol and its derivative cholesterol sulfate have also been demonstrated to play important roles in inducing or regulating the differentiation process[9]. It has been observed that an inhibition of the cholesterol synthesis as well as a depletion of cholesterol counteract the differentiation of keratinocytes[15], whilst a cholesterol

enrichment facilitates this process. In this context, it has been shown that cholesterol enhances the formation of cornified envelopes, a protein-lipid layer that replaces the plasma membrane of corneocytes[16].

A dysregulation of epidermal growth can lead to chronic skin diseases, such as *psoriasis vulgaris*, a non-infectious, inflammatory dermatological disorder that is characterised by an accelerated turnover of keratinocytes[17]. In affected individuals, keratinocytes cross the epidermis about four times faster than in healthy people. This results in an enhanced fraction of partially differentiated keratinocytes at the skin surface and an impaired barrier function. In case of atopic dermatitis, a disease with an increasing prevalence in developed countries, patients exhibit keratinocyte proliferation and differentiation defects[18]. The pathogenesis of this disease is poorly understood, but results obtained so far indicate the participation of keratinocytes and immune cells. Further diseases are also associated with changes of the proliferation capacity of keratinocytes. Such may be due to altered signalling cascades that sustain an increased cell proliferation and promote the development of skin cancers like basal cell and squamous cell carcinoma[19]. These are indeed the most common forms of non-melanoma skin tumours in the elderly.

1.2.3 Migration of keratinocytes

Keratinocytes move either in a three-dimensional direction during physiological turnover or as flat sheets during the reepithelialisation phase of wound healing[20,21]. In various respects, sheet migration resembles the movement of individual cells, including cytoskeletal reorientations or chemotactic guidance. However, in case of sheet migration, additional factors such as cell junctions mediate cell-superordinated behaviours that influence the initiation, maintenance and direction of keratinocyte movement. Similarly, migration is also affected by chemokines, growth factors and electrical signals.

During sheet migration, planar cell polarity can be observed: keratinocytes at the leading edge of the cell assembly, the so-called "leading cells", adopt a polarised shape[20,21]. Towards the leading edge, these cells extend lamellipodia. At the same time, the connection to those cells following is maintained throughout the whole process. The polarised morphology of migrating cells is accompanied by an asymmetric front-to-back distribution of signalling proteins and lipids. The most prominent example for a lipid gradient is that of phosphatidylinositol(3,4,5)-trisphosphate. This gradient results from distinct distribution patterns of activated phosphoinositide 3-kinases and the phosphatases SHIP and PTEN[22]. With respect to cholesterol, migrating endothelial cells display a front-to-back viscosity gradient in their plasma membranes[23], which has been attributed to a polarised distribution of cholesterol. Diverse studies addressed the polarity of lipid rafts in migrating cells (summarised by Mañes[24]), but results obtained so far are highly contradictory. This is probably due to variations in cell models and experimental approaches used, as well as due to the existence of distinct kinds of lipid rafts with altering compositions. Conflicting data has also been reported with regard to

the influence of cholesterol on cell migration. Depletion of cholesterol decreases the migration of different cell types[23,25–29], but on the other hand, cholesterol enrichment may also effectively inhibit cell migration, as has been demonstrated in macrophages[30,31] and T cells[32].

1.3 TRP channels

The family of transient receptor potential (TRP) channels consists of 28 mammalian genes that encode cation channel subunits[33]. TRP channels are expressed in virtually all cell types, contribute to sensory perception and decode environmental signals of versatile nature. Hence, TRP channels play crucial roles in a broad spectrum of cellular and physiological processes.

A functional TRP channel is assembled of four subunits[33], each containing six transmembrane-spanning segments and intracellularly located N- and C-termini (Fig. 3 A). It has been proposed that the fifth and sixth membrane segments in combination with their connecting loop form the centrally located channel pore, which bears the selectivity filter and channel gate(s). Based on sequence homology, the family of mammalian TRP channels can be divided into six subfamilies: the canonical (TRPC), vanilloid (TRPV), melastatin (TRPM), mucolipidin (TRPMP), polycystin (TRPP), and ankyrin-rich (TRPA) TRP channels.

1.3.1 Structure and biophysical characteristics of TRPV3

TRPV3 belongs to the vanilloid branch of TRP channels, a subfamily that has first been defined when TRPV1, a heat-stimulated channel that is also activated by vanilloid compounds like capsaicin, has been described. Among the TRPV channels, TRPV1 to TRPV4 are heat-activated, non-selective cation channels, whereas TRPV5 and TRPV6 are transcriptionally regulated, Ca^{2+}-selective channels, which contribute to the vitamin D3-controlled Ca^{2+} homeostasis. In some TRPV channels, alternative splicing or unconventional translation initiation can further increase the complexity of functional channels. In TRPV3, three different splice variants have been observed[34], but doubts remain whether these translate into functional variations. At their intracellular N- and C-termini, TRPV3 channels bear conserved domains and motifs, such as ankyrin repeats, the TRP domain, several putative phosphorylation sites, and a PDZ recognition site[34–36].

TRPV3 is a moderately Ca^{2+}-selective cation channel. TRPV3-mediated currents exhibit outwardly rectifying current-voltage relations with reversal potentials close to 0 mV[34–37]. During prolonged activation, TRPV3 channels are being stabilised in the open pore conformation, and the current-voltage relation adopts a more linear shape[38]. Accordingly, TRPV3 signals exhibits a characteristic sensitisation following repetitive activation[35,36,39], a feature that distinguishes TRPV3 from other TRP channels. Sensitisation results in boosted signals and occurs independently of the kind of

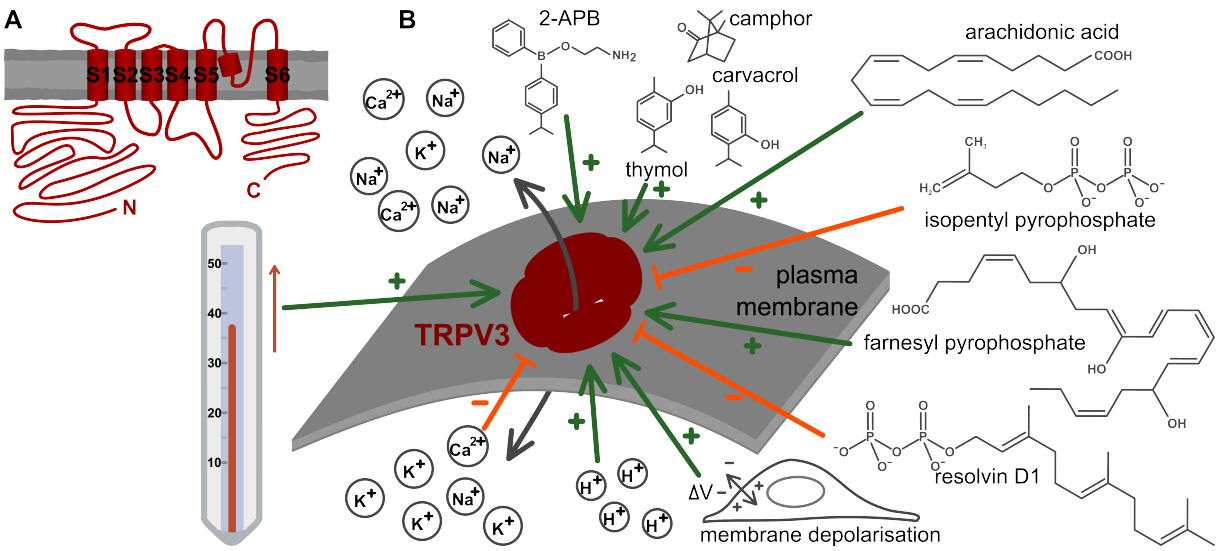

Figure 3: Structure and regulation of TRPV3 channels; **A** Structure of a single TRP channel subunit with six membrane-spanning helical segments (S1-S6) and intracellular N- and C-termini. A recursive loop between S5 and S6 dips into the plasma membrane and features the selectivity filter. **B** Schematic representation of some factors regulating TRPV3 channel activity, including exogenous modulators, such as 2-APB or camphor, and endogenous modulators, like the membrane potential, carbohydrate pyrophosphates, unsaturated fatty acids, or protons.

stimulus.

1.3.2 Expression profile and functions of TRPV3

TRPV3 has been discovered by three independent laboratories in 2002 [34–36], and has been characterised as a cation channel that is activated by innocuous warm temperatures. A few years later, TRPV3 knockout mice revealed a defective temperature recognition [40]. Thus, TRPV3 belongs to the group of the so-called thermoTRPs, which comprises several members of different TRP subfamilies. However, further studies demonstrated no obvious alterations in thermal preference behaviour of TRPV3 knockout mice [41]. This indicates that the development of a temperature sensing dysfunction probably depends on the genetic background of the animals or on compensatory mechanisms that are triggered by a lack of TRPV3 expression.

TRPV3 is predominantly localised on the plasma membrane of keratinocytes in the basal and suprabasal epidermal layers [35,36]. It has also been detected in keratinocyte-derived cell lines, such as the HaCaT (human adult low calcium high temperature) [42] cell line [43,44]. Further sites of expression of TRPV3 have been found in other tissues, including cells of the oral cavity and nose [45,46], embryonic stem cells [47], some brain tissues [48] and sensory neurons of dorsal root ganglia (DRG) in humans and primates [34,35].

To date, various physiological and pathophysiologial functions have been suggested for TRPV3.

These range from hot temperature perception, nociception and inflammatory hyperalgesia [49,50], to hair growth [13,51]. In addition, it seems that TRPV3 is directly involved in the formation and maintenance of the epidermal barrier. Cheng et al. demonstrated that TRPV3 forms a signalling complex with the epidermal growth factor receptor and, thus, probably regulates keratinocyte differentiation processes [13]. This conclusion is supported by the fact that TRPV3 knockout mice display anomalies regarding the formation of the epidermal barrier [13]. Consistent with these findings, temperatures that activate TRPV3 accelerate the epidermal barrier recovery after mechanical skin disruption [52]. Moreover, the activation of TRPV3 results in an elevated nitric oxide production [53], and this molecule plays a key role in wound healing processes [54]. Novel results indicate TRPV3 to be associated with cell cycle and differentiation regulation of several cell types [46,47,51,55,56].

Consequently, it has been evaluated whether TRPV3 is involved in the pathogenesis of skin diseases [57]. Indeed, an increased TRPV3 expression has been observed in dermal cells of patients suffering from rosacea [58]. It is noteworthy that mice bearing a mutated, constitutively active TRPV3 variant display symptoms that resemble those observed in patients suffering from atopic dermatitis, e.g. pruritus, inflammation, and hyperkeratosis [59–62]. In humans, various constitutively active mutations of TRPV3 are associated with the Olmsted syndrome [63], the only established hereditary channelopathy involving TRPV3. Olmsted syndrome is a rare skin disease accompanied by severe pruritus and hyperkeratosis due to enhanced keratinocyte turnover and apoptosis.

1.3.3 Regulation of TRPV3 channel activity

Like many other TRP channels, TRPV3 is influenced by a multitude of different factors (reviewed by Nilius [37], Fig. 3 B), some of which are introduced in the following section. As mentioned above, TRPV3 is temperature-sensitive and responds to warm temperatures, with thresholds ranging between 32°C and 39°C. Similar to the majority of temperature-regulated TRP channels, TRPV3 exhibits an intrinsic voltage dependence. In the absence of physical or chemical activators, voltage-induced channel gating is only achieved at unphysiologically positive voltages. Upon exposure to chemical activators or temperature changes, the threshold for voltage-dependent channel gating shifts towards more negative, physiological membrane potentials [64,65], thereby allowing the channels to open in response to the respective stimuli.

Like TRPV1, TRPV3 can alternatively be activated by heat or by non-thermal stimuli. 2-APB (2-aminoethoxydiphenyl borate) has been the first identified chemical activator of TRPV3 [66]. Since 2-APB modulates members of almost all TRP subfamilies in a positive or negative way [67], its action on TRPV3 is non-specific. Subsequently, camphor has been shown to activate TRPV3 [40]. Other TRPV3 stimulators have been recognised later on, with many of them being herbal ingredients, e.g. carvacrol, eugenol, and thymol, which share the terpene structure of camphor [45]. Other modulators of TRPV3 are lipids. Unsaturated fatty acids, like arachidonic acid, are considered endogenous reg-

ulators of TRPV3 activity[68]. They directly potentiate TRPV3 currents evoked by stimulation with 2-APB, but fail to activate these channels alone. In contrast farnesyl pyrophosphate, an intermediate of the mevalonate pathway, directly activates TRPV3, and may be involved in TRPV3-mediated nociception[49].

On the other hand, lipid modulators of TRPV3 may also inhibit channel activity, as is the case of farnesyl pyrophosphate, a precursor of isopentenyl pyrophosphate[69]. Resolvin D1[70], an anti-inflammatory agent produced by the cyclooxygenase 2 pathway, and phosphatidylinositol 4,5-bisphosphate[71] also attenuate TRPV3 channel activity. Moreover, the divalent cations Ca^{2+} and Mg^{2+} are among the negative regulators of TRPV3[39,72], a feature that is displayed by several TRP channels. Furthermore, the TRPM8 activator icilin[44] and the unspecific TRP channel blocker ruthenium red inhibit TRPV3 channel activity[34–36]. In the last years, some more selective TRPV3 antagonists have been described[57], but their pharmacodynamic or pharmacokinetic properties impeded any further development towards a possible therapeutic application.

1.3.4 Cholesterol-dependent regulation of temperature-mediated TRPs

The local cholesterol content of biological membranes strongly influences the signalling properties of numerous ion channels and other transmembrane proteins. In this context, the effect of cholesterol on the activity of TRP channels has been intensely studied. Concerning TRPV1, published results indicate a stimulus- or cell-type-dependent modulation of the channel's activity[73]. On the one side, in TRPV1-transfected HEK293 (human embryonic kidney) cells, cholesterol enrichment decreases the susceptibility of TRPV1 to hot temperatures by raising its activation threshold[74]. On the other hand, cholesterol extraction reduced channel activity during prolonged activation of TRPV1 in CHO cells expressing this channel[75]. By contrast, other reports found no significant changes of TRPV1 activity upon cholesterol depletion[74]. Accordingly, different ideas have been put forward to explain the cholesterol-dependent modulation of TRPV1. Liu et al. observed a reduced plasma membrane fraction of TRPV1 in cholesterol-depleted DRG neurons[76]. The group of Rosenbaum identified a cholesterol-binding motif in rat and human TRPV1 that may be responsible for a cholesterol-dependent inhibition of TRPV1 activity[77].

Regarding the cholesterol dependence of the cold receptor TRPM8, channel activity increased upon cholesterol depletion, which was possibly induced by the translocation of TRPM8 from rafts to non-raft regions[78]. A changed glycosylation pattern of TRPM8 may be the trigger of this channel's lipid raft segregation. The heat-activated channel TRPM3 is inhibited by cholesterol enrichment, whereas it is directly activated by pregnenolone sulphate, a cholesterol-derived steroid hormone[79]. Concerning TRPV3, findings regarding the cholesterol dependence of this ion channel have not yet been published.

Objective

Although cholesterol is an essential substance for the water-impermeability of the epidermis, little is known about the function of cholesterol with regards to keratinocyte migration. Since this lipid strongly determines the physical properties of biological membranes, we examined the microviscosity and the distribution of cholesterol in the plasma membrane of migrating keratinocytes. For this purpose, we performed fluorescence redistribution after photobleaching (FRAP) and fluorescence lifetime measurements combined with illumination under total internal reflection (TIR) conditions. For our experiments, we used HaCaT keratinocytes since this cell line is known to adopt a polarised morphology with extended lamellipodia, a feature resembling migrating keratinocytes. In addition, we monitored local plasma membrane cholesterol concentrations with filipin, a cholesterol-binding fluorophore. To address the question how the cholesterol transporters ABCA1 and ABCG1 influence the plasma membrane's microviscosity, we deactivated these transporters using pharmacological inhibitors or specifically knocked down their expression applying a small interference RNA-based approach. To quantify the migration capacity of HaCaT cells, we carried out a wound healing-resembling scratch assay with subsequent analysis by means of automated multiwell time-lapse microscopy.

The pivotal roles of calcium and cholesterol in the decision-making programme of terminal keratinocyte differentiation and the prominent TRPV3 expression in these cells prompted us to research whether the activity of TRPV3 may be regulated by cholesterol. Consequently, we investigated the effects of cholesterol on TRPV3 channel signalling with fluorometric Ca^{2+} influx measurements and electrophysiological patch clamp experiments. We focused on the response of recombinantly expressed or native TRPV3 in keratinocytes to heat and to chemical activators. Temperature threshold changes of TRPV3 activation induced by a modified plasma membrane's cholesterol content were monitored. Results from this study are expected to contribute to the understanding of the role of TRPV3 in the calcium- and cholesterol-dependent terminal differentiation and apoptosis induction of keratinocytes.

EXPERIMENTAL CELL RESEARCH 318 (2012) 809–818

Available online at www.sciencedirect.com

SciVerse ScienceDirect

www.elsevier.com/locate/yexcr

Research Article

HaCaT keratinocytes exhibit a cholesterol and plasma membrane viscosity gradient during directed migration

Anke S. Klein[a], *Michael Schaefer*[a], *Thomas Korte*[b], *Andreas Herrmann*[b], *Astrid Tannert*[a,*]

[a]*Rudolf-Boehm-Institut für Pharmakologie und Toxikologie, Universität Leipzig, Germany*
[b]*Institut für Biologie/Biophysik, Humboldt-Universität zu Berlin, Germany*

ARTICLE INFORMATION

Article Chronology:
Received 23 September 2011
Revised version received 27 January 2012
Accepted 8 February 2012
Available online 15 February 2012

Keywords:
ABCA1
Cholesterol
HaCaT migration
Wound healing
FRAP
FLIM

ABSTRACT

Keratinocyte migration plays an important role in cutaneous wound healing by supporting the process of reepithelialisation. During directional migration cells develop a polarised shape with an asymmetric distribution of a variety of signalling molecules in their plasma membrane. Here, we investigated front-to-back differences of the physical properties of the plasma membrane of migrating keratinocyte-like HaCaT cells. Using FRAP and fluorescence lifetime analysis, both under TIR illumination, we demonstrate a reduced viscosity of the plasma membrane in the lamellipodia of migrating HaCaT cells compared with the cell rears. This asymmetry is most likely caused by a reduced cholesterol content of the lamellipodia as demonstrated by filipin staining. siRNA-mediated silencing of the cholesterol transporter ABCA1, which is known to redistribute cholesterol from rafts to non-raft regions, as well as pharmacological inhibition of this transporter with glibenclamide, strongly diminished the viscosity gradient of the plasma membrane. In addition, HaCaT cell migration was inhibited by glibenclamide treatment. These data suggest a preferential role of non-raft cholesterol in the establishment of the asymmetric plasma membrane viscosity.

Introduction

Cell migration contributes to a multitude of physiological as well as pathophysiological processes, including development, wound healing, inflammation, and tumour dissemination. To migrate directionally, cells develop a polarised shape accompanied by cytoskeletal reorientation and a polarised redistribution of signalling proteins and lipids in the plasma membrane. The most prominent example in lipid polarisation is the lateral asymmetric distribution of PIP_3, which is generated by the interplay between locally activated PI3K and PTEN or SHIP-1 in *Dictyostelium* or neutrophils, respectively [1]. The role of other lipid components or physical membrane properties on cell migration is less well understood. Furthermore, there are very few investigations analysing the overall physical membrane properties of migrating cells which are highly influenced by the lipid composition. Ghosh et al. examined the viscosity of the plasma membrane of migrating endothelial cells [2], eliciting a slightly enhanced migration by stiffening the

* *Corresponding author at:* Rudolf-Boehm-Institut für Pharmakologie und Toxikologie, Universität Leipzig, Härtelstr. 16-18, D-04107 Leipzig, Germany. Fax: +49 341 9724609.
E-mail address: astrid.tannert@medizin.uni-leipzig.de (A. Tannert).

Abbreviations: ABC, ATP binding cassette; CLSM, confocal laser scanning microscopy; DiI, 1,1′-di-octa-decyl-3,3,3′,3′-tetra-methyl-indo-carbocya-nine perchlorate; FAST DiO, 3,3′-dilinoleyloxacarbocyanine perchlorate; FLIM, fluorescence lifetime imaging microscopy; FRAP, fluorescence redistribution after photobleaching; IRF, instrument response function; NBD-PC, 1-palmitoyl-2-(6-[N-(7-nitrobenz-2-oxa-1,3-diazol-4-yl)amino]caproyl)-*sn*-glycero-3-phosphocholine; TIRF, total internal reflection fluorescence.

0014-4827/$ – see front matter © 2012 Elsevier Inc. All rights reserved.
doi:10.1016/j.yexcr.2012.02.007

membrane with α-tocopherol and an inhibited migration by reducing the microviscosity upon lyso-lipid incorporation. In a follow up publication, this group showed that these cells reveal a front-to-back gradient of plasma membrane microviscosity with an enhanced viscosity at the front of the migrating endothelial cells using FRAP and fluorescence polarisation experiments [3].

Cholesterol strongly influences the physical membrane properties [4]. The cholesterol content of the plasma membrane of a cell is regulated by the cellular cholesterol biosynthesis as well as its uptake from and release to serum lipoproteins. Release of cholesterol to serum lipoproteins is facilitated by the plasma membrane cholesterol transporters ABCA1 and ABCG1, which presumably mediate a transversal, ATP-dependent transport of cholesterol from the inner to the outer membrane leaflet [5]. Expression of functional ABCA1 was shown to alter the fluidity of plasma membranes [6]. Furthermore, studies using cholesterol-enriched macrophages, which play a role in atherosclerosis, show not only that functional ABCA1 inhibits migration of these macrophages due to an enhanced fraction of cholesterol in their plasma membrane [7], but also that deletion of ABCA1 and ABCG1 leads to an inhibited macrophage mobility [5].

Cutaneous wound healing depends on the recruitment of fibroblasts, endothelial cells, and keratinocytes [8], the migration of the latter determines the process of reepithelialisation [9]. Keratinocytes typically migrate in cell assemblies, and cells at the edge form pronounced lamellipodia. Among other factors, keratinocyte migration is stimulated by activation of the EGF receptor [10]. Here, using FRAP and fluorescence lifetime measurements under total internal reflection (TIR) illumination, we show that migrating keratinocyte-like HaCaT cells exhibit a polarised cholesterol distribution when stimulated with EGF, leading to a reduced microviscosity of their lamellipodia compared to the cell rears. Pharmacological inhibition of the cholesterol transporter ABCA1, which is expressed in HaCaT cells [11], diminished cell migration tested by a scratch assay and reduced the microviscosity gradient in polarised HaCaT cells. In addition, after silencing ABCA1 with siRNA, no plasma membrane microviscosity gradient was observable in polarised HaCaT keratinocytes.

Materials and methods

Cell culture

The spontaneously immortalised, untransformed human keratinocyte cell line HaCaT was kindly provided by Dr. U. Anderegg (Department of Dermatology, University of Leipzig, Germany). The cells were maintained in Dulbecco's modified Eagles medium with 1 g/l glucose, supplemented with 10% (v/v) foetal calf serum (FCS), 1% glutamine, 100 U/ml penicillin, and 100 μg/ml streptomycin (all PAA Laboratories, Pasching, Austria) and cultured at 37 °C in an atmosphere of 5% CO_2. For passaging, cells were washed, incubated for 10 min with PBS supplemented with 0.8 mM EDTA at 37 °C and trypsinised. For measurements, cells were seeded onto glass coverslips in 35-mm cell culture dishes.

Transfection of HaCaT cells

HaCaT cells were transiently transfected with Lipofectamine 2000 (Invitrogen). For cotransfection, siRNA and plasmid DNA transfection solutions were prepared separately in OptiMEM (Invitrogen) with 500 ng DNA and 25 pmol siRNA per 1.5 μl Lipofectamine 2000. The final concentration of siRNA against ABCA1 or ABCG1 (Supplementary Table 2, stealth siRNA, containing 3 different sequences at equal portions, Invitrogen) was 25 nM siRNA and 500 ng/ml plasmid DNA. After transfection of HaCaT cells, we used media devoid of antibiotics to enhance cell viability; however we observed no change in transfection efficiency in the presence or absence of FCS in culture medium.

Fluorescence redistribution after photobleaching measurements under TIR illumination (TIR/FRAP)

The fluorescence redistribution after photobleaching (FRAP) experiments were done 1 day after seeding, when no additional activation of the cells was performed. To investigate the effect of defined concentrations of the human epidermal growth factor (EGF, Sigma-Aldrich), cells were cultured under serum-free conditions for 24 h followed by the addition of EGF and, optionally, inhibitors of different ABC transporters (Sigma-Aldrich), or DMSO as control for further 12–15 h. HaCaT cells were stained with 2.5 ng/ml of the plasma membrane probe FAST DiO (carbocyanine with diunsaturated $\Delta^{9,12}$-C18 alkyl substituents, Invitrogen) diluted in HEPES-buffered solution (HBS) containing 134 mM NaCl, 6 mM KCl, 1 mM $MgCl_2$, 1 mM $CaCl_2$, 5.5 mM glucose, 10 mM HEPES (pH 7.4) and 0.2% (w/v) bovine serum albumin for 20 min at room temperature (RT). After washing with HBS, cells at the edge of larger cell assemblies were examined. A sketch and a detailed explanation of the used setup for FRAP measurements using TIR excitation can be found in a previous publication [12]. For imaging of FAST DiO-stained HaCaT cells, we used the attenuated 488 nm line of an Ar^+ laser (Lasos, Jena, Germany) selected by an AOTF (AA Opto-Electronic, Orsay Cedex, France). A 514 nm beamsplitter (Chroma, Rockingham, VT) allowed for the separation of excitation and emission, and the emission light was filtered by a 514 nm RazorEdge longpass filter (Semrock, Rochester, NY). The 514 nm line was employed for bleaching of a diffraction-limited spot in the plasma membrane of the cells. Images were acquired using an EMCCD camera (iXon DV887, Andor, Belfast, UK) controlled by the TILLvisION software (TILL Photonics, Gräfelfing, Germany). One FRAP cycle consisted of 16 prebleach images, acquired every 20 ms, followed by a 5-ms lasting spot bleaching and immediate acquisition of 20 images in 20-ms intervals. This protocol was 10 times repeated every 10 s. After background correction of the images, the diffusion coefficient was approximated by a convolution-based algorithm as described previously [13].

For FRAP measurements with siRNA-mediated knockdown of ABC transporters in HaCaT cells, we cotransfected HaCaT cells with appropriate siRNA constructs and with a plasmid coding for an RFP-labelled nuclear protein to identify the transfected cells or with the plasmid encoding the nuclear RFP alone for control measurements. Due to its locally restricted cellular expression, the nuclear RFP did not influence the TIR/FRAP measurements and additionally possessed spectral properties that could be sufficiently separated from those of DiO (excitation of the RFP occurred with the 488 nm line of the Ar^+ laser and emission was filtered with a 685/40 nm bandpass filter). Seven hours after transfection, HaCaT cells were starved for 4 h, followed by an incubation of 12–15 h in 10 ng/ml EGF-containing, serum-free cell culture medium prior to FRAP measurements.

Fluorescence lifetime measurements under TIR illumination

For fluorescence lifetime measurements, HaCaT cells were seeded onto glass coverslips and labelled with NBD-PC (1-palmitoyl-palmitoyl-2-(6-[N-(7-nitrobenz-2-oxa-1,3-diazol-4-yl)amino]caproyl)-*sn*-glycero-3-phosphocholine, a phosphatidylcholine carrying an NBD group on one acyl chain, Invitrogen). NBD-PC was dissolved in chloroform, evaporated under a stream of nitrogen and resuspended to a final concentration of 4 μM in HBS. Cells were stained for 20 min at RT, washed with HBS and measured. For fluorescence lifetime measurements, we used the previously described TIRF microscope [12], which was upgraded by a 470 nm picosecond pulsed diode laser (LDH-D-C-470, PicoQuant, Berlin, Germany). Excitation light was cleaned by a Z463/25 X-HT filter (Chroma) and coupled into the excitation path instead of the Ar^+ laser. For NBD excitation, the pulse frequency was set to 20 MHz. An aperture in the excitation pathway enabled the selective measurement of distinct areas of the cells by constricting the excitation spot. The emission light was filtered by a 488 nm RazorEdge longpass filter (488-RU, Semrock), split by polarisation and directed onto two photomultiplier tubes (PMT). Data were recorded by the TimeHarp software (PicoQuant), using time-correlated single photon counting (TCSPC) at a rate of 10^5 counts/s until reaching 10^4 counts in the peak of the histogram. The instrument response function (IRF) was recorded using an empty coverslip to enable reconvolution of the TCSPC data. The fluorescence decay of NBD was approximated on a triexponential function [14] using an anisotropy model and reconvolving the measured IRF by the FluoFit Pro software (PicoQuant).

Confocal laser scanning microscopy-based fluorescence lifetime measurements

Confocal laser scanning microscopy (CLSM)-based fluorescence lifetime imaging (FLIM) of NBD-PC-labelled HaCaT was performed as described previously [14]. Cells were stained with NBD-PC as described above. Images were acquired by an inverted CLSM (Fluoview 1000, Olympus, Tokyo, Japan) equipped with a FLIM upgrade kit (PicoQuant) using a 60×/1.35 oil-immersion objective. NBD was excited with a 470 nm pulsed diode laser at a pulse frequency of 10 MHz. Emission was filtered using a 540/40 nm bandpass filter and recorded by a single-photon avalanche photodiode. About 100 frames of 512×512 pixels were acquired and summed up. The IRF was recorded using a clean coverslip and no emission filter. FLIM data analysis was performed with the SymPhoTime software (PicoQuant) using a triexponential model function, and reconvolving it with the IRF. Prior to FLIM analysis, the values of the two short lifetimes τ_1 and τ_2 were estimated from the whole image by summing up all pixel histograms. To calculate the average lifetimes of the FLIM image, the original image was binned 4× to a final size of 128×128 pixels. Again, the triexponential decay model function was reconvolved with the IRF and fitted with short lifetimes τ_1 and τ_2 (calculated as described above) fixed, while the environment-dependent long lifetime τ_3 was freely varied for each individual pixel.

Confocal laser scanning microscopy and filipin staining of HaCaT

The cholesterol content of the plasma membrane of HaCaT cells was visualised by staining with filipin (Sigma-Aldrich) [15], a known cholesterol marker. The plasma membrane was counterstained with different commercially available plasma membrane probes, i.e. FAST DiO (20 min, 2.5 ng/ml, RT) or DiI (20 min, 2.5 ng/ml, 37 °C, carbocyanine with saturated C18 alkyl substituents, Invitrogen) in HBS. After washing the cells with PBS, cells were fixed with 3% paraformaldehyde (PFA) in PBS for 20 min at RT, washed and incubated with 50 μg/ml filipin in PBS for 2 h at RT. Cells were observed using an inverted confocal laser scanning microscope (LSM 510Meta, Carl Zeiss AG, Oberkochen, Germany), with a C-Apochromat 40×/1.2 water immersion objective. For monitoring FAST DiO, we used the 488 nm line (Ar^+ laser) for excitation, a UV/488 beamsplitter and a 505 nm longpass filter. For visualising the DiI, we used the 543 nm laser line (He–Ne laser), a UV/488/543/633 beamsplitter and a 560 nm longpass emission filter. Excitation of filipin occurred with the 364 nm line (Enterprise UV laser), and we used a 385 nm longpass emission filter. Image analysis was performed with ImageJ (US National Institutes of Health, Bethesda, MD) [16].

Scratch wound healing assay

For wound healing assays $2 \cdot 10^5$ HaCaT cells per well were seeded into 24-well plates. After 1 day, medium was exchanged and after 2 days, confluently grown cells were starved for 4 h in culture medium without FCS and supplemented with 5 μg/ml mitomycin C (AppliChem GmbH, Darmstadt, Germany) to inhibit cell proliferation [17]. Afterwards an artificial wound was caused by scratching the cell monolayer with a 200-μl pipette tip. Transmission images of the cells on the scratch were recorded with a 5× objective using a cooled CCD camera (SensiCam, PCO AG, Kehlheim, Germany). Cells were incubated with various agents diluted in serum-free medium under cell culture conditions for 12–24 h. Additional images were recorded at the same locations at various time points using an automated microscope with a motorised stage (Axio Observer.Z1, Zeiss). The microscope and the image acquisition were controlled by the Micro-Manager 1.3 software (US National Institutes of Health) [18]. The wound healing was quantified, using ImageJ, by measuring the width of the cell-free scratch, which allowed to calculate the distance the cells migrated.

Results

Polarised HaCaT cells exhibit a plasma membrane viscosity gradient

To analyse the plasma membrane viscosity, we performed FRAP experiments in polarised HaCaT cells using a commercially available plasma membrane dye and analysing its distribution under TIR excitation [12]. We chose FAST DiO as fluorophore, which shows a bright plasma membrane staining in HaCaT cells, and analysed single cells at the edge of larger cell assemblies, which resemble border cells at the edge of a wound. These cells formed lamellipodia and their rears contacted other cells. On the lamellipodia of HaCaT cells, grown in culture medium containing FCS but without further growth factors, we found a mean diffusion coefficient of $1.30 \pm 0.06\ \mu m^2/s$ of FAST DiO, which was slightly but statistically significantly higher than that at the cell rears ($1.21 \pm 0.07\ \mu m^2/s$, Fig. 1a). This plasma membrane viscosity gradient was found in about 83% of the analysed cells. A gradient in the plasma membrane properties was also detectable using fluorescence lifetime measurements of NBD-PC-

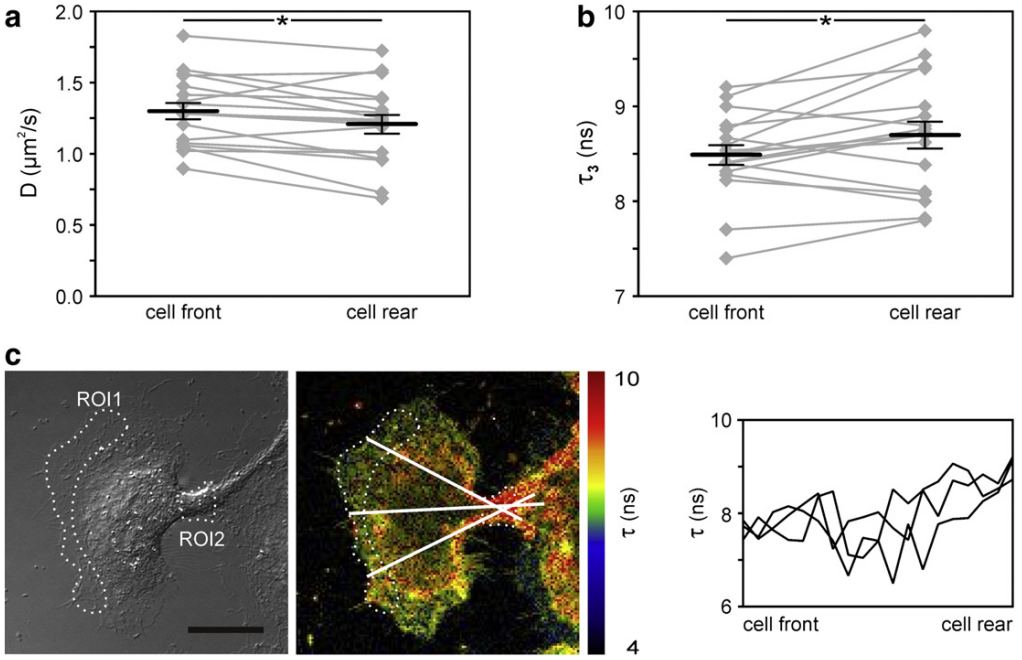

Fig. 1 – Migrating HaCaT cells reveal an asymmetric plasma membrane viscosity. a: HaCaT cells were cultured under normal cell culture conditions in FCS-containing medium, and stained with the plasma membrane marker FAST DiO 1 day after seeding. a: Diffusion coefficients at the lamellipodia and rears of spontaneously polarised cells at the border of large cell assemblies were determined with TIRF-based FRAP experiments. b: Fluorescence lifetime τ_3 measured at the fronts and rears of NBD-PC-stained HaCaT cells under TIR excitation. c: Space-resolved fluorescence lifetime image of a NBD-PC-stained HaCaT cell. The DIC image (left) and the corresponding pseudocoloured photon-weighted image of averaged fluorescence lifetimes (right) are shown. Average lifetime values of the depicted regions of interest are for ROI1 $\tau = 7.4$ ns and ROI2 $\tau = 8.6$ ns. Profiles of averaged fluorescence lifetimes of NBD-PC indicated by white lines are illustrated in the adjacent diagram. Scale bar: 20 µm. (a and b each with $n = 18$ from at least 3 independent experiments; mean ± SEM, single measurements are depicted in grey; paired Student's *t*-test $^*p < 0.05$.)

labelled HaCaT cells under TIR illumination. NBD exhibits three fluorescence lifetimes, of which the longest lifetime τ_3 (about 6–14 ns in different cell types) strongly depends on the physicochemical properties of the environment of the fluorophore. The two shorter lifetimes of about 0.2–0.5 ns and 2–3 ns are relatively independent of the environment [14] and were, therefore, not considered for the analysis of the viscosity gradient (Supplementary Fig. 1). The long fluorescence lifetimes of NBD at the cell fronts of HaCaT (8.49 ± 0.10 ns) were statistically significantly lower than at the cell rears (8.70 ± 0.14 ns) (Fig. 1b). Similar results were obtained in spatially resolved fluorescence lifetime images of NBD-PC-stained HaCaT cells (Fig. 1c). Slower diffusion of membrane markers as well as longer fluorescence lifetimes of NBD indicate a higher membrane viscosity at the cell rears.

Viscosity differences are related to altered membrane cholesterol contents

The membrane cholesterol content strongly influences the membrane properties [4]. It is therefore possible that the microviscosity gradient is caused by a heterogeneous distribution of cholesterol in the plasma membrane of polarised HaCaT cells. To further investigate this hypothesis, we stained polarised HaCaT cells with filipin that binds specifically to cholesterol [15], and visualised the cells by confocal microscopy. Thin membrane structures that are stacked like filipodia and lamellipodia may not be resolved in the *z*-axis by CLSM, leading to an apparent increase in fluorescence intensity, because the sum of fluorescence intensities of two membrane layers is recorded [19]. Therefore, we counterstained the cells with the lipophilic plasma membrane markers DiI or FAST DiO as reference (Fig. 2). The recorded fluorescence intensity of filipin was related to that of the plasma membrane markers, revealing a lower cholesterol content at the lamellipodia compared with the cell bodies of polarised HaCaT cells. These data suggest that a heterogeneous cholesterol concentration contributes to the viscosity gradient of the plasma membrane found in migrating HaCaT cells.

Activation of HaCaT cells promotes the development of a plasma membrane viscosity gradient

Keratinocyte migration is known to be enhanced in the presence of growth factors that bind to the EGF receptor [10]. Thus, we wanted to elucidate the impact of EGF on the observed microviscosity gradient. To eliminate the influence of growth factors contained in the FCS, we kept HaCaT cells in serum-free medium for 24 h, and subsequently added defined concentrations of EGF for about 12 h. Scratch experiments with HaCaT cells revealed highest migration rates at concentrations of 10 ng/ml EGF (Fig. 3a) and a decreasing migration rate at higher EGF concentrations, consistent with literature data [10]. Interestingly, HaCaT cells activated with

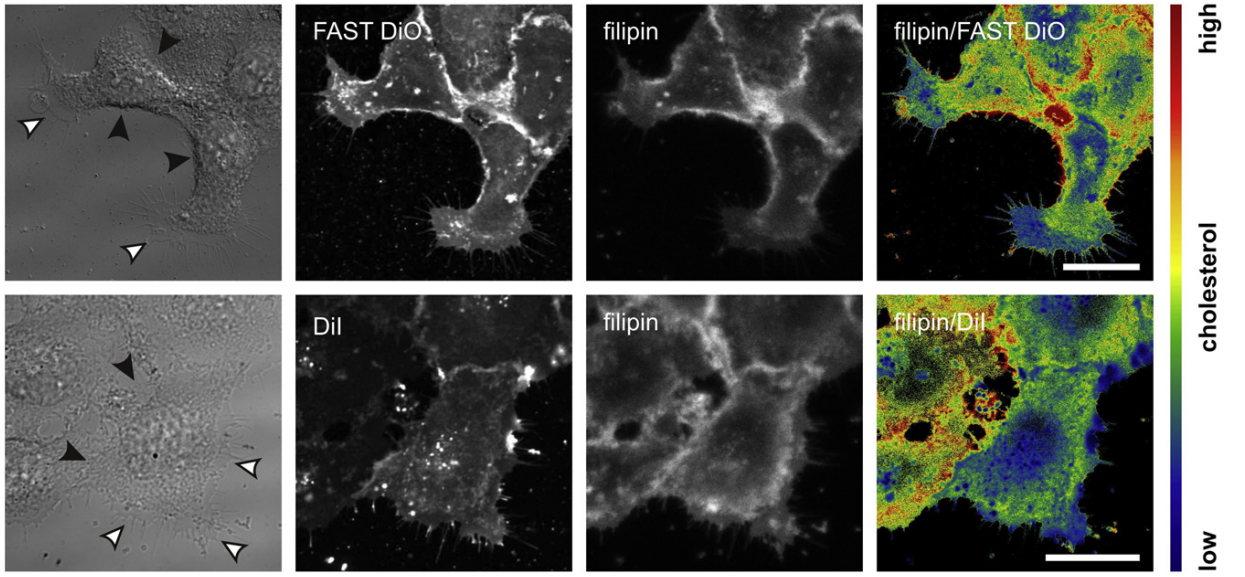

Fig. 2 – Cholesterol staining of polarised HaCaT cells. HaCaT cells were seeded in culture medium, counterstained with the plasma membrane markers FAST DiO or DiI, fixed, stained with filipin and imaged by CLSM. Representative images of spontaneously polarised HaCaT cells are shown with transmission light acquisition (left column), fluorescence image of the plasma membrane marker (middle left column), and filipin fluorescence (middle right column). The right panel shows pseudocoloured images of the ratio of the intensity images of filipin and the corresponding plasma membrane markers (high cholesterol content is indicated in red, low cholesterol content in blue). Scale bar: 20 μm. Filled arrow heads: plasma membrane regions without lamellipodia, empty arrow heads: lamellipodia.

10 ng/ml EGF also developed the most significant viscosity gradient determined by the FRAP approach ($1.23 \pm 0.04\ \mu m^2/s$ and $1.10 \pm 0.04\ \mu m^2/s$ at the fronts and the rears, respectively, Fig. 3b). Starvation of HaCaT cells led to a reduction of the viscosity gradient in the plasma membrane compared with EGF-treated cells (Fig. 3) or cells grown in culture medium containing FCS (Fig. 1). When cells were treated with higher EGF concentrations (100 ng/ml), *in vitro* wound healing was impaired, and the viscosity gradient was again not statistically significant ($p = 0.08$, 1.15 ± 0.06 versus $1.04 \pm 0.05\ \mu m^2/s$ at the cell fronts and backs, respectively) and only detectable in 65% of the cells. We observed an overall increase in microviscosity by stimulating HaCaT cells with EGF. In the presence of 100 ng/ml EGF, diffusion coefficients decreased by 17% and 24% at the cell fronts and rears, respectively, when compared with serum-starved cells. In agreement with these data, EGF treatment increased the cellular cholesterol content by over 40% (Supplementary Fig. 2).

In HaCaT cells that were not located at the border of an assembly but following the leaders, we did not observe a microviscosity gradient (Supplementary Fig. 3). These cells also did not adopt such a pronounced polarised morphology with lamellipodia like the leaders.

ABCA1 influences the membrane viscosity gradient

The plasma membrane cholesterol content and domain formation may be influenced by specialised proteins. To investigate the influence of cholesterol transporters of the ABC transporter protein family, we pharmacologically inhibited ABCA1 by glibenclamide [20] and analysed the cell migration and the microviscosity gradient. Scratch assays revealed that glibenclamide reduced HaCaT cell migration in response to 10 ng/ml EGF (Fig. 4a). We noted that at higher concentrations of glibenclamide (400 μM) the number of polarised HaCaT cells is reduced and staining with FAST DiO was less efficient. For FRAP measurements we reduced the glibenclamide concentration to values that allowed the cells to form a polarised shape. HaCaT cells treated with 200 μM glibenclamide still appeared polarised but the microviscosity gradient in the presence of EGF was abolished (Fig. 4b). Inhibition of other cholesterol transporters ABCG1 or ABCB1 with 20 μM benzamil [21] or verapamil [22], respectively, did not significantly influence the observed plasma membrane viscosity gradient (Supplementary Fig. 4). Since glibenclamide is a relative poorly specific inhibitor of different ABC transporters, we verified the influence of ABCA1 on the microviscosity gradient by siRNA-assisted knockdown in FRAP experiments. We proved the knockdown of mRNA with reverse transcription–polymerase chain reaction. In our hands, the mRNA of ABCA1 and ABCG1 was most efficiently downregulated after 24 h using 25 nM siRNA (Supplementary Fig. 5). Consistent with the pharmacological inhibition of ABCA1, HaCaT cells treated with siRNA against ABCA1 exhibited randomly distributed viscosity gradients, whereas cells with silenced ABCG1 still possessed uniformer plasma membrane viscosity gradients with a higher diffusion at their lamellipodia compared with their rears (Fig. 5).

Discussion

Cell migration is a highly regulated and complex process. It involves large rearrangements of the plasma membrane, which are mediated in part by interaction with cytoskeletal proteins and

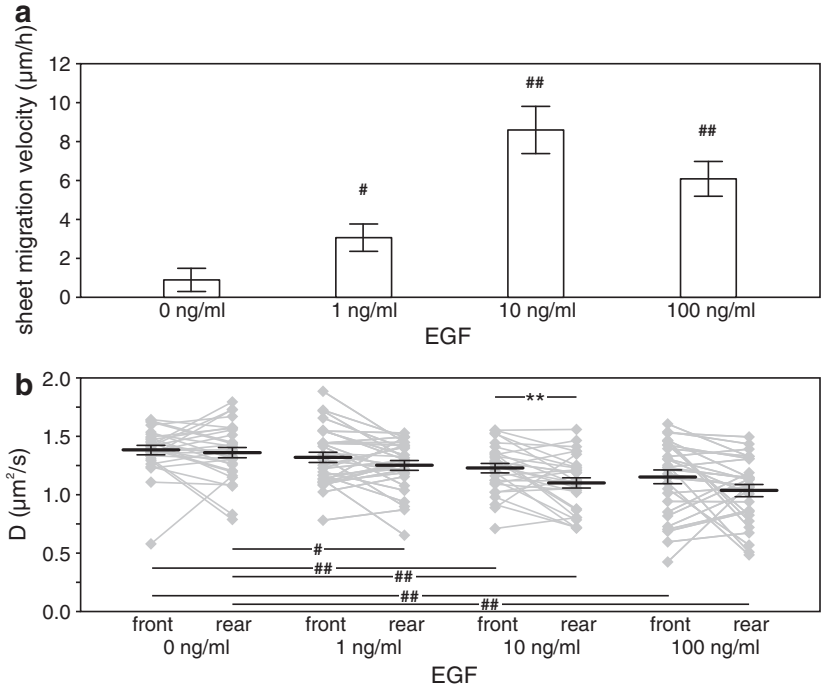

Fig. 3 – Upon activation with EGF, HaCaT cells are stimulated to migrate and develop a front-to-back asymmetry of their plasma membrane viscosity. a: HaCaT cell migration in different concentrations of EGF was measured using a wound healing assay. Migration was quantified at minimal 12 h after scratching by determining the distance, the cells migrated into the scratched area ($n = 6$). b: HaCaT were seeded, starved, and incubated for 12–15 h with different concentrations of EGF. After staining with FAST DiO, diffusion coefficients were determined by TIR/FRAP experiments at the cells fronts and rears ($n = 30$ from at least 4 independent experiments). (a and b: mean ± SEM, paired Student's *t*-test $^{**}p < 0.008$; unpaired Student's *t*-test $\#p < 0.05$, $\#\#p < 0.008$ compared with corresponding values in the absence of EGF.)

the asymmetric accumulation of adhesive structures. We investigated the migration of the spontaneously immortalised, untransformed keratinocyte cell line HaCaT that is often used as a cell model to study keratinocyte movements and to simulate wound healing [10,23]. Different signalling proteins, like chemoattractants, receptors or further signal transduction proteins, as well as lipids are involved in the migration process and partly show an asymmetric front-to-back distribution in the plasma membranes of these cells. Cholesterol makes up a large fraction of plasma membrane components [4] that greatly influence the physical properties of membranes; hence we were interested in its influence on keratinocyte migration. Many studies addressed the distribution of rafts, small cholesterol- and sphingomyelin-rich lipid domains, in migrating cells, although sometimes leading to inconsistent conclusions, probably due to different cell models, experimental approaches, and different kinds of lipid rafts with altering compositions [24]. Studies modifying the cellular cholesterol content indicate that the plasma membrane cholesterol plays an important role in cell migration. Cholesterol depletion decreases migration of different cell types [3,25–27]. Intriguingly, enrichment of cholesterol can also inhibit effective cell migration, as demonstrated for macrophages [28] and T cells [29]. It is argued that both methods destroy plasma membrane rafts, leading, amongst others, to a disturbed signalling of the small GTPases RhoA and Rac1 [25,28].

Up to now, there are only few studies addressing the plasma membrane properties of migrating keratinocytes. Thus, we investigated the plasma membrane lipid composition of polarised keratinocyte-like HaCaT cells. The plasma membrane at the lamellipodia on the cells fronts revealed a higher fluidity compared with the cells rears. The lateral asymmetry of plasma membrane viscosity was consistently detected using different fluorescence techniques on living HaCaT cells, including FRAP and fluorescence lifetime measurements of an environment-sensitive plasma membrane marker. These methods are independent of the fluorescence intensity, and are, thus, less prone to staining irregularities. The additional application of TIR illumination enabled a relative selective plasma membrane excitation [30]. Fluorescence lifetimes of NBD in a similar range to that reported here have been measured previously [14]. The diffusion coefficients of FAST DiO of about 1.0–1.5 $\mu m^2/s$ measured by our approach are also similar to previously published data measured for dialkylcarbocyanines in fish keratocytes [31].

Since it is known that cholesterol can influence the viscosity of biomembranes, we visualised cholesterol in fixed HaCaT cells with filipin. We related the filipin staining to the distribution of different plasma membrane markers, revealing a lower cholesterol content at the lamellipodia compared with the cells rears. We conclude that cholesterol contributes to the difference in plasma membrane viscosity of polarised HaCaT.

HaCaT cells required activation, for example with EGF, a known stimulator of keratinocyte migration, to stably form a microviscosity gradient. They developed the most pronounced viscosity gradients at an EGF concentration, which also elicited the strongest response in migration, as quantified by scratch wound healing assays. Moreover, at this EGF concentration, a gradient with lower

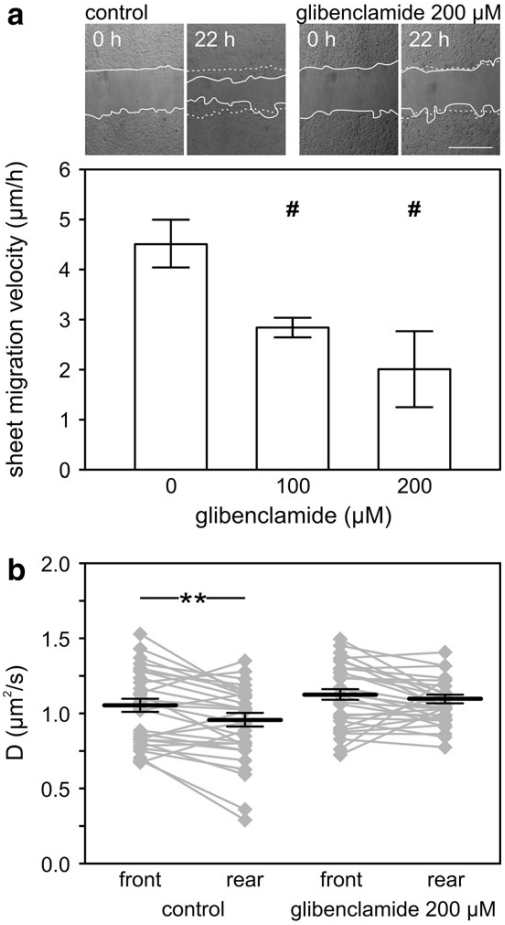

Fig. 4 – Pharmacological inhibition of ABCA1 reduces HaCaT cell migration and impedes on the microviscosity gradient. a: Quantification of HaCaT migration stimulated with 10 ng/ml EGF in the presence of different concentrations of glibenclamide determined by scratch assays ($n = 6$, scale bar: 250 µm). b: Diffusion coefficients of polarised HaCaT cells incubated with 10 ng/ml EGF or 200 µM glibenclamide and 10 ng/ml EGF extracted from TIR/FRAP experiments of FAST DiO-stained cells ($n > 30$). (a and b: mean ± SEM, paired Student's t-test $^{**}p < 0.008$; unpaired Student's t-test $\#p < 0.05$.)

viscosity at the leading edge was found in about 80% of the investigated cells, whereas in the absence of EGF and other serum-derived growth factors, we could not detect a viscosity gradient. The minority of EGF-treated cells that did not display a lower viscosity at the leading edge might represent cells that appeared polarised to the investigator but are probably non-migrating. Additionally, EGF enhanced the overall membrane viscosity of HaCaT cells, which is in agreement with a higher cholesterol content in EGF-treated cells that we confirmed by determining the cellular cholesterol content. The reason for this cholesterol increase is probably an EGF-induced gain in cholesterol synthesis reported previously [32]. Similarly, Ghosh et al. detected a growth factor-induced increase in plasma membrane microviscosity of endothelial cells [2,3]. However, by the same group (Vasanji et al.), it was shown that endothelial cells exhibit a higher viscosity at their cell fronts compared with their rears [3]. The authors also detected an enhanced cholesterol accumulation at the cells front visualised by labelling the cells with NBD-cholesterol.

This apparent discrepancy with our data may be caused by several factors. Firstly, Vasanji et al. used endothelial cells, measured by FRAP of the DiI-C16 with saturated alkyl substituents and fluorescence anisotropy of TMA-DPH. Our study addressed keratinocyte migration investigated mainly with FRAP using FAST DiO under TIR illumination. Using TIRF, the axial excitation depth is about 100–150 nm, leading to an excitation of the ventral plasma membrane that is adherent to the coverslip and parts of the adjacent cytosol. Since we analysed only the ventral plasma membrane, this fact or the use of different membrane dyes that possibly prefer different membrane regions may account for some discrepancies with other studies. Secondly, Vasanji et al. used NBD-labelled cholesterol to investigate the front-to-back cholesterol distribution. This analogue exhibits an up-side-down orientation in the membrane and, therefore, is not well suited to represent the endogenous cholesterol distribution [33]. Thirdly, cholesterol can change the viscosity of biomembranes in different manners, depending on other components of the membrane and there are hints that cholesterol might even reduce the viscosity of the plasma membrane of aortic endothelial cells [34]. Thus, an increase rather than a reduction of the microviscosity in the lamellipodia of endothelial cells compared to keratinocytes might also be attributed to a generally different composition and cholesterol content of the plasma membrane in these cells. Another possibility is that migrating cells rather require a distinct local viscosity or cholesterol content at certain parts of their plasma membrane, e.g. at the lamellipodium, than the formation of a viscosity gradient. Fourthly, the development and direction of plasma membrane microviscosity gradients might be cell type-specific. Indeed, other studies found no differences in the plasma membrane viscosity of migrating neutrophils [35], which is consistent with our results on migrating differentiated HL-60 cells, in which we could not detect plasma membrane viscosity gradients (data not shown). Weisswange et al. also found no differences in the diffusion coefficient of a dialkylcarbocyanine dye of migrating fish keratocytes between the leading and the trailing edges [31]. Moreover, these authors observed a diffusion barrier at the leading edge by labelling the cells at the top and examining the spreading of the dye to the bottom of the cells, indicating a faster diffusion at the trailing edge. Their data apparently contradict our results, but the different cellular systems might not be comparable. Moreover, the detected diffusion barrier might be caused by a dense, locally restricted protein arrangement, as discussed by these authors, and probably does not represent general plasma membrane viscosity at the leading edge.

Whereas some cell types, e.g. immune cells, move as single cells, processes associated with wound closure usually involve sheet migration [36]. We investigated polarised HaCaT keratinocytes in front of sheets and found a microviscosity gradient in their ventral cell membrane. In following HaCaT cells within the cell assembly, which did not adopt a pronounced polarised morphology, we detected a more uniform microviscosity. Other studies addressed for example single cell movement, and found no gradient or a viscosity gradient inverse to the observed membrane viscosity in HaCaT cells. Thus, the establishment of a viscosity gradient might also be a feature of the different forms of individual or collective cell movement.

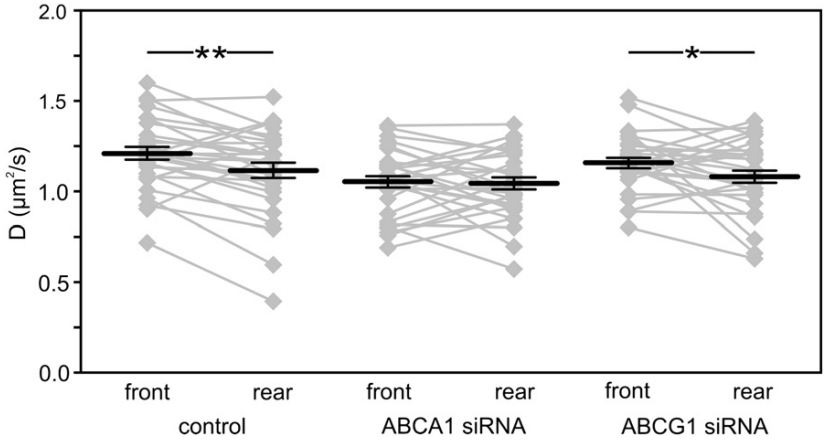

Fig. 5 – siRNA-mediated silencing of ABCA1 but not of ABCG1, results in a random distribution of microviscosity gradients in HaCaT cells. HaCaT cells were transfected with siRNA against ABCA1 (middle panel) or ABCG1 (right panel) and a nuclear-located RFP-coding plasmid or with the plasmid alone (control, left panel). Twenty-four hours after transfection and 12 h after addition of 10 ng/ml EGF, we determined the diffusion at the fronts and rears of HaCaT cells at the edge of large cell assemblies under TIR illumination ($n = 31$; mean ± SEM; paired Student's t-test $^{**}p < 0.008$, $^{*}p < 0.05$).

It is an open question how migrating cells establish and maintain a microviscosity gradient. One possibility is that specific proteins are responsible for the formation of the viscosity gradient by locally regulating the plasma membrane cholesterol content. Therefore, we focussed on a cholesterol transporter of the ABC family, ABCA1, whose main function is to facilitate the cholesterol export to ApoA-I. Previous studies indicating that ABCA1 can affect the physical properties of its membrane environment support the hypothesis that this transport protein is involved in the establishment of a plasma membrane viscosity gradient [6]. In addition to a decreased cell migration, pharmacological inhibition of ABCA1 also diminished differences between the viscosity at the fronts and rears of HaCaT cells in the presence of EGF. These data support an important role of cholesterol in the establishment of the microviscosity gradient in migrating keratinocytes. Inhibition of ABCG1, another ABC transporter that is known to be involved in cholesterol transport, with benzamil did not significantly alter the plasma membrane viscosity gradient and inhibited cell migration to a lesser extent than glibenclamide treatment (data not shown). We cannot completely exclude that the observed effects of the pharmacological inhibitors might involve other mechanisms as glibenclamide is known to inhibit several different ABC transporters. It is commonly used as antidiabetic drug, since it blocks ABCC8 at low concentrations, which is not expressed in HaCaT cells [11], however. At higher concentrations, glibenclamide also blocks ABCB1 (MDR1), ABCC9 (SUR2), ABCC7 (CFTR) in addition to ABCA1 [37–39]. Whereas ABCC9 and ABCC7 are transporters for small ions, ABCB1 is indeed also a cholesterol transporter, though its main function is the exclusion of a variety of amphiphatic substrates from cells [40]. However, inhibiting ABCB1 with verapamil, a known MDR inhibitor [22], did not diminish the observed microviscosity gradient in polarised HaCaT cells.

Furthermore, the specific involvement of ABCA1, but not ABCG1, in the gradient formation was confirmed by an siRNA approach. The mechanisms by which these ABC transporters mediate cholesterol efflux seem to be not identical. Whereas ABCA1 is thought to promote an accumulation of cholesterol outside of detergent-resistant membrane patches [41], ABCG1 probably operates preferentially within lipid rafts [42]. Our data are, thus, consistent with a redistribution of cholesterol from the raft to the non-raft phase by ABCA1.

Future investigations should decipher the molecular mechanisms by which the microviscosity gradient influences cell motility. One possible mechanism is an altered activity of small G proteins like Rac1 at the cell fronts and rears. Recently it was demonstrated that ABCA1 and ABCG1 activities influence the activation of Rac1 in macrophages [5,7]. Alternatively, an established microviscosity gradient might be important for the interaction of the cytoskeleton with the plasma membrane, and efficient actin polymerisation at the leading edge might require a defined microviscosity [3].

It is also conceivable that different cholesterol concentrations at the leading and trailing edges have a direct effect on keratinocyte migration, and that the observed effects on plasma membrane microviscosity are secondary. A direct influence of cholesterol on cell migration may be due to the interaction of cholesterol with certain proteins that are important for cell migration and that may require a defined cholesterol concentration to operate efficiently. For instance, cholesterol depletion is known to alter the organisation of the actin cytoskeleton [43]. The membrane-cytoskeleton adhesion was recently demonstrated to be strengthened upon cholesterol depletion [44]. Similarly, it is established that cholesterol depletion of plasma membranes promotes the spontaneous activity of EGF receptors and increases the HB-EGF release [45,46].

Conclusions

Thus, we demonstrated that migrating keratinocytes establish a cholesterol gradient leading to a lower microviscosity at the leading edge of these cells. This gradient can be diminished by siRNA-mediated silencing or pharmacologically inhibiting ABCA1, which also dramatically reduces the ability of keratinocytes to migrate.

We conclude that the establishment and maintenance of a lateral cholesterol asymmetry is important for wound healing and is at least partly mediated by the activity of ABCA1 in keratinocytes.

Conflicts of interest

The authors indicate no potential conflicts of interest.

Acknowledgments

This work was supported by the Deutsche Forschungsgemeinschaft (FOR 806, to M.S.), and a formel.1 grant of the Medical Faculty of the University of Leipzig (to A.T.). We thank Marion Leonhardt and Helga Sobottka for technical support and Christian Hellwig and Tanja Plötz for critically reading the manuscript.

Appendix A. Supplementary data

Supplementary data to this article can be found online at doi:10.1016/j.yexcr.2012.02.007.

REFERENCES

[1] L. Stephens, L. Milne, P. Hawkins, Moving towards a better understanding of chemotaxis, Curr. Biol. 18 (2008) R485–R494.
[2] P.K. Ghosh, A. Vasanji, G. Murugesan, S.J. Eppell, L.M. Graham, P.L. Fox, Membrane microviscosity regulates endothelial cell motility, Nat. Cell Biol. 4 (2002) 894–900.
[3] A. Vasanji, P.K. Ghosh, L.M. Graham, S.J. Eppell, P.L. Fox, Polarization of plasma membrane microviscosity during endothelial cell migration, Dev. Cell 6 (2004) 29–41.
[4] P.L. Yeagle, Cholesterol and the cell membrane, Biochim. Biophys. Acta 822 (1985) 267–287.
[5] T.A. Pagler, M. Wang, M. Mondal, A.J. Murphy, M. Westerterp, K.J. Moore, F.R. Maxfield, A.R. Tall, Deletion of ABCA1 and ABCG1 impairs macrophage migration because of increased Rac1 signaling, Circ. Res. 108 (2011) 194–200.
[6] A. Zarubica, A.P. Plazzo, M. Stöckl, T. Trombik, Y. Hamon, P. Müller, T. Pomorski, A. Herrmann, G. Chimini, Functional implications of the influence of ABCA1 on lipid microenvironment at the plasma membrane: a biophysical study, FASEB J. 23 (2009) 1775–1785.
[7] M.P. Adorni, E. Favari, N. Ronda, A. Granata, S. Bellosta, L. Arnaboldi, A. Corsini, R. Gatti, F. Bernini, Free cholesterol alters macrophage morphology and mobility by an ABCA1 dependent mechanism, Atherosclerosis 215 (2011) 70–76.
[8] R. Gillitzer, M. Goebeler, Chemokines in cutaneous wound healing, J. Leukoc. Biol. 69 (2001) 513–521.
[9] M.M. Santoro, G. Gaudino, Cellular and molecular facets of keratinocyte reepithelization during wound healing, Exp. Cell Res. 304 (2005) 274–286.
[10] L. Koivisto, G. Jiang, L. Häkkinen, B. Chan, H. Larjava, HaCaT keratinocyte migration is dependent on epidermal growth factor receptor signaling and glycogen synthase kinase-3α, Exp. Cell Res. 312 (2006) 2791–2805.
[11] D. Kielar, W.E. Kaminski, G. Liebisch, A. Piehler, J.J. Wenzel, C. Möhle, S. Heimerl, T. Langmann, S.O. Friedrich, A. Böttcher, S. Barlage, W. Drobnik, G. Schmitz, Adenosine triphosphate binding cassette (ABC) transporters are expressed and regulated during terminal keratinocyte differentiation: a potential role for ABCA7 in epidermal lipid reorganization, J. Invest. Dermatol. 121 (2003) 465–474.
[12] A. Tannert, P. Voigt, S. Burgold, S. Tannert, M. Schaefer, Signal amplification between Gβγ release and PI3Kγ-mediated PI(3,4,5)P3 formation monitored by a fluorescent Gβγ biosensor protein and repetitive two component total internal reflection/fluorescence redistribution after photobleaching analysis, Biochemistry 47 (2008) 11239–11250.
[13] A. Tannert, S. Tannert, S. Burgold, M. Schaefer, Convolution-based one and two component FRAP analysis: theory and application, Eur. Biophys. J. 38 (2009) 649–661.
[14] M. Stöckl, A.P. Plazzo, T. Korte, A. Herrmann, Detection of lipid domains in model and cell membranes by fluorescence lifetime imaging microscopy of fluorescent lipid analogues, J. Biol. Chem. 283 (2008) 30828–30837.
[15] S. Mukherjee, X. Zha, I. Tabas, F.R. Maxfield, Cholesterol distribution in living cells: fluorescence imaging using dehydroergosterol as a fluorescent cholesterol analog, Biophys. J. 75 (1998) 1915–1925.
[16] M.D. Abràmoff, P.J. Magalhães, S.J. Ram, Image processing with ImageJ, Biophotonics Int. 11 (2004) 36–42.
[17] M. Carretero, M.J. Escámez, M. García, B. Duarte, A. Holguín, L. Retamosa, J.L. Jorcano, M.D. Río, F. Larcher, In vitro and in vivo wound healing-promoting activities of human cathelicidin LL-37, J. Invest. Dermatol. 128 (2008) 223–236.
[18] N. Stuurman, N. Amdodaj, R.D. Vale, μManager: open source software for light microscope imaging, Microsc. Today 15 (2007) 42–43.
[19] S. Dewitt, R.L. Darley, M.B. Hallett, Translocation or just location? Pseudopodia affect fluorescent signals, J. Cell Biol. 184 (2009) 197–203.
[20] K. Takahashi, Y. Kimura, N. Kioka, M. Matsuo, K. Ueda, Purification and ATPase activity of human ABCA1, J. Biol. Chem. 281 (2006) 10760–10768.
[21] L. Seres, J. Cserepes, N.B. Elkind, D. Törocsik, L. Nagy, B. Sarkadi, L. Homolya, Functional ABCG1 expression induces apoptosis in macrophages and other cell types, Biochim. Biophys. Acta 1778 (2008) 2378–2387.
[22] W.D. Stein, Kinetics of the multidrug transporter (P-glycoprotein) and its reversal, Physiol. Rev. 77 (1997) 545–590.
[23] X. Yang, J. Wang, S.L. Guo, K.J. Fan, J. Li, Y.L. Wang, Y. Teng, X. Yang, miR-21 promotes keratinocyte migration and re-epithelialization during wound healing, Int. J. Biol. Sci. 7 (2011) 685–690.
[24] S. Mañes, R.A. Lacalle, C. Gómez-Moutón, C. Martínez-A, From rafts to crafts: membrane asymmetry in moving cells, Trends Immunol. 24 (2003) 320–326.
[25] L.M. Pierini, R.J. Eddy, M. Fuortes, S. Seveau, C. Casulo, F.R. Maxfield, Membrane lipid organization is critical for human neutrophil polarization, J. Biol. Chem. 278 (2003) 10831–10841.
[26] S. Mañes, E. Mira, C. Gómez-Moutón, R.A. Lacalle, P. Keller, J.P. Labrador, C. Martínez-A, Membrane raft microdomains mediate front–rear polarity in migrating cells, EMBO J. 18 (1999) 6211–6220.
[27] C. Gómez-Móuton, J.L. Abad, E. Mira, R.A. Lacalle, E. Gallardo, S. Jiménez-Baranda, I. Illa, A. Bernad, S. Mañes, C. Martínez-A, Segregation of leading-edge and uropod components into specific lipid rafts during T cell polarization, Proc. Natl. Acad. Sci. U. S. A. 98 (2001) 9642–9647.
[28] T. Nagao, C. Qin, I. Grosheva, F.R. Maxfield, L.M. Pierini, Elevated cholesterol levels in the plasma membranes of macrophages inhibit migration by disrupting RhoA regulation, Arterioscler. Thromb. Vasc. Biol. 27 (2007) 1596–1602.
[29] D.H. Nguyen, J.C. Espinoza, D.D. Taub, Cellular cholesterol enrichment impairs T cell activation and chemotaxis, Mech. Ageing Dev. 125 (2004) 641–650.
[30] D. Axelrod, Selective imaging of surface fluorescence with very high aperture microscope objectives, J. Biomed. Opt. 6 (2001) 6–13.
[31] I. Weisswange, T. Bretschneider, K.I. Anderson, The leading edge is a lipid diffusion barrier, J. Cell Sci. 118 (2005) 4375–4380.

[32] I.R. Harris, H. Höppner, W. Siefken, A.M. Farrell, K.P. Wittern, Regulation of HMG-CoA synthase and HMG-CoA reductase by insulin and epidermal growth factor in HaCaT keratinocytes, J. Invest. Dermatol. 114 (2000) 83–87.
[33] H.A. Scheidt, P. Müller, A. Herrmann, D. Huster, The potential of fluorescent and spin-labeled steroid analogs to mimic natural cholesterol, J. Biol. Chem. 278 (2003) 45563–45569.
[34] F.J. Byfield, H. Aranda-Espinoza, V.G. Romanenko, G.H. Rothblat, I. Levitan, Cholesterol depletion increases membrane stiffness of aortic endothelial cells, Biophys. J. 87 (2004) 3336–3343.
[35] R.G. Sitrin, T.M. Sassanella, J.J. Landers, H.R. Petty, Migrating human neutrophils exhibit dynamic spatiotemporal variation in membrane lipid organization, Am. J. Respir. Cell Mol. Biol. 43 (2010) 498–506.
[36] P. Rørth, Collective cell migration, Annu. Rev. Cell Dev. Biol. 25 (2009) 407–429.
[37] P.E. Golstein, A. Boom, J. van Geffel, P. Jacobs, B. Masereel, R. Beauwens, P-glycoprotein inhibition by glibenclamide and related compounds, Pflugers Arch. 437 (1999) 652–660.
[38] M. Meyer, F. Chudziak, C. Schwanstecher, M. Schwanstecher, U. Panten, Structural requirements of sulphonylureas and analogues for interaction with sulphonylurea receptor subtypes, Br. J. Pharmacol. 128 (1999) 27–34.
[39] D.N. Sheppard, M.J. Welsh, Effect of ATP-sensitive K^+ channel regulators on cystic fibrosis transmembrane conductance regulator chloride currents, J. Gen. Physiol. 100 (1992) 573–591.
[40] A. Garrigues, A.E. Escargueil, S. Orlowski, The multidrug transporter, P-glycoprotein, actively mediates cholesterol redistribution in the cell membrane, Proc. Natl. Acad. Sci. U. S. A. 99 (2002) 10347–10352.
[41] Y.D. Landry, M. Denis, S. Nandi, S. Bell, A.M. Vaughan, X. Zha, ATP-binding cassette transporter A1 expression disrupts raft membrane microdomains through its ATPase-related functions, J. Biol. Chem. 281 (2006) 36091–36101.
[42] K. Nagao, Y. Kimura, M. Mastuo, K. Ueda, Lipid outward translocation by ABC proteins, FEBS Lett. 584 (2010) 2717–2723.
[43] J. Kwik, S. Boyle, D. Fooksman, L. Margolis, M.P. Sheetz, M. Edidin, Membrane cholesterol, lateral mobility, and the phosphatidylinositol 4,5-bisphosphate-dependent organization of cell actin, Proc. Natl. Acad. Sci. U. S. A. 100 (2003) 13964–13969.
[44] M. Sun, N. Northup, F. Marga, T. Huber, F.J. Byfield, I. Levitan, G. Forgacs, The effect of cellular cholesterol on membrane-cytoskeleton adhesion, J. Cell Sci. 120 (2007) 2223–2231.
[45] X. Chen, M.D. Resh, Cholesterol depletion from the plasma membrane triggers ligand-independent activation of the epidermal growth factor receptor, J. Biol. Chem. 277 (2002) 49631–49637.
[46] S. Giltaire, S. Lambert, Y. Poumay, HB-EGF synthesis and release induced by cholesterol depletion of human epidermal keratinocytes is controlled by extracellular ATP and involves both p38 and ERK1/2 signaling pathways, J. Cell. Physiol. 226 (2011) 1651–1659.

Cell Calcium 55 (2014) 59–68

Contents lists available at ScienceDirect

Cell Calcium

journal homepage: www.elsevier.com/locate/ceca

Cholesterol sensitises the transient receptor potential channel TRPV3 to lower temperatures and activator concentrations

Anke S. Klein, Astrid Tannert[1], Michael Schaefer*

Rudolf-Boehm-Institut für Pharmakologie und Toxikologie, Universität Leipzig, Leipzig, Germany

ARTICLE INFO

Article history:
Received 10 September 2013
Received in revised form 4 December 2013
Accepted 7 December 2013
Available online 17 December 2013

Keywords:
Intracellular calcium homeostasis
Vanilloid receptors
Non-selective cation channel
Keratinocyte differentiation
Heat-activated ionic currents
Thymol
Camphor
Carvacrol

ABSTRACT

TRPV3, a thermosensitive cation channel, is predominantly expressed in keratinocytes. It contributes to physiological processes such as thermosensation, nociception, and skin development. TRPV3 is polymodally regulated by chemical agonists, innocuous heat, intracellular acidification or by membrane depolarization. By manipulating the content of plasma membrane cholesterol, a key modulator of the physicochemical properties of biological membranes, we here addressed the question, how the lipid environment influences TRPV3. Cholesterol supplementation robustly potentiated TRPV3 channel activity by sensitising it to lower concentrations of chemical activators. In addition, the thermal activation of TRPV3 is significantly shifted to lower temperatures in cholesterol-enriched cells. The sensitising effect of cholesterol was not caused by an increased plasma membrane targeting of the channel. In HaCaT keratinocytes, which natively express TRPV3, a cholesterol-mediated sensitisation of TRPV3-like responses was reproduced. The cholesterol-dependent modulation of TRPV3 activity may provide a molecular mechanism to interpret its involvement in keratinocyte differentiation.

1. Introduction

The epidermis, as the interface between an individual and its environment, has to perform different essential functions. It protects an organism against harmful external influences, pathogens, and dehydration. Keratinocytes are the major cell type of the epidermis and bear responsible for the formation of an outer barrier, the stratum corneum. To generate this barrier, keratinocytes undergo a complex differentiation programme that terminates in apoptosis and cornification [1]. Differentiation is accompanied by synthesis of several structural proteins and lipids, like ceramides, fatty acids and cholesterol. To prevent skin barrier dysfunction, the proliferation and differentiation of keratinocytes needs to be tightly regulated. Multiple factors are known to influence the balance between keratinocyte proliferation and differentiation, including growth factors, extracellular calcium concentrations, cell density, or lipids like ceramides, cholesterol and cholesterol-derived metabolites.

Another function of keratinocytes, together with neurons that extend into the epidermis, is to recognise environmental factors, some of which are decoded by members of the transient receptor potential (TRP) family of cation channels. For instance, TRPV3, a member of the vanilloid subfamily, is predominantly expressed in keratinocytes of all epidermal layers [2,3]. Its activity is polymodally regulated by chemical and physical queues. TRPV3 can be activated by numerous, poorly selective compounds like 2-aminoethoxydiphenyl borate (2-APB) [4], and by secondary plant metabolites, such as camphor [5], carvacrol, eugenol and thymol [6]. TRPV3 is activated by temperatures above 33 °C [2,3,7]. The initial characterisation of TRPV3-deficient mice indicated that TRPV3 participates in heat perception [5], but more recent data demonstrate that this effect strongly depends on the genetic background of the investigated animals [8]. In addition, cytosolic acidification [9], membrane potential [3], and various lipid factors [10–13] are known to influence TRPV3 activity. Apart from thermosensation, TRPV3 is discussed to be involved in physiological and pathophysiological processes, including nociception [14,15], hair growth [16], inflammation [10], and skin diseases [17–19]. Recent findings demonstrated that the epidermal barrier in TRPV3$^{-/-}$ mice is defective [16], pointing to a role of TRPV3 in regulating keratinocyte differentiation and cornification. Since former studies have demonstrated that cholesterol also plays an important role in keratinocyte physiology we wondered about the influence of cholesterol on TRPV3 signalling.

* Corresponding author at: Rudolf-Boehm-Institut für Pharmakologie und Toxikologie, Universität Leipzig, Härtelstr. 16-18, 04107 Leipzig, Germany.
Tel.: +49 341 9724600; fax: +49 341 9724609.
E-mail address: michael.schaefer@medizin.uni-leipzig.de (M. Schaefer).
[1] Current affiliation: Leibniz Institute for Zoo and Wildlife Research (IZW), Berlin, Germany.

0143-4160/$ – see front matter © 2013 Elsevier Ltd. All rights reserved.
http://dx.doi.org/10.1016/j.ceca.2013.12.001

In the present study, we introduce cholesterol as a new regulator of TRPV3 channel activity. We modified the cholesterol content of HEK293 cells stably expressing mouse TRPV3 and performed calcium and whole-cell patch clamp analyses. These experiments revealed that cholesterol enrichment robustly potentiates TRPV3 by shifting its sensitivity to lower activator concentrations and by sensitising TRPV3 to lower temperatures. The influence of cholesterol on TRPV3 activity was not restricted to the recombinant expression model, but also observed in HaCaT keratinocytes, which endogenously express TRPV3 [20,21], and are widely used to study keratinocyte physiology [22].

2. Methods

2.1. Cell culture and transfections

HEK293 cells were maintained in Earle's minimum essential medium (MEM), supplemented with 10% foetal calf serum (FCS, v/v), 2 mM L-glutamine, 100 units/ml penicillin, and 100 μg/ml streptomycin (all PAA Laboratories, Pasching, Austria). To obtain a HEK293 cell line stably expressing mouse TRPV3 (HEK_{mTRPV3}), cells were transfected with a pcDNA3.1 plasmid encoding a C-terminally CFP-tagged mTRPV3. All transfections were performed with a Fugene HD lipofection reagent (Promega, Madison, USA), according to the manufacturer's instructions. Individual clones were picked under optical control in an epifluorescence microscope, reseeded in serial dilutions, and grown in culture medium supplemented with 1 mg/ml G418. After clonal selection and initial expansion, the established HEK_{mTRPV3} cell line was grown in medium containing 0.4 mg/ml G418.

The spontaneously immortalised, untransformed human keratinocyte cell line HaCaT (human adult low calcium high temperature) was cultured in Dulbecco's modified Eagle's medium (DMEM) with 1 g/l glucose, supplemented with 10% FCS, 2 mM L-glutamine, 100 units/ml penicillin, and 100 μg/ml streptomycin. After reaching a density of about 70%, HaCaT cells were washed and incubated for 10 min in PBS supplemented with 0.8 mM EDTA at 37 °C, harvested by mild trypsinisation, and reseeded. All cells were grown at 37 °C in a humidified atmosphere with 5% CO_2.

2.2. Cholesterol modification

Modification of the cellular cholesterol content was achieved using methyl-β-cyclodextrin (MβCD). MβCD is known to extract cholesterol from living cells or, when preloaded with cholesterol, to enrich cells with cholesterol [23]. To generate MβCD–cholesterol complexes, cholesterol (Sigma–Aldrich) was dissolved in ethanol (20 mg/ml), heated and added to a MβCD-containing solution (200 mM in PBS, Sigma–Aldrich). We used saturated mixtures with a molar ratio of MβCD:cholesterol of 10:1 [23]. Unless otherwise stated, cholesterol depletion or enrichment was performed by incubating the cells for 15 min at 37 °C in HEPES-buffered solution (HBS) containing 134 mM NaCl, 6 mM KCl, 1 mM $MgCl_2$, 1 mM $CaCl_2$, 5.5 mM glucose and 10 mM HEPES (pH 7.4, adjusted with NaOH), and supplemented with 10 mM MβCD or 2.5 mM MβCD–cholesterol, respectively. These conditions have only minor effects on cellular viability [24]. As a control, we incubated cells in HBS without MβCD supplement at 37 °C.

2.3. Calcium measurement

All calcium measurements were performed at room temperature in HBS. Cells were loaded for 30 min at 37 °C with 3 μM of either fura-2/AM of fluo-4/AM (Invitrogen) in HBS supplemented with 0.2% (w/v) bovine serum albumin. Subsequently, cellular cholesterol content was modulated. After washing the cells with HBS without MβCD or MβCD–cholesterol, calcium measurements were performed.

Concentration response curves were monitored in fluo-4-loaded cell suspensions. To this end, cell suspensions were dispensed into 384-well plates and mounted on the stage of a custom-made fluorescence imaging plate reader [25] built within a robotic liquid handling station (Freedom Evo 150, Tecan, Switzerland). Modulators or agonists were applied with the 96-tip multichannel arm. The image acquisition was controlled by the MicroManager software (Version 1.3; US National Institutes of Health, Bethesda, MD) [26], and image evaluation was performed with ImageJ (US National Institutes of Health) [27]. Mean fluorescence intensities of individual wells were determined, corrected for background signals, and normalised to initial intensities (F/F_0). Intensity values at the end of the measurement (2.5 min after agonist application) were extracted, and concentration-dependent effects were parameterised by fitting the data obtained with various activator concentrations to a four parameter Hill equation:

$$E = \frac{E_{min} + (E_{max} - E_{min})}{1 + ([A]/EC_{50})^{-nH}},$$

where E represents the observed effect, $[A]$ is the concentration of activator, EC_{50} the activator concentration yielding a half-maximal effect, and nH the Hill coefficient.

For single cell calcium measurements, cells were grown on glass coverslips, loaded with the ratiometric calcium indicator fura-2/AM, and imaged with an inverted microscope (Fluar 10×/0.5; Axiovert 100 microscope, Carl Zeiss, Jena, Germany). For excitation we used a fibre-coupled monochromator device (Polychrome V, Till-Photonics, Gräfelfing, Germany) at alternating wavelengths of 340, 358, and 380 nm. Emission was imaged with a cooled CCD camera (Sensicam, PCO, Kelheim, Germany) through a dichroic beam splitter (DCXR-510, Chroma, Rockingham, VT) and a 515 nm long-pass filter (OG515, Schott, Jena, Germany). Fluorescence intensities were averaged over regions of individual cells. Background signals were subtracted, and intracellular calcium concentrations where calculated with a spectral fingerprinting method as described [28].

2.4. Confocal laser scanning microscopy

Cells were imaged using an inverted confocal laser scanning microscope (LSM510-META, Carl Zeiss AG, Oberkochen, Germany), with a C-Apochromat 40×/1.2 water immersion objective. CFP-tagged TRP channels were excited with the 458-nm line of an Ar^+ laser, and emission was detected through a 500/50 nm band-pass filter.

2.5. Electrophysiological procedures

For the electrophysiological characterisation of TRPV3, HEK293 cells were seeded on poly-L-lysin-coated (0.02%, Sigma–Aldrich) glass coverslips, and cultured for 24 h. Unless otherwise indicated, whole-cell recordings were made at room temperature, using an EPC9 amplifier controlled by the PULSE software (HEKA, Lambrecht, Germany). The standard extracellular solution contained 140 mM NaCl, 5 mM KCl, 1 mM $MgCl_2$, 10 mM glucose, 10 mM HEPES and 1 mM $CaCl_2$ (adjusted to pH 7.4 with NaOH, and to 305 mosmol/l with mannitol). The pipette solution included 110 mM CsCl, 4 mM $MgCl_2$, 10 mM EGTA and 10 mM HEPES (pH 7.2 with CsOH). For whole-cell recordings, patch pipettes had a resistance of 3–5 MΩ. Serial resistances were always less then 10 MΩ and compensated by 80%. Liquid junction potentials added up to +4.1 mV and were not compensated in the illustrated figures.

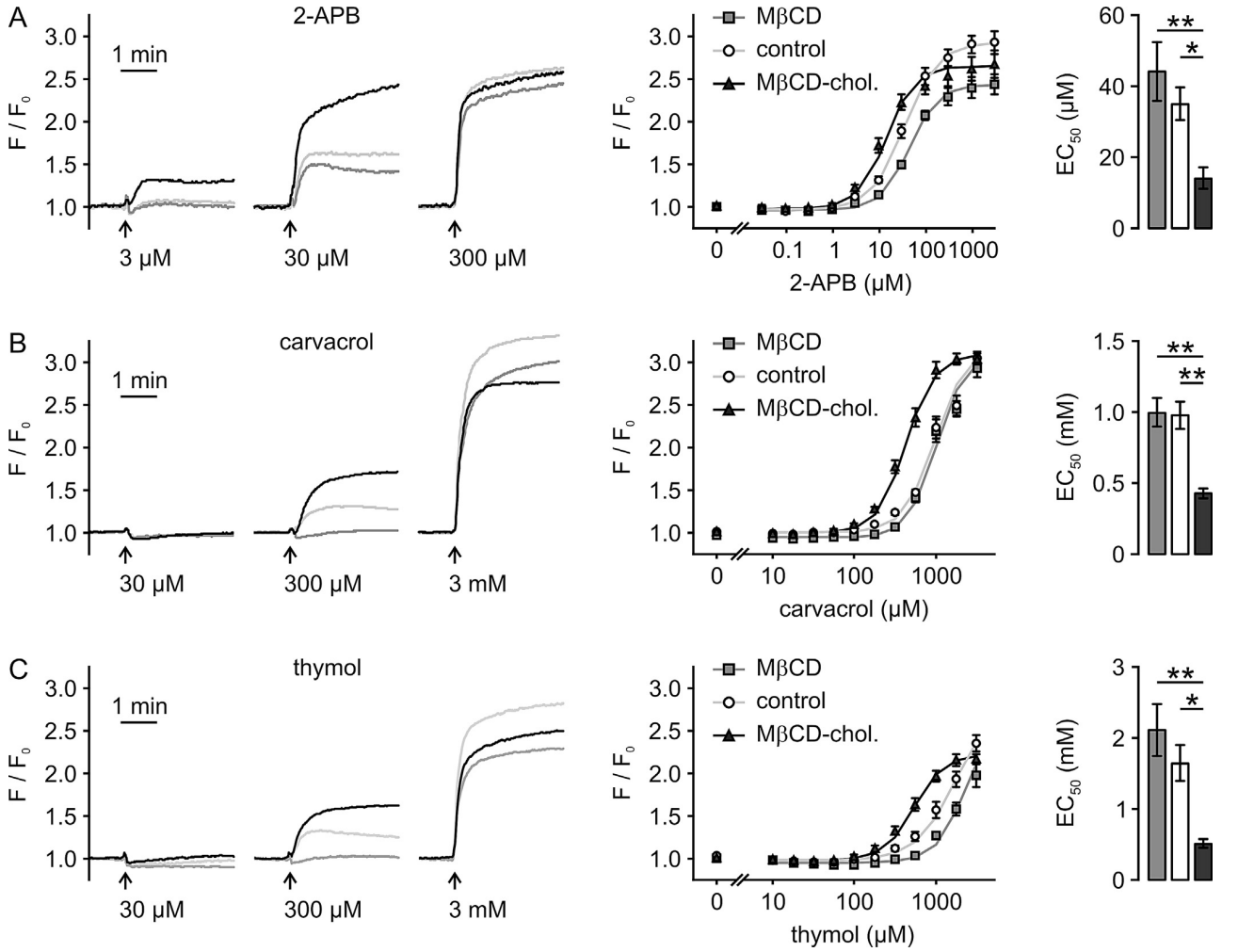

Fig. 1. Cholesterol enrichment sensitises mTRPV3 to lower agonist concentrations. HEK_{mTRPV3} cells were loaded with the Ca^{2+} indicator dye fluo-4, and cellular cholesterol was depleted or enriched via incubation in MβCD (10 mM) or MβCD–cholesterol (10:1; 2.5 mM) for 15 min at 37 °C, respectively. After washing with HBS, fluo-4 fluorescence was recorded during stimulation with the TRPV3 activators 2-APB (A, $n = 7$), carvacrol (B, $n = 6$), and thymol (C, $n = 6$) applied at the indicated concentrations. Fluorescence intensities were background-corrected and normalised to the initial fluorescence intensity F_0 (left panels). Concentration-dependent increases in F/F_0 were fitted to a four parameter Hill equation (middle panels) and calculated EC_{50} values are depicted (right panels; $^*p < 0.05$, $^{**}p < 0.01$, one way ANOVA).

Slow voltage ramps (0.12 mV/ms) ranging from −60 to +60 mV were applied every 2 s, filtered at 0.3 kHz and sampled with 1 kHz. Chemical activators were applied with a gravity-driven perfusion system. Recorded current intensities at −60 and +60 mV were normalised to the cell size using the corresponding capacity. To investigate the heat activation of TRPV3, we used an inline solution heater (TC-324B, Warner Instruments). The temperature of the bath solution ranged between 20 °C and 40 °C, and was recorded with a thermistor electrode placed in the vicinity of the patched cell. Since currents (at $V_h = 60$ mV) in untransfected control cells rose by less than 3.5-fold during the exposure to buffer solutions heated from 20 °C to 40 °C, whereas TRPV3-expressing cells exhibited larger increases, we defined the factor of 3.5 as the lower level of detection (LLD) of current contributions arising from thermal activation of TRPV3. The corresponding temperature at which currents exceeded the LLD was termed T_{LLD}. Temperature coefficients (Q_{10}) were calculated for the temperature ranges of 21–27 °C, 28–32 °C and 33–39 °C, according to:

$$Q_{10} = \left(\frac{I_2}{I_1}\right)^{10/\Delta T},$$

where I_1 and I_2 were obtained from Arrhenius plots for a given temperature increment ΔT by linear regression analysis.

2.6. Statistical analysis

Results are depicted as means ± S.E.M. To test for statistically significant differences, we used the Student's *t*-test for two normally distributed data groups or the ANOVA test combined with Tukey's test for more then two data groups.

3. Results

3.1. Cholesterol enrichment sensitises mTRPV3 to lower agonist concentrations

TRPV3 channels are differently regulated by physical and chemical stimuli, hence the question arose, if TRPV3 activity is dependent on the content of cellular cholesterol. To address this question, we modulated the cholesterol content of fluo-4-loaded HEK_{mTRPV3} cells, and performed calcium measurements in a plate imaging-based approach. We generated concentration response curves with

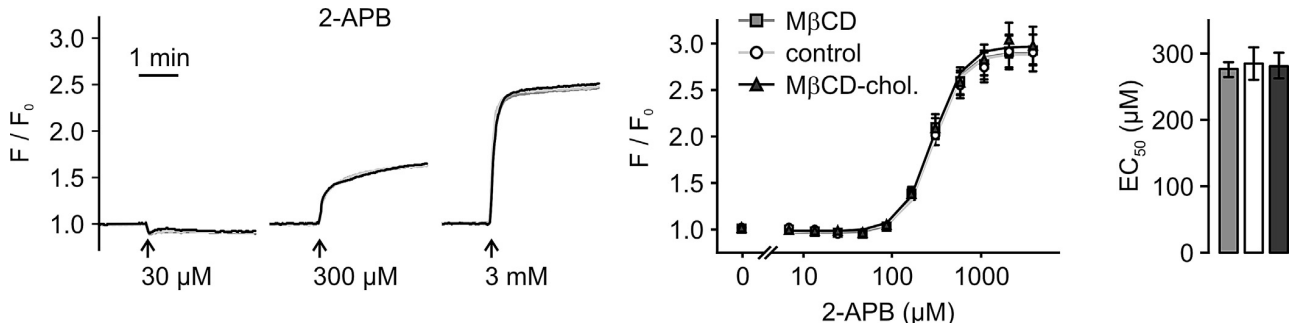

Fig. 2. TRPV2 signalling is not affected by modification of cellular cholesterol. Measurements were performed as described in Fig. 1, but with HEK293 expressing TRPV2. Cells were activated with 2-APB at different concentrations to generate concentration–response curves. Depicted are single traces of representative normalised fluorescence time courses (left panel), aggregated data of several experiments performed with various activator concentrations (middle panel, $n = 6$), and the calculated EC_{50} values (right panel).

the known TRPV3 activators 2-APB, carvacrol and thymol (Fig. 1). Without manipulating the cholesterol content, the respective EC_{50} values were in agreement with established literature data [29]. Interestingly, the EC_{50} of the cholesterol-treated samples significantly shifted to lower agonist concentrations compared to cholesterol-depleted or unmodified HEK_{mTRPV3} cells. The sensitisation was observed with all tested TRPV3 activators. Compared with untreated control cells, the EC_{50} of 2-APB and thymol to activate TRPV3 appeared higher in cholesterol-extracted cells, but the differences were not statistically significant. The E_{max} and Hill slopes *nH* were not significantly altered between the different approaches (not shown). On the basis of these results, we conclude that cholesterol enrichment enhances the sensitivity of HEK_{mTRPV3} towards all used TRPV3 activators.

To test if the potentiating effect of cholesterol is a more general feature of temperature-activated TRP channels, we analysed the influence of cholesterol on rat TRPV2, a closely related and 2-APB-sensitive member of the TRPV subfamily. In contrast to the findings with TRPV3, TRPV2 responses to 2-APB were not discernibly affected by cholesterol modification (Fig. 2).

3.2. Electrophysiological properties of cholesterol-enhanced mTRPV3 currents

In order to confirm and to quantify the impact of cholesterol supplementation on TRPV3-mediated cation currents, we performed whole-cell patch clamp experiments with HEK_{mTRPV3} cells. After variation of cellular cholesterol content, we patched the cells and activated them by adding 30 µM 2-APB to the bath solution. HEK_{mTRPV3} cells responded with typical outwardly rectifying currents that increased during repetitive activation (Fig. 3) [4]. HEK_{mTRPV3} cells that were incubated in MβCD–cholesterol showed about 6.3-fold and 5.2-fold higher current densities in response to the initial 2-APB stimulation compared to buffer-treated control cells at −60 mV and +60 mV, respectively. The current facilitation in cholesterol-supplemented HEK_{mTRPV3} cells during the first and following pulses of 2-APB stimulation was highly significant ($p < 0.01$, ANOVA test). Accordingly, the typical current run-up during repetitive activation [30] with a non-saturating concentration (30 µM) of 2-APB was not observed in cholesterol-supplemented cells. In the absence of 2-APB, basal current densities in cholesterol-supplemented cells were slightly smaller compared to untreated cells (Fig. 3C). The capacity that correlates with cell size and plasma membrane thickness (C_{slow}) was significantly decreased by about 20% upon cholesterol enrichment (14.1 ± 0.7 pF in control cells, 11.4 ± 0.8 pF in cholesterol-enriched cells, Student's *t*-test $p < 0.05$). HEK_{mTRPV3} cells that were cholesterol-depleted by preincubation in MβCD displayed a trend towards smaller 2-APB-induced currents, but differences did not reach statistical significance when compared to the current densities in buffer-treated control cells.

3.3. Temperature-dependent activation of TRPV3 is sensitised by cholesterol enrichment

To test if thermal activation of TRPV3 is influenced by cholesterol, we investigated heat-induced currents in HEK_{mTRPV3} cells by electrophysiological patch clamp experiments in the whole-cell mode. As expected [30], repeated application of temperature ramps (from 20 °C to 38–40 °C) resulted in a time-dependent augmentation of outwardly rectifying currents in control HEK_{mTRPV3} cells. Upon cholesterol supplementation, mean current densities were significantly increased (two way ANOVA, $p < 0.01$, Fig. 4A–C). During the sixth application of buffer heated to 37 °C, an about 11-fold and 20-fold augmentation compared to untreated control HEK_{mTRPV3} cells was observed at −60 mV and +60 mV, respectively.

Since heat-induced gating of thermosensory TRP channels does not exhibit a sharp threshold temperature at which channel opening begins, shifts of the temperature sensitivity of mTRPV3 were assessed by measuring the temperature T_{LLD} when currents densities rose in TRPV3-expressing cells increased by more than 3.5-fold – a factor that was not reached in untransfected control cells (Fig. 4D). At the first two temperature-induced activation cycles, only 44% of investigated, buffer-treated HEK_{mTRPV3} cells showed TRPV3-like currents that met this criterion, and the T_{LLD} of responsive cells was 35.8 ± 1.0 °C. During the sixth activation cycle, significant heat-induced currents were observed in about 78% of tested cells, and the T_{LLD} was 36.6 ± 1.1 °C. In experiments with cholesterol-enriched HEK_{mTRPV3} cells, 72% of investigated cells showed TRPV3-like currents, and the T_{LLD} of responsive cells was 34.0 ± 1.1 °C during the first two activation cycles. During the third to sixth temperature cycles, all cells displayed large TRPV3 currents, and T_{LLD} was already achieved at 31.1 ± 0.6 °C (see Fig. 4D).

Comparisons between buffer-treated and cholesterol-enriched cells become more sensitive by analysing aggregated data of all patched cells ($n = 9$ cells each). In Arrhenius plots (Fig. 5A and B), significance of temperature sensitisation by cholesterol feeding was reached at temperatures above 33 °C during the third temperature ramp and further shifted to lower temperatures (above 27 °C) during the sixth temperature ramp. We therefore defined temperature ranges of 21–27 °C, 28–32 °C, and 33–39 °C for calculating Q_{10} values of temperature-activated TRPV3 currents. During the third temperature ramp, buffer-treated HEK_{mTRPV3} cells did not show discernible increases in Q_{10} values at temperatures up to 40 °C (Fig. 5C). By contrast, cholesterol-treated HEK_{mTRPV3} displayed steeper slopes (see Fig. 5A) and higher Q_{10} values at temperatures above 28 °C (Fig. 5C). During the sixth temperature ramp,

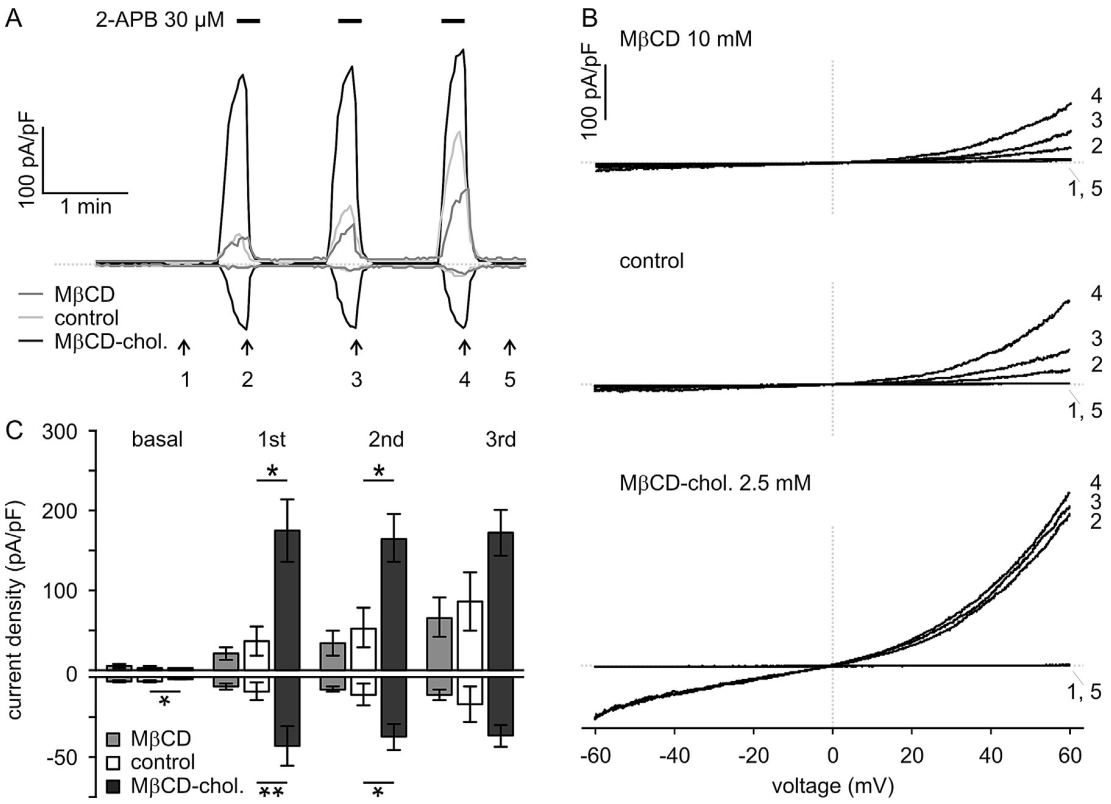

Fig. 3. Whole-cell patch-clamp recordings of TRPV3 currents in cholesterol-modified HEK_{mTRPV3} cells. Adherent HEK_{mTRPV3} cells were incubated in HBS (control) or in HBS supplemented either with 10 mM MβCD, or with 2.5 mM cholesterol-preloaded MβCD (MβCD–chol.) for 15 min at 37 °C. Subsequently, whole-cell currents were recorded during repetitive stimulation with 30 µM 2-APB. Data were extracted from repeatedly (every 2 s) applied voltage ramps (−60 to 60 mV; 0.12 mV/ms). (A) Representative traces of recorded current densities at −60 and +60 mV. (B) Current densities during voltage ramps obtained at the time points indicated in (A). (C) Aggregated data of all cells measured as shown in (A) ($n = 7$ each, $^{*}p < 0.05$, $^{**}p < 0.01$).

buffer-treated HEK_{mTRPV3} cells displayed a minor increase in the Q_{10} value at temperatures above 32 °C, whereas cholesterol-supplemented HEK_{mTRPV3} cells yielded about 3-fold higher Q_{10} values at temperature ranges of 28–32 °C and of 33–39 °C compared to the buffer-pretreated controls (Fig. 5D). Thus, TRPV3 is sensitised to lower temperatures and confers markedly higher current amplitudes at 37 °C after cellular cholesterol enrichment.

3.4. Intracellular fraction of TRPV3 is increased by cholesterol enrichment

To investigate if the cellular localisation of TRPV3 channels is affected by cholesterol treatment, we modulated cellular cholesterol, and subsequently monitored the localisation of mTRPV3-CFP in HEK_{mTRPV3} cells by confocal laser scanning microscopy. In buffer-treated cells, mTRPV3-CFP was mostly located at the plasma membrane (Fig. 6A), and only a minor fraction of the protein was observed in intracellular compartments, most likely on endomembranes. Upon cholesterol extraction with MβCD, cell rounding occurred, but TRPV3 was still predominantly located in the plasma membrane and to a small extent in intracellular compartments. By contrast, cholesterol enrichment led to an enhancement of the intracellular fraction of TRPV3-CFP. HEK293 cells expressing TRPV2-CFP showed a similar shift of localisation by cholesterol modulation (Fig. 6B). Thus, the potentiating effect of cholesterol on TRPV3 currents cannot be attributed to an enhanced surface localisation.

3.5. Calcium responses to TRPV3 activators are increased in HaCaT keratinocytes endogenously expressing TRPV3

The human keratinocyte cell line HaCaT, like primary keratinocytes, expresses TRPV3 [20,21]. To investigate if cholesterol modifies human TRPV3 channel activity in a system that natively expresses TRPV3, single cell calcium measurements with HaCaT keratinocytes were carried out. These cells showed more spontaneous calcium signals when cholesterol-enrichment occurred at 37 °C. We therefore chose conditions with 5 mM MβCD–cholesterol in HBS and room temperature for more gentle enrichment. Cholesterol supplementation resulted in a more than 2-fold enhancement of $[Ca^{2+}]_i$ increases upon stimulation with the TRPV3 activators carvacrol (500 µM) and camphor (10 mM) (Fig. 7; $p < 0.05$, two way ANOVA). We therefore conclude that cholesterol also potentiates the activity of TRPV3 natively expressed in HaCaT keratinocytes.

4. Discussion

In the present study, we showed for the first time an enhanced TRPV3 activity as a result of cellular cholesterol supplementation. Applying $[Ca^{2+}]_i$ analyses and patch clamp experiments, we found that cholesterol enrichment led to a robust increase in TRPV3 sensitivity to chemical and physical modes of TRPV3 activation. Cholesterol enrichment shifted the concentration dependence of TRPV3 to lower activator concentrations, and lowered the temperature at which TRPV3 currents became detectable in TRPV3-expressing cells. Similarly, cholesterol-supplemented

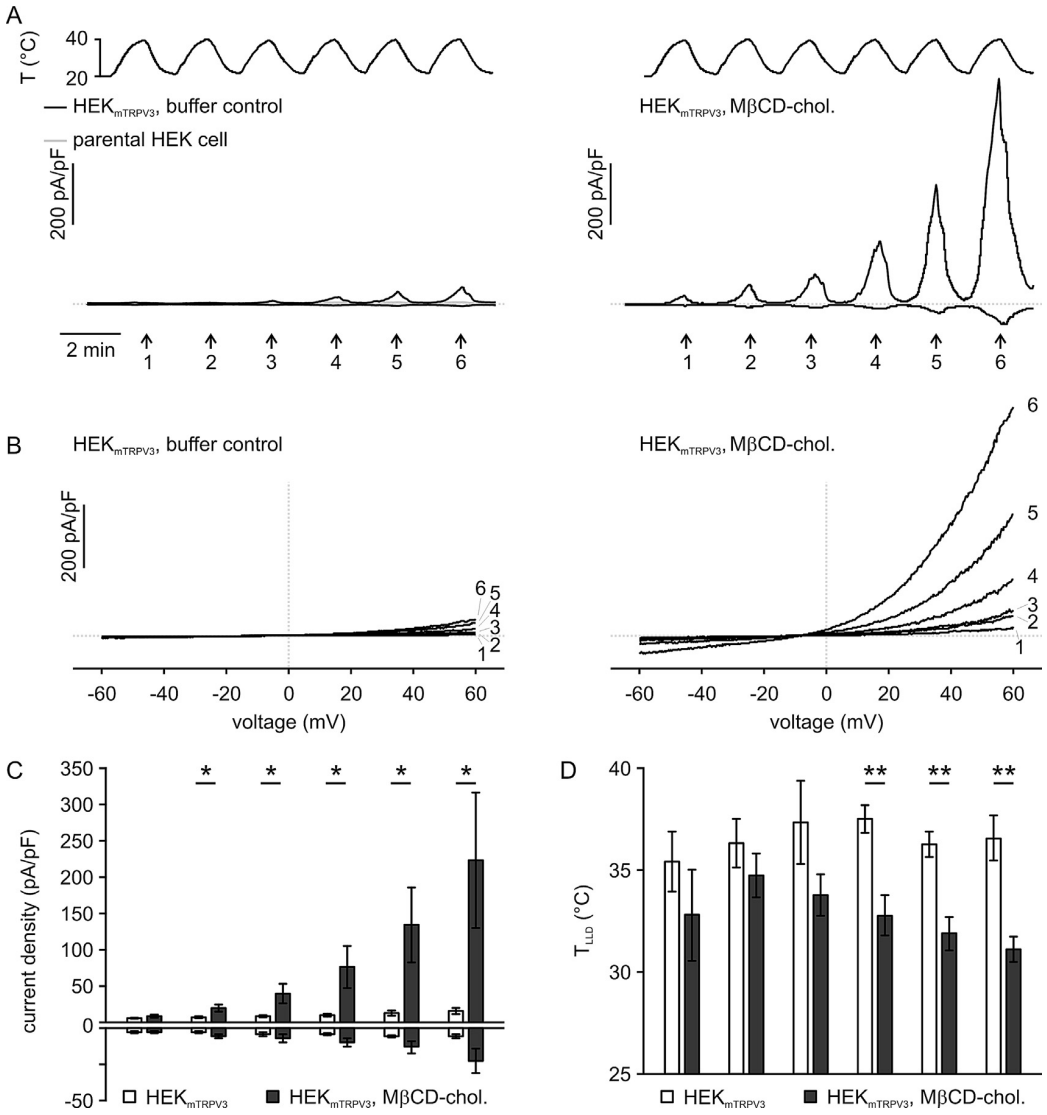

Fig. 4. Cholesterol enrichment strongly potentiates heat-induced TRPV3 currents. After modification of cellular cholesterol in HEK$_{mTRPV3}$ cells, whole-cell currents were recorded during repeated activation of TRPV3 by temperature ramps from 20 °C to 40 °C. (A) Typical time course of currents at −60 and +60 mV in an untransfected parental HEK293 cell (grey line), in a buffer-treated HEK$_{mTRPV3}$ cell (black line; left panel), and in a cholesterol-enriched HEK$_{mTRPV3}$ cell (right panel). Note the different scaling of the panels. (B) Current voltage traces recorded in a buffer-treated HEK$_{mTRPV3}$ cell (left panel), and in a cholesterol-enriched HEK$_{mTRPV3}$ cell (right panel). Data correspond to the time points indicated in (A). (C) Statistical analysis of temperature-induced current densities measured at 37 °C during the rising phase of the temperature ramps. (D) Lowest temperatures at which TRPV3-related currents became evident (T_{LLD}) in temperature ramp experiments performed as shown in (A). (C and D) Results depict means and S.E.M. of $n = 9$ patched cells for each condition during six consecutive applications of temperature ramps (*$p < 0.05$, **$p < 0.01$).

HaCaT keratinocytes exhibited higher $[Ca^{2+}]_i$ increases in response to different TRPV3 activators.

TRPV3-induced currents observed in cholesterol-enriched HEK$_{mTRPV3}$ cells exhibited typical features of TRPV3, including outward rectification and sensitisation by repeated activation. Cholesterol supplementation of HEK$_{mTRPV3}$ already gave rise to strongly increased current densities during the first activation cycle. During repeated challenging with 2-APB, TRPV3 currents then exhibited no further run-up, indicating that 30 μM 2-APB represent a saturating activator concentration under these conditions, whereas higher 2-APB concentrations or repeated activation cycles are required in untreated HEK$_{mTRPV3}$ cells to obtain full activation of TRPV3. Since we neither found increases in basal $[Ca^{2+}]_i$ nor recorded augmented basal current densities in the absence of a chemical activator in cholesterol-enriched HEK$_{mTRPV3}$ cells, cholesterol itself does not appear to activate TRPV3 at room temperature. Considering that the skin temperature in vivo is typically lower than the values that are required to trigger TRPV3 activation in a recombinant setting, the cholesterol-induced shift of the thermal sensitivity of TRPV3 to lower temperatures may provide a mechanistic basis for TRPV3 regulation by physiological temperatures in the skin.

To pursue the matter if cholesterol-dependent potentiation is a common feature of temperature-activated TRPV channels, we examined TRPV2-mediated responses to 2-APB stimulation in cholesterol-modified HEK293 cells. In our hands, there was no influence of cholesterol on TRPV2 signalling. The role of cholesterol in the regulation of TRPV1, the best characterised, heat-activated member of the TRP family has intensively been investigated in different studies, but the documented effects are controversial. Cholesterol enrichment led to an increased activation temperature in rat TRPV1-expressing HEK293 cells [31], and, in another study,

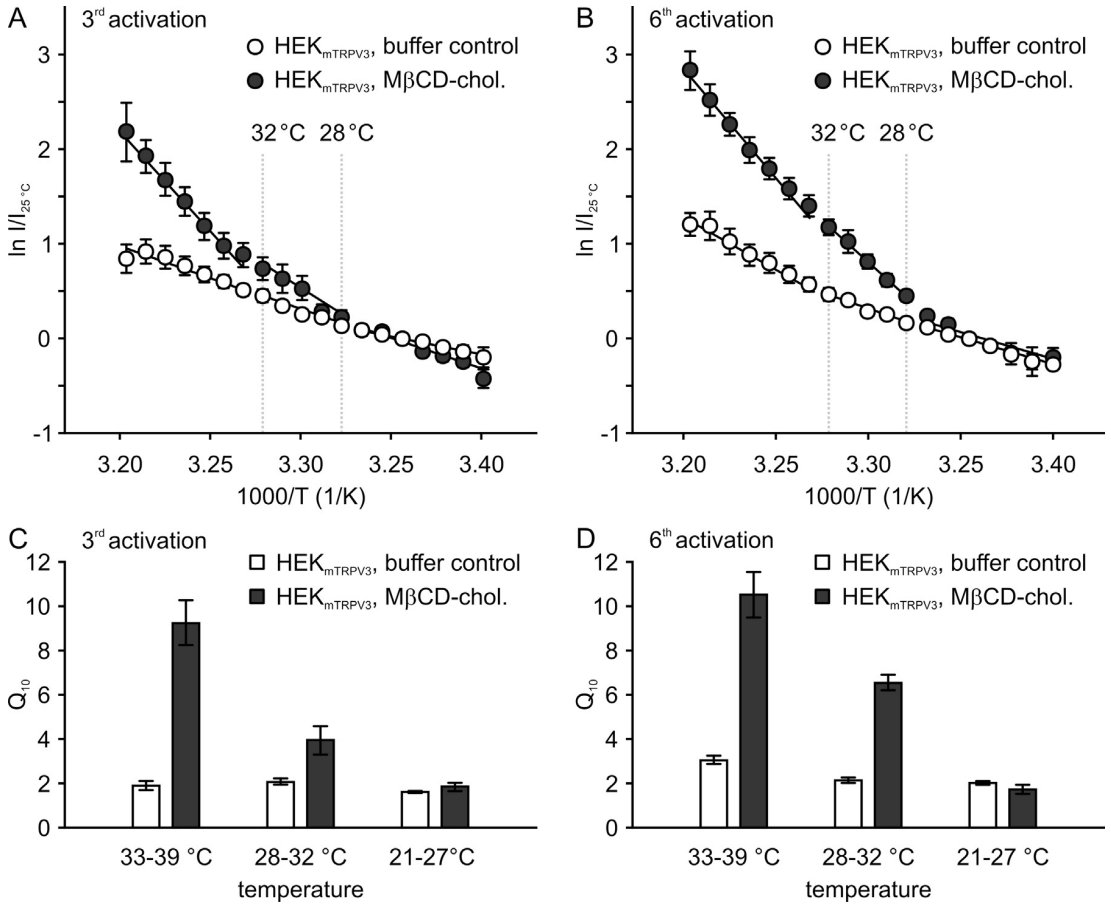

Fig. 5. Temperature dependence and Q_{10} values of heat-induced currents measured in cholesterol-enriched HEK_{mTRPV3} cells. Current densities at +60 mV recorded as shown in Fig. 4 during the rising phases of temperature ramps were normalised to current densities measured at 25 °C, and plotted against the actual temperature during the 3rd (A) or 6th (B) temperature ramp. Current densities were averaged over 1-°C temperature steps. Data represent mean current densities of $n = 9$ cells. Slopes of temperature-correlated increases in current densities were calculated by linear regression analysis for temperature ranges of 21–27 °C, 28–32 °C, and 33–39 °C, respectively. (C and D) Q_{10} values of TRPV3-induced currents were calculated for the temperature ranges described in (A) and (B).

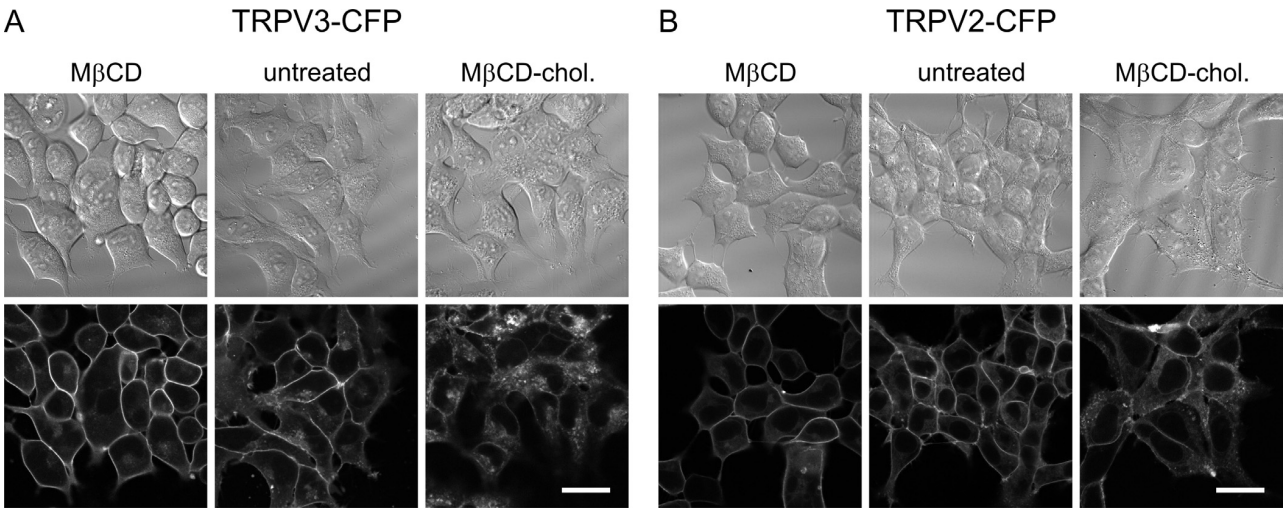

Fig. 6. Cellular localisation of heterologously expressed mTRPV3-CFP. Living HEK293 cells expressing TRPV3-CFP (A) or TRPV2-CFP (B) were imaged after cholesterol depletion (left panels), without cholesterol modification (middle panels), or after cholesterol supplementation (right panels). Upper panels: Nomarski differential contrast (DIC) images; lower panels: confocal laser scanning microscope images (scale bar: 25 μm).

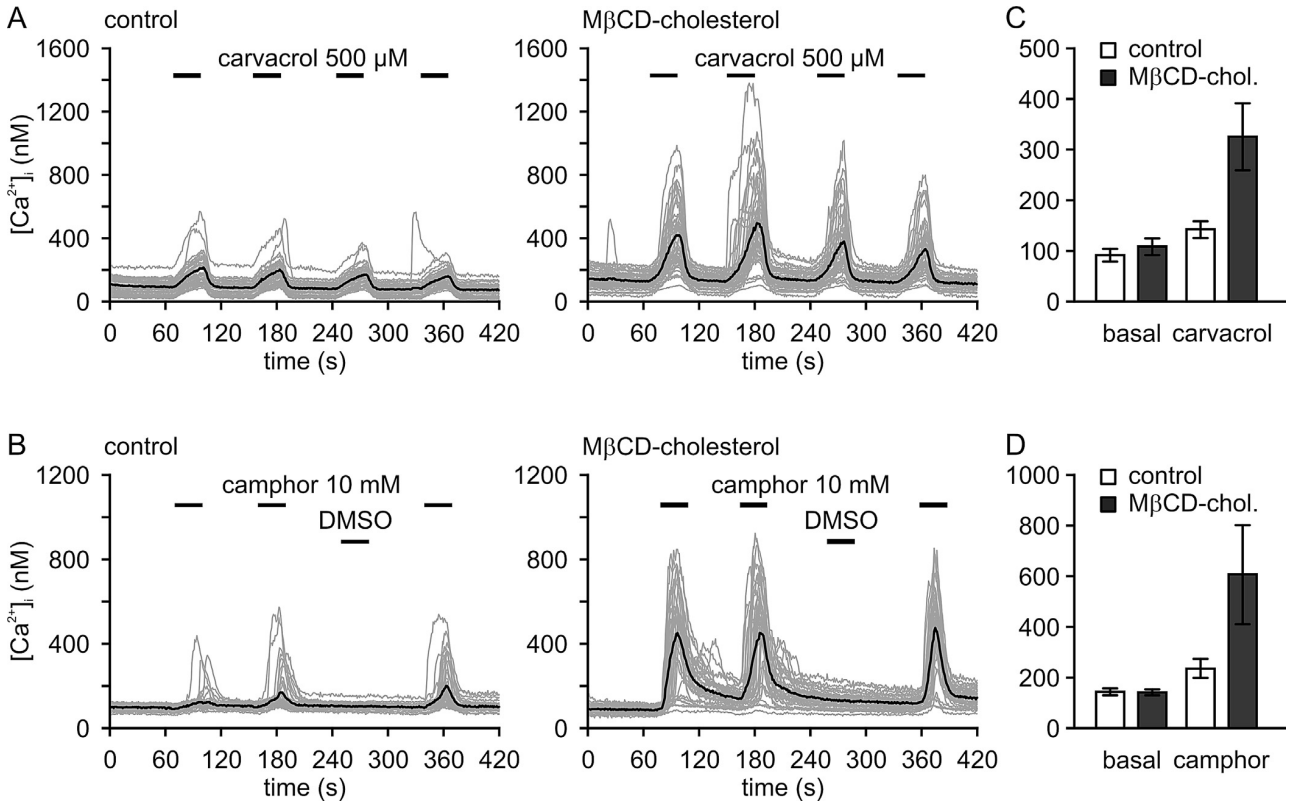

Fig. 7. Activation of TRPV3 in cholesterol-modified HaCaT cells. HaCaT cells were loaded with the calcium indicator fura-2 and incubated for 15 min at room temperature in HBS (control) or in HBS supplemented with 5 mM MβCD–cholesterol. Subsequently, calcium responses to repeatedly applied carvacrol (A) or camphor (B) were monitored. Shown are responses in single cells (grey lines) and the averaged signal (black line) of representative measurements. (C and D) Aggregated analysis of experiments performed as shown in (A) and (B), calculated from 4 (carvacrol stimulation) and 12 (camphor stimulation) independent $[Ca^{2+}]_i$ imaging experiments performed in buffer- or cholesterol-treated HEK_{mTRPV3} cells, each. Shown are basal $[Ca^{2+}]_i$ values immediately before agonist application and peak concentrations during the first application of the agonist.

decreased capsaicin-induced TRPV1 currents [32]. On the other side, cholesterol depletion inhibits the formation of large TRPV1 pores evoked by prolonged activation of TRPV1 in CHO cells [33]. Similarly, cholesterol extraction diminishes the TRPV1 response to capsaicin and resiniferatoxin (RTX) stimulation in trigeminal neurons [34], and to capsaicin and acidification in DRG neurons [35], but in transfected CHO cells, only the capsaicin response was reduced and stimulation with RTX or low pH was not influenced by MβCD [34]. In other studies, cholesterol depletion did not significantly change TRPV1 activation properties [31,33]. TRPM3 channels, recently shown to be warm sensitive [36], are inhibited by cholesterol supplementation [37]. The cold sensing member of TRP channels, TRPM8, however, is potentiated by cholesterol depletion [38,39]. Thus, cholesterol-mediated potentiation seems not to be a common hallmark of temperature-activated TRP channels, hinting to a specific physiological importance of the cholesterol-enhanced TRPV3 signalling.

Different mechanisms of the impact of cholesterol on TRP channel activity are conceivable. Cholesterol may indirectly affect TRP channels by promoting the interaction with intracellular signal cascades. For instance, TRPC6 has been shown to be sensitised to mechanical activation by a cholesterol-mediated binding of podocin [40]. TRPV3 signalling is facilitated by EGF receptor stimulation [16]. Indeed, the EGF receptor activity is regulated by plasma membrane cholesterol, but several studies have demonstrated that cholesterol depletion led to autoactivation of EGF receptors and its activity is rather abrogated by cholesterol supplementation [41]. Another possibility is the phospholipase C-mediated TRPV3 potentiation [11,16]. Cholesterol loading may lead to phospholipase C activation [42] resulting in a decreased level of PIP_2 at the plasma membrane, a lipid known to inhibit TRPV3 activity [11]. Applying the cholesterol supplementation protocol used in the actual study, we found no significant activation of phospholipase C, as monitored in living cells by observing the plasma membrane translocation of PKCε-YFP, a diacylglycerol-sensitive fluorescent biosensor protein [43] (data not shown). In addition, PIP_2 depletion would also facilitate TRPV2 desensitisation [44], but we noticed no enhanced desensitisation of TRPV2-mediated calcium signals in cholesterol-enriched cells.

Another possibility of indirect modulation may involve the plasma membrane targeting of TRPV3. Cholesterol depletion has been demonstrated to reduce the plasma membrane fraction of TRPV1 in DRG neurons, leading to diminished functional activity in these cells [35]. Studies with TRPM8 showed that cholesterol depletion potentiates TRPM8 activity by shifting its localisation between raft and non-rafts regions and thereby causes different glycosylation patterns that in turn influence its temperature and menthol sensitivity [38]. In addition, cholesterol depletion has been shown to enhance TRPM8 signals by increasing the number of channels located in the plasma membrane, an effect that closely resembles our observations concerning the cellular localisation of TRPV2 and TRPV3. The authors suggested that a decreased rate of endocytosis is responsible for the accumulation of TRPM8 channels in cholesterol-extracted plasma membranes [39].

Since various protein domains are known to interact with cholesterol, a direct binding to the channel protein may account for its functional modulation. Rat TRPV1 has been reported to contain a cholesterol-binding domain in its S5 helix [32]. The

homologous region in TRPV3, however, more closely resembles that of the cholesterol-independent human TRPV1 ortholog [32]. Thus, other motifs or non-linear binding epitopes may serve the binding site for cholesterol in TRPV3. At present, we cannot discriminate between direct interaction and membrane perturbation as the mechanism of TRPV3 sensitisation by cholesterol.

Cholesterol strongly affects the biophysical properties of lipid membranes, including their rigidity, fluidity, and thickness. Since voltage sensitivity and temperature detection of temperature-sensing TRP channels are highly intertwined and require only minute movement of their gating charge within the electrical field of the membrane [45,46], it is obvious that subtle changes in their membrane environment may suffice to strongly affect the gating behaviour. Indeed, the sensitisation to lower temperatures indicates that TRPV3 modulation by cholesterol critically involves the voltage-sensing mechanism of the channel protein. An allosteric mechanism of cholesterol bound to moieties of the channel that are not exposed to the electrical field cannot formally be excluded. However, a more simple explanation would be that cholesterol-induced changes of biophysical properties of lipid membranes, including their fluidity and thickness or cholesterol binding to TRPV3 within the electrical field facilitate the gating of the channel by shifting its voltage dependence towards physiological potentials.

TRPV3 is expressed in different cell types, but exerts an outstanding role in keratinocytes. Recent data of Cheng et al. demonstrated that TRPV3-deficient mice have curly hair and an impaired skin barrier formation [16]. These mice exhibited an increase in the thickness of keratin-1- and keratin-10-positive epidermal layers, as well as a diminished number of cornified envelopes, indicating that TRPV3 is critical for the progression of late differentiation processes [16]. During differentiation, keratinocytes actively synthesise and accumulate lipids like ceramides, cholesterol and fatty acids. These lipids are stored in granules, which are released into the extracellular space in the upper epidermal layers, where they prevent transepidermal water loss. A growing body of evidence suggests that cholesterol plays an important role in differentiation control and induction of the cornification [47–49]. Thus, future work will be directed to solve the question whether the increased cholesterol content in differentiating keratinocytes and upper epidermal layers, via TRPV3 sensitisation and Ca^{2+} entry contribute to late keratinocyte differentiation. Of note, TRPV4 is a second heat-activated TRP channel in keratinocytes, which participates in epidermal barrier formation by stabilising cell–cell junctions [50]. It may be interesting to investigate whether cholesterol also enhances TRPV4 activity and, thus, possibly supports skin integrity via a second mechanism.

The functional interaction between cholesterol and TRPV3 may also explain some pathophysiological effects. It is established, that gain-of-function variants of TRPV3 are involved in the development of pruritus and hyperkeratosis [17–19] associated with inflammatory skin disorders like atopic dermatitis or with psoriasis. Thus, functional modulation of TRPV3 channel activity may provide a target for pharmacological intervention not only with respect to nociception, but also to control keratinocyte functions in skin disorders [51].

Conflict of interest statement

None declared.

Acknowledgments

HaCaT cells were kindly provided by Dr. Ulf Anderegg (Department of Dermatology, University of Leipzig, Germany). This work was supported by the Deutsche Forschungsgemeinschaft (FOR806 to M.S.).

References

[1] E. Proksch, J.M. Brandner, J.M. Jensen, The skin: an indispensable barrier, Exp. Dermatol. 17 (2008) 1063–1072.
[2] A.M. Peier, A.J. Reeve, D.A. Andersson, et al., A heat-sensitive TRP channel expressed in keratinocytes, Science 296 (2002) 2046–2049.
[3] H. Xu, I.S. Ramsey, S.A. Kotecha, et al., TRPV3 is a calcium-permeable temperature-sensitive cation channel, Nature 418 (2002) 181–186.
[4] M.K. Chung, H. Lee, A. Mizuno, M. Suzuki, M.J. Caterina, 2-Aminoethoxydiphenyl borate activates and sensitizes the heat-gated ion channel TRPV3, J. Neurosci. 24 (2004) 5177–5182.
[5] A. Moqrich, S.W. Hwang, T.J. Earley, et al., Impaired thermosensation in mice lacking TRPV3, a heat and camphor sensor in the skin, Science 307 (2005) 1468–1472.
[6] H. Xu, M. Delling, J.C. Jun, D.E. Clapham, Oregano, thyme and clove-derived flavors and skin sensitizers activate specific TRP channels, Nat. Neurosci. 9 (2006) 628–635.
[7] G.D. Smith, M.J. Gunthorpe, R.E. Kelsell, et al., TRPV3 is a temperature-sensitive vanilloid receptor-like protein, Nature 418 (2002) 186–190.
[8] S.M. Huang, X. Li, Y. Yu, J. Wang, M.J. Caterina, TRPV3 and TRPV4 ion channels are not major contributors to mouse heat sensation, Mol. Pain 7 (2011) 37.
[9] X. Cao, F. Yang, J. Zheng, K. Wang, Intracellular proton-mediated activation of TRPV3 channels accounts for the exfoliation effect of α-hydroxyl acids on keratinocytes, J. Biol. Chem. 287 (2012) 25905–25916.
[10] H.Z. Hu, R. Xiao, C. Wang, et al., Potentiation of TRPV3 channel function by unsaturated fatty acids, J. Cell. Physiol. 208 (2006) 201–212.
[11] J.F. Doerner, H. Hatt, I.S. Ramsey, Voltage- and temperature-dependent activation of TRPV3 channels is potentiated by receptor-mediated $PI(4,5)P_2$ hydrolysis, J. Gen. Physiol. 137 (2011) 271–288.
[12] S. Bang, S. Yoo, T.J. Yang, H. Cho, S.W. Hwang, Isopentenyl pyrophosphate is a novel antinociceptive substance that inhibits TRPV3 and TRPA1 ion channels, Pain 152 (2011) 1156–1164.
[13] S. Bang, S. Yoo, T.J. Yang, H. Cho, S.W. Hwang, 17(R)-resolvin D1 specifically inhibits transient receptor potential ion channel vanilloid 3 leading to peripheral antinociception, Br. J. Pharmacol. 165 (2012) 683–692.
[14] S. Bang, S. Yoo, T.J. Yang, H. Cho, S.W. Hwang, Farnesyl pyrophosphate is a novel pain-producing molecule via specific activation of TRPV3, J. Biol. Chem. 285 (2010) 19362–19371.
[15] S.M. Huang, H. Lee, M.K. Chung, et al., Overexpressed transient receptor potential vanilloid 3 ion channels in skin keratinocytes modulate pain sensitivity via prostaglandin E2, J. Neurosci. 28 (2008) 13727–13737.
[16] X. Cheng, J. Jin, L. Hu, et al., TRP channel regulates EGFR signaling in hair morphogenesis and skin barrier formation, Cell 141 (2010) 331–343.
[17] T. Yoshioka, K. Imura, M. Asakawa, et al., Impact of the Gly573Ser substitution in TRPV3 on the development of allergic and pruritic dermatitis in mice, J. Invest. Dermatol. 129 (2009) 714–722.
[18] K. Imura, T. Yoshioka, T. Hirasawa, T. Sakata, Role of TRPV3 in immune response to development of dermatitis, J. Inflamm. (Lond.) 6 (2009) 17.
[19] Z. Lin, Q. Chen, M. Lee, et al., Exome sequencing reveals mutations in TRPV3 as a cause of Olmsted syndrome, Am. J. Hum. Genet. 90 (2012) 558–564.
[20] P. Boukamp, R.T. Petrussevska, D. Breitkreutz, J. Hornung, A. Markham, N.E. Fusenig, Normal keratinization in a spontaneously immortalized aneuploid human keratinocyte cell line, J. Cell. Biol. 106 (1988) 761–771.
[21] M.A. Sherkheli, H. Benecke, J.F. Doerner, et al., Monoterpenoids induce agonist-specific desensitization of transient receptor potential vanilloid-3 (TRPV3) ion channels, J. Pharm. Pharm. Sci. 12 (2009) 116–128.
[22] L. Micallef, F. Belaubre, A. Pinon, et al., Effects of extracellular calcium on the growth-differentiation switch in immortalized keratinocyte HaCaT cells compared with normal human keratinocytes, Exp. Dermatol. 18 (2009) 143–151.
[23] R. Zidovetzki, I. Levitan, Use of cyclodextrins to manipulate plasma membrane cholesterol content: evidence, misconceptions and control strategies, Biochim. Biophys. Acta 1768 (2007) 1311–1324.
[24] A.M. Hartmann, P. Blaesse, T. Kranz, et al., Opposite effect of membrane raft perturbation on transport activity of KCC2 and NKCC1, J. Neurochem. 111 (2009) 321–331.
[25] W. Nörenberg, H. Sobottka, C. Hempel, et al., Positive allosteric modulation by ivermectin of human but not murine P2X7 receptors, Br. J. Pharmacol. 167 (2012) 48–66.
[26] A. Edelstein, N. Amodaj, K. Hoover, R. Vale, N. Stuurman, Computer control of microscopes using μManager, Curr. Protoc. Mol. Biol. 92 (2010) 14.20.1–14.20.17.
[27] M.D. Abràmoff, P.J. Magalhães, S.J. Ram, Image processing with ImageJ, Biophoton. Int. 11 (2004) 36–42.
[28] J.C. Lenz, H.P. Reusch, N. Albrecht, G. Schultz, M. Schaefer, Ca^{2+}-controlled competitive diacylglycerol binding of protein kinase C isoenzymes in living cells, J. Cell. Biol. 159 (2002) 291–302.
[29] A.K. Vogt-Eisele, K. Weber, M.A. Sherkheli, et al., Monoterpenoid agonists of TRPV3, Br. J. Pharmacol. 151 (2007) 530–540.
[30] B. Liu, J. Yao, M.X. Zhu, F. Qin, Hysteresis of gating underlines sensitization of TRPV3 channels, J. Gen. Physiol. 138 (2011) 509–520.

[31] B. Liu, K. Hui, F. Qin, Thermodynamics of heat activation of single capsaicin ion channels VR1, Biophys. J. 85 (2003) 2988–3006.
[32] G. Picazo-Juárez, S. Romero-Suárez, A. Nieto-Posadas, et al., Identification of a binding motif in the S5 helix that confers cholesterol sensitivity to the TRPV1 ion channel, J. Biol. Chem. 286 (2011) 24966–24976.
[33] E.T. Jansson, C.L. Trkulja, A. Ahemaiti, et al., Effect of cholesterol depletion on the pore dilation of TRPV1, Mol. Pain 9 (2013) 1.
[34] E. Szoke, R. Börzsei, D.M. Tóth, et al., Effect of lipid raft disruption on TRPV1 receptor activation of trigeminal sensory neurons and transfected cell line, Eur. J. Pharmacol. 628 (2010) 67–74.
[35] M. Liu, W. Huang, D. Wu, J.V. Priestley, TRPV1, but not P2X, requires cholesterol for its function and membrane expression in rat nociceptors, Eur. J. Neurosci. 24 (2006) 1–6.
[36] J. Vriens, G. Owsianik, T. Hofmann, et al., TRPM3 is a nociceptor channel involved in the detection of noxious heat, Neuron 70 (2011) 482–494.
[37] J. Naylor, J. Li, C.J. Milligan, et al., Pregnenolone sulphate- and cholesterol-regulated TRPM3 channels coupled to vascular smooth muscle secretion and contraction, Circ. Res. 106 (2010) 1507–1515.
[38] C. Morenilla-Palao, M. Pertusa, V. Meseguer, H. Cabedo, F. Viana, Lipid raft segregation modulates TRPM8 channel activity, J. Biol. Chem. 284 (2009) 9215–9224.
[39] L.A. Veliz, C.A. Toro, J.P. Vivar, et al., Near-membrane dynamics and capture of TRPM8 channels within transient confinement domains, PLoS ONE 5 (2010) e13290.
[40] T.B. Huber, B. Schermer, R.U. Müller, et al., Podocin and MEC-2 bind cholesterol to regulate the activity of associated ion channels, Proc. Natl. Acad. Sci. U.S.A. 103 (2006) 17079–17086.
[41] T. Ringerike, F.D. Blystad, F.O. Levy, I.H. Madshus, E. Stang, Cholesterol is important in control of EGF receptor kinase activity but EGF receptors are not concentrated in caveolae, J. Cell Sci. 115 (2002) 1331–1340.
[42] Y.S. Chun, S. Shin, Y. Kim, et al., Cholesterol modulates ion channels via down-regulation of phosphatidylinositol 4,5-bisphosphate, J. Neurochem. 112 (2010) 1286–1294.
[43] D. Sinnecker, M. Schaefer, Real-time analysis of phospholipase C activity during different patterns of receptor-induced Ca^{2+} responses in HEK293 cells, Cell Calcium 35 (2004) 29–38.
[44] J. Mercado, A. Gordon-Shaag, W.N. Zagotta, S.E. Gordon, Ca^{2+}-dependent desensitization of TRPV2 channels is mediated by hydrolysis of phosphatidylinositol 4,5-bisphosphate, J. Neurosci. 30 (2010) 13338–13347.
[45] R. Latorre, S. Brauchi, G. Orta, C. Zaelzer, G. Vargas, ThermoTRP channels as modular proteins with allosteric gating, Cell Calcium 42 (2007) 427–438.
[46] B. Nilius, K. Talavera, G. Owsianik, J. Prenen, G. Droogmans, T. Voets, Gating of TRP channels: a voltage connection? J. Physiol. 567 (2005) 35–44.
[47] F. Spörl, M. Wunderskirchner, O. Ullrich, et al., Real-time monitoring of membrane cholesterol reveals new insights into epidermal differentiation, J. Invest. Dermatol. 130 (2010) 1268–1278.
[48] K.R. Feingold, M.Q. Man, E. Proksch, G.K. Menon, B.E. Brown, P.M. Elias, The lovastatin-treated rodent: a new model of barrier disruption and epidermal hyperplasia, J. Invest. Dermatol. 96 (1991) 201–209.
[49] R. Schmidt, E.J. Parish, V. Dionisius, et al., Modulation of cellular cholesterol and its effect on cornified envelope formation in cultured human epidermal keratinocytes, J. Invest. Dermatol. 97 (1991) 771–775.
[50] T. Sokabe, T. Fukumi-Tominaga, S. Yonemura, A. Mizuno, M. Tominaga, The TRPV4 channel contributes to intercellular junction formation in keratinocytes, J. Biol. Chem. 285 (2010) 18749–18758.
[51] B. Nilius, T. Biro, G. Owsianik, TRPV3: time to decipher a poorly understood family member!, J. Physiol. (2013), http://dx.doi.org/10.1113/jphysiol.2013.255968 (Epub ahead of print).

Summary

The major task of keratinocytes is to protect the organism against harmful external influences. Thus, they compose a complex outer barrier, the epidermis, where cell proliferation, differentiation, and migration of keratinocytes are of fundamental significance. In cooperation with neurons, keratinocytes also play pivotal roles in recognising environmental factors. Amongst other receptors and ion channels, keratinocytes express temperature-sensitive TRPV3 channels[34,35], whose role in keratinocyte physiology and pathophysiology is still poorly understood.

Cholesterol is an important lipid for epidermal development. Maturing keratinocytes actively synthesise and accumulate cholesterol and other lipids that are enriched in upper epidermal layers with the objective to maintain a barrier impermeable to water[7,9]. Moreover, cholesterol chiefly influences physical properties of membranes like thickness and viscosity[1,2]. It is also known to participate in several signalling pathways, either by direct interaction or indirectly via recruiting and clustering transmembrane or membrane-associated proteins.

4.1 HaCaT keratinocytes exhibit a cholesterol and plasma membrane viscosity gradient during directed migration

During the reepithelialisation phase of wound healing, keratinocytes migrate in cell assemblies. Cells at the edge adopt a polarised morphology characterised by extended lamellipodia at their front, while their rears remain in contact with adjacent cells[20,21]. For years, the involvement of signalling lipids like phosphatidylinositols in cell migration as well as their distribution in the plasma membrane of migrating cells has intensively been investigated[22]. However, the influence of cholesterol on the migration capacity of keratinocytes is less well understood. Furthermore, the importance of local differences of physical membrane properties of polarised keratinocytes has been neglected. Thus, we analysed the plasma membrane consistency and cholesterol content of keratinocyte-like HaCaT cells with pronounced lamellipodia at the edge of larger cell assemblies. These cells strongly resemble keratinocytes at a wound's leading edge.

4.1.1 Results

- We performed FRAP measurements of FAST DiO-stained HaCaT cells under TIR illumination[80]. This fluorophore homogeneously labels the plasma membrane in living cells. The diffusion coefficients of FAST DiO measured at the lamellipodia of polarised HaCaT cells were significantly higher than those at the cell rears, indicating a plasma membrane viscosity front-to-back gradient in these keratinocytes with a lower viscosity at their lamellipodia.

- The fluorescence lifetime of NBD depends on the physicochemical properties of its environment[81]. Using fluorescence lifetime measurements of HaCaT cells that were labelled with phosphatidylcholine carrying the NBD group on one acyl chain (NBD-PC) and that were excited under TIR conditions, we verified the results of the above described FRAP experiment. In addition, spatially resolved fluorescence lifetime images of NBD-PC-stained HaCaT cells were obtained for a direct visualisation of this gradient.
- Fixed HaCaT cells that were stained with the cholesterol-binding, fluorescent dye filipin[82], were analysed by confocal laser scanning microscopy (CLSM). The polarised cells showed a weaker filipin staining intensity at their lamellipodia when compared with their cell bodies.
- Exposure to epidermal growth factor (EGF) accelerates keratinocyte migration[20,83] in wound healing models. Applying FRAP and scratch assays, we found a bell-shaped dependence of cell migration and viscosity gradients on EGF concentrations. Of note, optimal EGF concentrations with regard to migration speed closely correlated with the most pronounced front-to-back viscosity gradients in plasma membranes of HaCaT cells.
- EGF supplementation led to an overall increase in plasma membrane viscosity and cholesterol content. This finding is in agreement with a previous report[84].
- The cholesterol transporter ABCA1 can alter the cholesterol content in the plasma membrane[85]. We investigated the impact of ABCA1 and ABCG1, two cholesterol transporters expressed in HaCaT cells[86], on the observed gradient. Pharmacological inhibition as well as small interference RNA-mediated gene silencing of these transporters indicated that ABCA1 but not ABCG1 is responsible for the formation or maintenance of the viscosity gradient in migrating HaCaT keratinocytes.

4.1.2 Condensed discussion

This study demonstrates that the polarisation of HaCaT keratinocytes is accompanied by the development of a microviscosity gradient in their plasma membranes, with a low viscosity observable at the lamellipodia. An inhomogeneous cholesterol distribution presumably contributes to this gradient, but further molecules may account for differences of the plasma membrane viscosity. Our findings underline the importance of cholesterol for keratinocyte migration and indicate that the local cholesterol distribution is strictly regulated in these cells. It is still an open question whether the membrane viscosity or rather distinct cholesterol contents are crucial for migrating keratinocytes. Since opposite viscosity and cholesterol gradients have been monitored in the plasma membrane of migrating endothelial cells[23], it is likely that viscosities optimal for cell migration are cell type-specific.

To identify mechanisms that induce or maintain the microviscosity gradient in migrating keratinocytes, we focused on the two cholesterol transporters ABCA1 and ABCG1. They are known to be

involved in macrophage migration via regulation of Rac1 [6,87], a monomeric GTPase participating in lamellipodia formation. Reduced ABCA1 activity led to a less pronounced microviscosity gradient in HaCaT cells, thus, indicating that this transporter affects the development of the cholesterol gradient. ABCA1 is presumably involved in the translocation of cholesterol from raft to non-raft regions [88], a fact that may imply a considerable importance of non-raft cholesterol for the microviscosity gradient.

The physiological relevance of the microviscosity gradient may lay in the regional regulation of signalling pathways. Diverse determinants of keratinocyte physiology are known to be modulated by cholesterol, including certain components of the cytoskeleton [89], of growth factor signalling cascades [90], and ion channels [73–79].

4.2 Cholesterol sensitises the transient receptor potential channel TRPV3 to lower temperatures and activator concentrations

Keratinocytes sense environmental changes via different receptors and ion channels like heat-sensitive TRPV3 channels. Regulation of TRPV3 channel activity is complex and only incompletely understood [37]. Since TRPV3 dysfunctions are known to favour the appearance of skin diseases [57–63], there is an increasing need for applicable, pharmacological modulators of this channel [50,57]. Whereas it has been established that cholesterol affects signalling events mediated by several temperature-regulated TRP channels [73–78], no such results have been provided regarding the activity of TRPV3. Hence, we investigated the cholesterol dependence of TRPV3 channel activation by chemical and thermal stimuli.

4.2.1 Results

- We modified the cholesterol content of HEK293 cells that stably expressed CFP-tagged mouse TRPV3 (HEK_{mTRPV3}) by subjecting these cells to methyl-β-cyclodextrin (MβCD) or MβCD preloaded with cholesterol [91]. Subsequently, we analysed the localisation of TRPV3 in these cells via CLSM. In buffer-treated and cholesterol-depleted cells, TRPV3 channels were mostly located at the plasma membrane. By contrast, cholesterol enrichment led to an intracellular accumulation of TRPV3-CFP and a lower number of channels at the plasma membrane.
- Multiwell-based $[Ca^{2+}]_i$ measurements in HEK_{mTRPV3} cells revealed that cholesterol extraction does not strongly change the sensitivity of TRPV3 towards the chemical activators 2-APB, carvacrol and thymol. In contrast, after cholesterol enrichment, significantly lower concentrations of the aforementioned TRPV3 activators sufficed to stimulate TRPV3-mediated Ca^{2+} influx.
- Carrying out the same assay, we showed that the response of the closely related channel TRPV2 to stimulation with 2-APB [67] could not be altered by cholesterol enrichment or depletion.

- The potentiation of TRPV3 responses by cholesterol enrichment was verified in electrophysiological whole-cell patch clamp experiments. Considerably larger TRPV3 currents were evoked in cholesterol-enriched cells by 2-APB application when compared with HEK_{mTRPV3} cells that were not supplemented with cholesterol. By contrast, no significant differences could be observed when comparing currents evoked in cholesterol-depleted cells and untreated controls.
- Patch clamp experiments showed that currents induced by temperature increases were robustly amplified in cholesterol-fed HEK_{mTRPV3} cells. Under these conditions, temperature thresholds for TRPV3 activation were lowered by approximately 5°C, and currents revealed considerably higher 10-degree temperature coefficients (Q_{10} values).
- We also tested the response of HaCaT keratinocytes[42] natively expressing TRPV3[43,44]. HaCaT keratinocytes displayed increases in $[Ca^{2+}]_i$ upon the application of carvacrol or camphor. These responses could be augmented by cholesterol supplementation.

4.2.2 Condensed discussion

Based on our previous findings indicating that keratinocytes strongly regulate the cholesterol content of their plasma membranes, we investigated the cholesterol dependence of TRPV3 function, a temperature-regulated ion channel expressed in these cells. Our results demonstrate that cholesterol enrichment strongly increases TRPV3 channel activity. Hence, it may be speculated that cholesterol serves as an endogenous modulator of TRPV3. However, the exact mechanism by which cholesterol affects these channels is still unknown. We could exclude an enhanced surface targeting of TRPV3 channels as a result of cholesterol supplementation, but a cholesterol-dependent lateral reorganisation within the plasma membrane possibly facilitates TRPV3 signalling. The possibility that cholesterol indirectly influences TRPV3 activity by interacting with other signalling cascades should also be considered. Alternatively, TRPV3 may directly bind cholesterol, as has been proposed for TRPV1[77]. Although the TRPV3 sequence does not feature the same cholesterol-binding motif as TRPV1, other, perhaps non-linear cholesterol-binding domains may exist in TRPV3. Since many TRP channels respond to physical stimuli, such as temperature changes or plasma membrane depolarisation[64,65], cholesterol-dependent modulation of TRPV3 may rely on complex physical processes.

Investigations of Cheng et al. indicate that TRPV3 is crucial for the progression of late differentiation processes of keratinocytes[13]. Our findings support the hypothesis that the increased cholesterol content in differentiating keratinocytes and the upper epidermal layer[9,10] results in a sensitisation of TRPV3, whose enhanced signalling is necessary to promote late keratinocyte differentiation. A growing body of evidence suggests that gain-of-function mutations in TRPV3 play a role in the development of skin disorders like the Olmsted syndrome[57–63]. A better understanding of TRPV3 regulation may pave the way towards an efficient treatment of this skin disease.

References

[1] Yeagle, P. L., Cholesterol and the cell membrane. 1985, *Biochim. Biophys. Acta.* 822:267–287. 7, 8, 38

[2] Song, Y., Kenworthy, A. K. and Sanders, C. R., Cholesterol as a co-solvent and a ligand for membrane proteins. 2014, *Protein Sci.* 23:1–22. 7, 8, 38

[3] Carquin, M., D'Auria, L., Pollet, H., Bongarzone, E. R. and Tyteca, D., Recent progress on lipid lateral heterogeneity in plasma membranes: From rafts to submicrometric domains. 2016, *Prog Lipid Res.* 62:1–24. 7

[4] Fantini, J. and Barrantes, F. J., How cholesterol interacts with membrane proteins: an exploration of cholesterol-binding sites including CRAC, CARC, and tilted domains. 2013, *Front Physiol.* 4:31. 8

[5] Soccio, R. E. and Breslow, J. L., Intracellular cholesterol transport. 2004, *Arterioscler. Thromb. Vasc. Biol.* 24:1150–1160. 9

[6] Pagler, T. A., Wang, M., Mondal, M., Murphy, A. J., Westerterp, M., Moore, K. J., Maxfield, F. R. and Tall, A. R., Deletion of ABCA1 and ABCG1 impairs macrophage migration because of increased Rac1 signaling. 2011, *Circ. Res.* 108:194–200. 9, 40

[7] Houben, E., De Paepe, K. and Rogiers, V., A keratinocyte's course of life. 2007, *Skin Pharmacol Physiol.* 20:122–132. 9, 10, 11, 38

[8] Baroni, A., Buommino, E., De Gregorio, V., Ruocco, E., Ruocco, V. and Wolf, R., Structure and function of the epidermis related to barrier properties. 2012, *Clin Dermatol.* 30:257–262. 9, 10, 11

[9] Feingold, K. R. and Elias, P. M., Role of lipids in the formation and maintenance of the cutaneous permeability barrier. 2014, *Biochim. Biophys. Acta.* 1841:280–294. 11, 38, 41

[10] Proksch, E., Brandner, J. M. and Jensen, J.-M., The skin: an indispensable barrier. 2008, *Exp. Dermatol.* 17:1063–1072. 11, 41

[11] Ponec, M., Gibbs, S., Weerheim, A., Kempenaar, J., Mulder, A. and Mommaas, A. M., Epidermal growth factor and temperature regulate keratinocyte differentiation. 1997, *Arch Dermatol Res.* 289:317–326. 11

[12] Elsholz, F., Harteneck, C., Muller, W. and Friedland, K., Calcium–a central regulator of keratinocyte differentiation in health and disease. 2014, *Eur J Dermatol.* 24:650–661. 11

[13] Cheng, X., Jin, J., Hu, L., Shen, D., Dong, X.-P., Samie, M. A., Knoff, J., Eisinger, B., Liu, M.-L., Huang, S. M., Caterina, M. J., Dempsey, P., Michael, L. E., Dlugosz, A. A., Andrews, N. C., Clapham, D. E. and Xu, H., TRP channel regulates EGFR signaling in hair morphogenesis and skin barrier formation. 2010, *Cell.* 141:331–343. 11, 15, 41

[14] Pillai, S., Mahajan, M. and Carlomusto, M., Ceramide potentiates, but sphingomyelin inhibits, vitamin D-induced keratinocyte differentiation: comparison between keratinocytes and HL-60 cells. 1999, *Arch Dermatol Res.* 291:284–289. 11

[15] Spörl, F., Wunderskirchner, M., Ullrich, O., Bömke, G., Breitenbach, U., Blatt, T., Wenck, H., Wittern, K.-P. and Schrader, A., Real-time monitoring of membrane cholesterol reveals new

insights into epidermal differentiation. 2010, *J. Invest. Dermatol.* 130:1268–1278. 11

[16] Schmidt, R., Parish, E. J., Dionisius, V., Cathelineau, C., Michel, S., Shroot, B., Rolland, A., Brzokewicz, A. and Reichert, U., Modulation of cellular cholesterol and its effect on cornified envelope formation in cultured human epidermal keratinocytes. 1991, *J. Invest. Dermatol.* 97:771–775. 12

[17] Lowes, M. A., Bowcock, A. M. and Krueger, J. G., Pathogenesis and therapy of psoriasis. 2007, *Nature.* 445:866-73. 12

[18] Proksch, E., Fölster-Holst, R. and Jensen, J.-M., Skin barrier function, epidermal proliferation and differentiation in eczema. 2006, *J Dermatol Sci.* 43:159-69. 12

[19] Arwert, E. N., Hoste, E. and Watt, F. M., Epithelial stem cells, wound healing and cancer. 2012, *Nat Rev Cancer.* 12:170–180. 12

[20] Friedl, P. and Gilmour, D., Collective cell migration in morphogenesis, regeneration and cancer. 2009, *Nat Rev Mol Cell Biol.* 10:445–457. 12, 38, 39

[21] Santoro, M. M. and Gaudino, G., Cellular and molecular facets of keratinocyte reepithelization during wound healing. 2005, *Exp. Cell Res.* 304:274–286. 12, 38

[22] Stephens, L., Milne, L. and Hawkins, P., Moving towards a better understanding of chemotaxis. 2008, *Curr. Biol.* 18:R485–R494. 12, 38

[23] Vasanji, A., Ghosh, P. K., Graham, L. M., Eppell, S. J. and Fox, P. L., Polarization of plasma membrane microviscosity during endothelial cell migration. 2004, *Dev. Cell.* 6:29–41. 12, 13, 39

[24] Mañes, S., Lacalle, R. A., Gómez-Moutón, C. and Martínez-A, C., From rafts to crafts: membrane asymmetry in moving cells. 2003, *Trends Immunol.* 24:320–326. 12

[25] Rose, J. J., Foley, J. F., Yi, L., Herren, G. and Venkatesan, S., Cholesterol is obligatory for polarization and chemotaxis but not for endocytosis and associated signaling from chemoattractant receptors in human neutrophils. 2008, *J. Biomed. Sci.* 15:441–461. 13

[26] Pierini, L. M., Eddy, R. J., Fuortes, M., Seveau, S., Casulo, C. and Maxfield, F. R., Membrane lipid organization is critical for human neutrophil polarization. 2003, *J. Biol. Chem.* 278:10831–10841.

[27] Bodin, S. and Welch, M. D., Plasma membrane organization is essential for balancing competing pseudopod- and uropod-promoting signals during neutrophil polarization and migration. 2005, *Mol. Biol. Cell.* 16:5773–5783.

[28] Mañes, S., Mira, E., Gómez-Moutón, C., Lacalle, R. A., Keller, P., Labrador, J. P. and Martínez-A, C., Membrane raft microdomains mediate front-rear polarity in migrating cells. 1999, *EMBO J.* 18:6211–6220.

[29] Gómez-Móuton, C., Abad, J. L., Mira, E., Lacalle, R. A., Gallardo, E., Jiménez-Baranda, S., Illa, I., Bernad, A., Mañes, S. and Martínez-A, C., Segregation of leading-edge and uropod components into specific lipid rafts during T cell polarization. 2001, *Proc. Natl. Acad. Sci. U.S.A.* 98:9642–9647. 13

[30] Qin, C., Nagao, T., Grosheva, I., Maxfield, F. R. and Pierini, L. M., Elevated plasma membrane cholesterol content alters macrophage signaling and function. 2006, *Arterioscler. Thromb. Vasc.*

Biol. 26:372–378. 13

[31] Nagao, T., Qin, C., Grosheva, I., Maxfield, F. R. and Pierini, L. M., Elevated cholesterol levels in the plasma membranes of macrophages inhibit migration by disrupting RhoA regulation. 2007, *Arterioscler. Thromb. Vasc. Biol.* 27:1596–1602. 13

[32] Nguyen, D. H., Espinoza, J. C. and Taub, D. D., Cellular cholesterol enrichment impairs T cell activation and chemotaxis. 2004, *Mech. Ageing Dev.* 125:641–650. 13

[33] Nilius, B. and Owsianik, G., The transient receptor potential family of ion channels. 2011, *Genome Biol.* 12:218. 13

[34] Smith, G. D., Gunthorpe, M. J., Kelsell, R. E., Hayes, P. D., Reilly, P., Facer, P., Wright, J. E., Jerman, J. C., Walhin, J.-P., Ooi, L., Egerton, J., Charles, K. J., Smart, D., Randall, A. D., Anand, P. and Davis, J. B., TRPV3 is a temperature-sensitive vanilloid receptor-like protein. 2002, *Nature.* 418:186–190. 13, 14, 16, 38

[35] Xu, H., Ramsey, I. S., Kotecha, S. A., Moran, M. M., Chong, J. A., Lawson, D., Ge, P., Lilly, J., Silos-Santiago, I., Xie, Y., DiStefano, P. S., Curtis, R. and Clapham, D. E., TRPV3 is a calcium-permeable temperature-sensitive cation channel. 2002, *Nature.* 418:181–186. 13, 14, 38

[36] Peier, A. M., Reeve, A. J., Andersson, D. A., Moqrich, A., Earley, T. J., Hergarden, A. C., Story, G. M., Colley, S., Hogenesch, J. B., McIntyre, P., Bevan, S. and Patapoutian, A., A heat-sensitive TRP channel expressed in keratinocytes. 2002, *Science.* 296:2046–2049. 13, 14, 16

[37] Nilius, B., Biro, T. and Owsianik, G., TRPV3: time to decipher a poorly understood family member! 2014, *J. Physiol.* 592:295-304. 13, 15, 40

[38] Chung, M.-K., Gler, A. D. and Caterina, M. J., Biphasic currents evoked by chemical or thermal activation of the heat-gated ion channel, TRPV3. 2005, *J. Biol. Chem.* 280:15928–15941. 13

[39] Xiao, R., Tang, J., Wang, C., Colton, C. K., Tian, J. and Zhu, M. X., Calcium plays a central role in the sensitization of TRPV3 channel to repetitive stimulations. 2008, *J. Biol. Chem.* 283:6162–6174. 13, 16

[40] Moqrich, A., Hwang, S. W., Earley, T. J., Petrus, M. J., Murray, A. N., Spencer, K. S. R., Andahazy, M., Story, G. M. and Patapoutian, A., Impaired thermosensation in mice lacking TRPV3, a heat and camphor sensor in the skin. 2005, *Science.* 307:1468–1472. 14, 15

[41] Huang, S. M., Li, X., Yu, Y., Wang, J. and Caterina, M. J., TRPV3 and TRPV4 ion channels are not major contributors to mouse heat sensation. 2011, *Mol Pain.* 7:37. 14

[42] Boukamp, P., Petrussevska, R. T., Breitkreutz, D., Hornung, J., Markham, A. and Fusenig, N. E., Normal keratinization in a spontaneously immortalized aneuploid human keratinocyte cell line. 1988, *J. Cell Biol.* 106:761–771. 14, 41

[43] Kang, D., Kim, S.-H., Hwang, E.-M., Kwon, O.-S., Yang, H.-Y., Kim, E.-S., Choi, T. H., Park, J.-Y., Hong, S.-G. and Han, J., Expression of thermosensitive two-pore domain K^+ channels in human keratinocytes cell line HaCaT cells. 2007, *Exp Dermatol.* 16:1016–1022. 14, 41

[44] Sherkheli, M. A., Benecke, H., Doerner, J. F., Kletke, O., Vogt-Eisele, A. K., Gisselmann, G. and Hatt, H., Monoterpenoids induce agonist-specific desensitization of transient receptor

potential vanilloid-3 (TRPV3) ion channels. 2009, *J Pharm Pharm Sci.* 12:116–128. 14, 16, 41

[45] Xu, H., Delling, M., Jun, J. C. and Clapham, D. E., Oregano, thyme and clove-derived flavors and skin sensitizers activate specific TRP channels. 2006, *Nat. Neurosci.* 9:628–635. 14, 15

[46] Aijima, R., Wang, B., Takao, T., Mihara, H., Kashio, M., Ohsaki, Y., Zhang, J.-Q., Mizuno, A., Suzuki, M., Yamashita, Y., Masuko, S., Goto, M., Tominaga, M. and Kido, M. A., The thermosensitive TRPV3 channel contributes to rapid wound healing in oral epithelia. 2015, *FASEB J.* 29:182–192. 14, 15

[47] Lo, I. C., Chan, H. C., Qi, Z., Ng, K. L., So, C. and Tsang, S. Y., TRPV3 channel negatively regulates cell cycle progression and safeguards the pluripotency of embryonic stem cells. 2016, *J Cell Physiol.* 231:403–413. 14, 15

[48] Moussaieff, A., Rimmerman, N., Bregman, T., Straiker, A., Felder, C. C., Shoham, S., Kashman, Y., Huang, S. M., Lee, H., Shohami, E., Mackie, K., Caterina, M. J., Walker, J. M., Fride, E. and Mechoulam, R., Incensole acetate, an incense component, elicits psychoactivity by activating TRPV3 channels in the brain. 2008, *FASEB J.* 22:3024–3034. 14

[49] Bang, S., Yoo, S., Yang, T.-J., Cho, H. and Hwang, S. W., Farnesyl pyrophosphate is a novel pain-producing molecule via specific activation of TRPV3. 2010, *J. Biol. Chem.* 285:19362–19371. 15, 16

[50] Huang, S. M. and Chung, M.-K., Targeting TRPV3 for the Development of Novel Analgesics. 2013, *Open Pain J.* 6:119–126. 15, 40

[51] Borbíró, I., Lisztes, E., Tóth, B. I., Czifra, G., Oláh, A., Szöllosi, A. G., Szentandrássy, N., Nánási, P. P., Péter, Z., Paus, R., Kovács, L. and Bíró, T., Activation of transient receptor potential vanilloid-3 inhibits human hair growth. 2011, *J Invest Dermatol.* 131:1605–1614. 15

[52] Denda, M., Sokabe, T., Fukumi-Tominaga, T. and Tominaga, M., Effects of skin surface temperature on epidermal permeability barrier homeostasis. 2007, *J. Invest. Dermatol.* 127:654–659. 15

[53] Miyamoto, T., Petrus, M. J., Dubin, A. E. and Patapoutian, A., TRPV3 regulates nitric oxide synthase-independent nitric oxide synthesis in the skin. 2011, *Nat Commun.* 2:369. 15

[54] Cals-Grierson, M.-M. and Ormerod, A. D., Nitric oxide function in the skin. 2004, *Nitric Oxide.* 10:179–193. 15

[55] Li, X., Zhang, Q., Fan, K., Li, B., Li, H., Qi, H., Guo, J., Cao, Y. and Sun, H., Overexpression of TRPV3 Correlates with Tumor Progression in Non-Small Cell Lung Cancer. 2016, *Int J Mol Sci.* 17:437. 15

[56] Cheung, S. Y., Huang, Y., Kwan, H. Y., Chung, H. Y. and Yao, X., Activation of transient receptor potential vanilloid 3 channel suppresses adipogenesis. 2015, *Endocrinology.* 156:2074–2086. 15

[57] Broad, L. M., Mogg, A. J., Eberle, E., Tolley, M., Li, D. L. and Knopp, K. L., TRPV3 in Drug Development. 2016, *Pharmaceuticals (Basel).* 9:55. 15, 16, 40, 41

[58] Sulk, M., Seeliger, S., Aubert, J., Schwab, V. D., Cevikbas, F., Rivier, M., Nowak, P., Voegel, J. J., Buddenkotte, J. and Steinhoff, M., Distribution and expression of non-neuronal transient receptor potential (TRPV) ion channels in rosacea. 2012, *J. Invest. Dermatol.* 132:1253–1262.

15

[59] Xiao, R., Tian, J., Tang, J. and Zhu, M. X., The TRPV3 mutation associated with the hairless phenotype in rodents is constitutively active. 2008, *Cell Calcium.* 43:334–343. 15

[60] Yoshioka, T., Imura, K., Asakawa, M., Suzuki, M., Oshima, I., Hirasawa, T., Sakata, T., Horikawa, T. and Arimura, A., Impact of the Gly573Ser substitution in TRPV3 on the development of allergic and pruritic dermatitis in mice. 2009, *J. Invest. Dermatol.* 129:714–722.

[61] Imura, K., Yoshioka, T., Hirasawa, T. and Sakata, T., Role of TRPV3 in immune response to development of dermatitis. 2009, *J Inflamm (Lond).* 6:17.

[62] Yamamoto-Kasai, E., Yasui, K., Shichijo, M., Sakata, T. and Yoshioka, T., Impact of TRPV3 on the development of allergic dermatitis as a dendritic cell modulator. 2013, *Exp Dermatol.* 22:820–824. 15

[63] Duchatelet, S. and Hovnanian, A., Olmsted syndrome: clinical, molecular and therapeutic aspects. 2015, *Orphanet J Rare Dis.* 10:33. 15, 40, 41

[64] Nilius, B., Talavera, K., Owsianik, G., Prenen, J., Droogmans, G. and Voets, T., Gating of TRP channels: a voltage connection? 2005, *J. Physiol.* 567:35–44. 15, 41

[65] Latorre, R., Brauchi, S., Orta, G., Zaelzer, C. and Vargas, G., ThermoTRP channels as modular proteins with allosteric gating. 2007, *Cell Calcium.* 42:427–438. 15, 41

[66] Chung, M.-K., Lee, H., Mizuno, A., Suzuki, M. and Caterina, M. J., 2-Aminoethoxydiphenyl borate activates and sensitizes the heat-gated ion channel TRPV3. 2004, *J. Neurosci.* 24:5177–5182. 15

[67] Hu, H.-Z., Gu, Q., Wang, C., Colton, C. K., Tang, J., Kinoshita-Kawada, M., Lee, L.-Y., Wood, J. D. and Zhu, M. X., 2-Aminoethoxydiphenyl borate is a common activator of TRPV1, TRPV2, and TRPV3. 2004, *J. Biol. Chem.* 279:35741–35748. 15, 40

[68] Hu, H.-Z., Xiao, R., Wang, C., Gao, N., Colton, C. K., Wood, J. D. and Zhu, M. X., Potentiation of TRPV3 channel function by unsaturated fatty acids. 2006, *J. Cell. Physiol.* 208:201–212. 16

[69] Bang, S., Yoo, S., Yang, T.-J., Cho, H. and Hwang, S. W., Isopentenyl pyrophosphate is a novel antinociceptive substance that inhibits TRPV3 and TRPA1 ion channels. 2011, *Pain.* 152:1156–1164. 16

[70] Bang, S., Yoo, S., Yang, T. J., Cho, H. and Hwang, S. W., 17(R)-resolvin D1 specifically inhibits transient receptor potential ion channel vanilloid 3 leading to peripheral antinociception. 2012, *Br J Pharmacol.* 165:683–692. 16

[71] Doerner, J. F., Hatt, H. and Ramsey, I. S., Voltage- and temperature-dependent activation of TRPV3 channels is potentiated by receptor-mediated PI(4,5)P_2 hydrolysis. 2011, *J. Gen. Physiol.* 137:271–288. 16

[72] Luo, J., Stewart, R., Berdeaux, R. and Hu, H., Tonic inhibition of TRPV3 by Mg^{2+} in mouse epidermal keratinocytes. 2012, *J. Invest. Dermatol.* 132:2158–2165. 16

[73] Szöke, , Börzsei, R., Tóth, D. M., Lengl, O., Helyes, Z., Sándor, Z. and Szolcsányi, J., Effect of lipid raft disruption on TRPV1 receptor activation of trigeminal sensory neurons and transfected cell line. 2010, *Eur. J. Pharmacol.* 628:67–74. 16, 40

[74] Liu, B., Hui, K. and Qin, F., Thermodynamics of heat activation of single capsaicin ion channels VR1. 2003, *Biophys. J.* 85:2988–3006. 16

[75] Jansson, E. T., Trkulja, C. L., Ahemaiti, A., Millingen, M., Jeffries, G. D. M., Jardemark, K. and Orwar, O., Effect of cholesterol depletion on the pore dilation of TRPV1. 2013, *Mol Pain.* 9:1. 16

[76] Liu, M., Huang, W., Wu, D. and Priestley, J. V., TRPV1, but not P2X, requires cholesterol for its function and membrane expression in rat nociceptors. 2006, *Eur. J. Neurosci.* 24:1–6. 16

[77] Picazo-Juárez, G., Romero-Suárez, S., Nieto-Posadas, A., Llorente, I., Jara-Oseguera, A., Briggs, M., McIntosh, T. J., Simon, S. A., Guevara, E. L., Islas, L. D. and Rosenbaum, T., Identification of a binding motif in the S5 helix that confers cholesterol sensitivity to the TRPV1 ion channel. 2011, *J. Biol. Chem.* 286:24966–24976. 16, 41

[78] Morenilla-Palao, C., Pertusa, M., Meseguer, V., Cabedo, H. and Viana, F., Lipid raft segregation modulates TRPM8 channel activity. 2009, *J. Biol. Chem.* 284:9215–9224. 16, 40

[79] Naylor, J., Li, J., Milligan, C. J., Zeng, F., Sukumar, P., Hou, B., Sedo, A., Yuldasheva, N., Majeed, Y., Beri, D., Jiang, S., Seymour, V. A. L., McKeown, L., Kumar, B., Harteneck, C., O'Regan, D., Wheatcroft, S. B., Kearney, M. T., Jones, C., Porter, K. E. and Beech, D. J., Pregnenolone sulphate- and cholesterol-regulated TRPM3 channels coupled to vascular smooth muscle secretion and contraction. 2010, *Circ. Res.* 106:1507–1515. 16, 40

[80] Axelrod, D., Selective imaging of surface fluorescence with very high aperture microscope objectives. 2001, *J. Biomed. Opt.* 6:6–13. 38

[81] Stöckl, M., Plazzo, A. P., Korte, T. and Herrmann, A., Detection of lipid domains in model and cell membranes by fluorescence lifetime imaging microscopy of fluorescent lipid analogues. 2008, *J. Biol. Chem.* 283:30828–30837. 39

[82] Mukherjee, S., Zha, X., Tabas, I. and Maxfield, F. R., Cholesterol distribution in living cells: fluorescence imaging using dehydroergosterol as a fluorescent cholesterol analog. 1998, *Biophys. J.* 75:1915–1925. 39

[83] Koivisto, L., Jiang, G., Häkkinen, L., Chan, B. and Larjava, H., HaCaT keratinocyte migration is dependent on epidermal growth factor receptor signaling and glycogen synthase kinase-3α. 2006, *Exp. Cell Res.* 312:2791–2805. 39

[84] Harris, I. R., Höppner, H., Siefken, W., Farrell, A. M. and Wittern, K. P., Regulation of HMG-CoA synthase and HMG-CoA reductase by insulin and epidermal growth factor in HaCaT keratinocytes. 2000, *J Invest Dermatol.* 114:83–87. 39

[85] Zarubica, A., Plazzo, A. P., Stöckl, M., Trombik, T., Hamon, Y., Müller, P., Pomorski, T., Herrmann, A. and Chimini, G., Functional implications of the influence of ABCA1 on lipid microenvironment at the plasma membrane: a biophysical study. 2009, *FASEB J.* 23:1775–1785. 39

[86] Kielar, D., Kaminski, W. E., Liebisch, G., Piehler, A., Wenzel, J. J., Möhle, C., Heimerl, S., Langmann, T., Friedrich, S. O., Böttcher, A., Barlage, S., Drobnik, W. and Schmitz, G., Adenosine triphosphate binding cassette (ABC) transporters are expressed and regulated during terminal keratinocyte differentiation: a potential role for ABCA7 in epidermal lipid reorganization. 2003, *J. Invest. Dermatol.* 121:465–474. 39

[87] Adorni, M. P., Favari, E., Ronda, N., Granata, A., Bellosta, S., Arnaboldi, L., Corsini, A., Gatti, R. and Bernini, F., Free cholesterol alters macrophage morphology and mobility by an ABCA1 dependent mechanism. 2011, *Atherosclerosis.* 215:70–76. 40

[88] Landry, Y. D., Denis, M., Nandi, S., Bell, S., Vaughan, A. M. and Zha, X., ATP-binding cassette transporter A1 expression disrupts raft membrane microdomains through its ATPase-related functions. 2006, *J. Biol. Chem.* 281:36091–36101. 40

[89] Sun, M., Northup, N., Marga, F., Huber, T., Byfield, F. J., Levitan, I. and Forgacs, G., The effect of cellular cholesterol on membrane-cytoskeleton adhesion. 2007, *J. Cell. Sci.* 120:2223–2231. 40

[90] Pike, L. J. and Casey, L., Cholesterol levels modulate EGF receptor-mediated signaling by altering receptor function and trafficking. 2002, *Biochemistry.* 41:10315–10322. 40

[91] Zidovetzki, R. and Levitan, I., Use of cyclodextrins to manipulate plasma membrane cholesterol content: evidence, misconceptions and control strategies. 2007, *Biochim. Biophys. Acta.* 1768:1311–1324. 40

HaCaT keratinocytes exhibit a cholesterol and plasma membrane viscosity gradient during directed migration: Supplemental Material

Methods

Quantification of cellular cholesterol content

Cholesterol was quantified using a cholesterol quantification kit (R-Biopharm AG, Darmstadt, Germany), following the manufacturers instructions with minor modifications. This technique is based on enzymatic oxidation of cholesterol, which results in an increase in absorbance at 405 nm. After starving HaCaT cells for 24 h, they were grown for 12 h in the presence or absence of EGF in serum-free medium under cell culture conditions. After detaching the cells with trypsin, cells where counted using a hemocytometer and centrifuged. The cell pellet (about $5–10 \cdot 10^5$ cells) was collected in 15 µl isopropanol and vortexed. The volumes of the used solutions were adapted onto a 384-well format. Absorbance was measured with a multiwell plate reader (Polarstar Omega, BMG Labtech, Offenburg, Germany). The cholesterol content was normalised to the cell count.

Reverse transcription-polymerase chain reaction

About $2 \cdot 10^5$ HaCaT cells were seeded in 35-mm cell culture dishes and transfected with siRNA and DNA for cytosolic GFP to evaluate the transfection efficiency. 24 or 48 h after transfection, total RNA was isolated (GeneJET, Fermentas, St. Leon-Rot, Germany) and reverse transcribed via random hexamer primer (SuperScript II, Invitrogen). Subsequently, the mRNA of ABC transporters and GAPDH, as an internal control, were amplified (GoTaq, Promega, Mannheim, Germany) with specific primers (Supplementary table 1). After denaturation for 2 min at 95℃ multiple PCR cycles proceeded consisting of 30 s at 95℃, 30 s at 50℃ for GAPDH, 60℃ for ABCA1 or 65℃ for ABCG1 followed by 30 s at 72℃. GAPDH mRNA was amplified by 23 cycles, ABCA1 mRNA and ABCG1 mRNA by 35 cycles.

		5' → 3'	product size (bp)
hABCA1 [1]	for.	GCACTGAGGAAGATGCTGAAA	205
	rev.	AGTTCCTGGAAGGTCTTGTTCAC	
hABCG1 [1]	for.	CAGTGACAGCCATCCCGGTGCT	252
	rev.	CGATGAAGTCCAGGTACAGCTTGGC	
hGAPDH	for.	CTCATTTCCTGGTATGAC	277
	rev.	GAGCACAGGGTACTTTAT	

Supplementary table 1: Primers used for RT-PCR.

hABCA1	HSS176437	CACUUCCUCCGAGUCAAGAAGUUAA
	HSS176438	GCCUUGGCAGUGUCCAGCAUCUAAA
	HSS176439	GACCAAAGUGAUGAUGACCACUUAA
hABCG1	HSS145231	UCGUCCAUGGAAGGCUGCCACAGCU
	HSS145233	UCUCGCUGAUGAAAGGGCUCGCUCA
	HSS190466	CAUAUUUGAGGGAUUUGGGUCUGAA

Supplementary table 2: siRNAs used for specific knockdown of ABCA1 or ABCG1.

References

[1] D. Kielar, W.E. Kaminski, G. Liebisch, A. Piehler, J.J. Wenzel, C. Möhle, S. Heimerl, T. Langmann, S.O. Friedrich, A. Böttcher, S. Barlage, W. Drobnik, G. Schmitz, Adenosine triphosphate binding cassette (ABC) transporters are expressed and regulated during terminal keratinocyte differentiation: a potential role for ABCA7 in epidermal lipid reorganization, J. Invest. Dermatol. 121 (2003) 465–474.

Figures

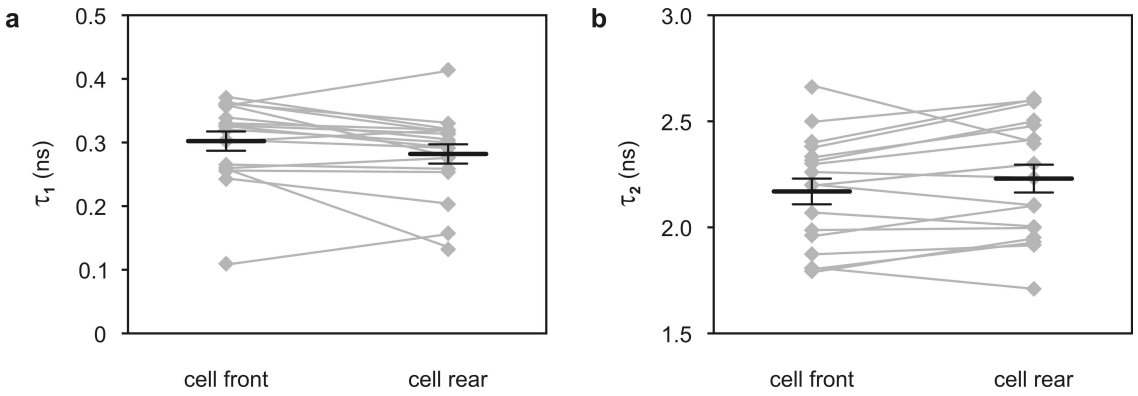

Supplementary figure 1: Short and intermediate lifetimes of NBD in NBD-PC-stained polarised HaCaT cells under TIR excitation. Evaluation of the fluorescence decay of NBD revealed three separate lifetimes, the longest lifetime being strongly dependent on lipid-induced physical properties of membranes. The shortest (a) and intermediate (b) lifetimes of NBD measured at the front of polarised HaCaT keratinocytes did not diverge statistically significantly from the values measured at the back of the cells ($p > 0.05$, mean $\pm$ SEM, the results of individual cells are depicted in gray). The shortest fluorescence lifetimes τ_1 measured at the fronts and rears of NBD-PC-stained HaCaT cells were 0.30 ± 0.02 ns and 0.28 ± 0.02 ns, respectively. The intermediate fluorescence lifetimes τ_2 were 2.17 ± 0.06 ns at the front and 2.23 ± 0.07 ns at the rear of HaCaT cells.

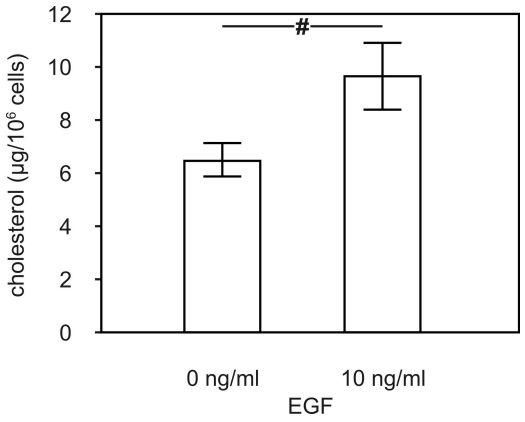

Supplementary figure 2: The cellular cholesterol content is elevated in HaCaT cells grown in the presence of EGF compared with starving cells. HaCaT were cultured for 12 h in media containing none or 10 ng/ml EGF followed by the determination of cellular cholesterol content that was normalised to the cell count ($n = 8$, unpaired Student's t-test # $p < 0.05$).

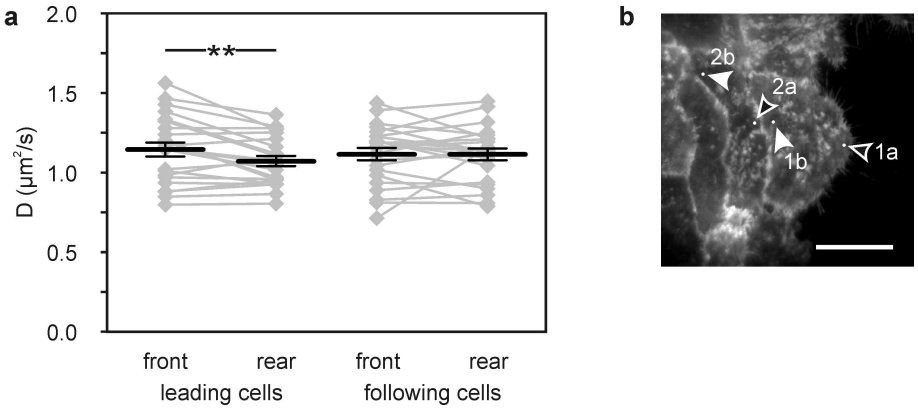

Supplementary figure 3: HaCaT keratinocytes adjacent to leading cells at the edge of a cell assembly do not possess a plasma membrane microviscosity gradient like polarised leading cells. a: Diffusion coefficients determined by a FRAP approach in polarised HaCaT cells that were stimulated by 10 ng/ml EGF at the edge of a cell assembly and at adjacent cells behind the leading cells ($n = 23$; mean $\pm$ SEM; paired Student's t-test $**$ $p < 0.008$). b: Example of a FRAP experiment on a polarised HaCaT cell and of a neighbouring cell behind the edge. White points mark the bleach regions, empty arrow heads indicate the fronts, filled arrow heads the rears of the cells (scale bar: 25 µm).

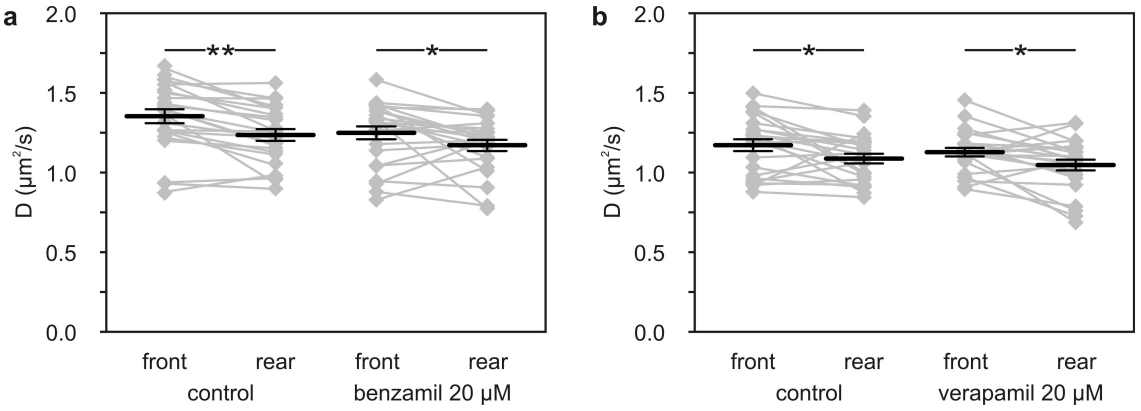

Supplementary figure 4: Benzamil and verapamil, inhibitors of ABCG1 and ABCB1, did not influence the microviscosity gradient in polarised HaCaT cells. Prior to FRAP experiments, we inhibited ABCG1 with 20 µM benzamil (a) and ABCB1 with 20 µM verapamil (b) in the presence of 10 ng/ml EGF for 12 h. Polarised HaCaT keratinocytes still exhibit a microviscosity gradient in the presence of ABCG1 or ABCB1 inhibitors ($n = 24$; mean ± SEM; paired Student's t-test $* \; p < 0.05$).

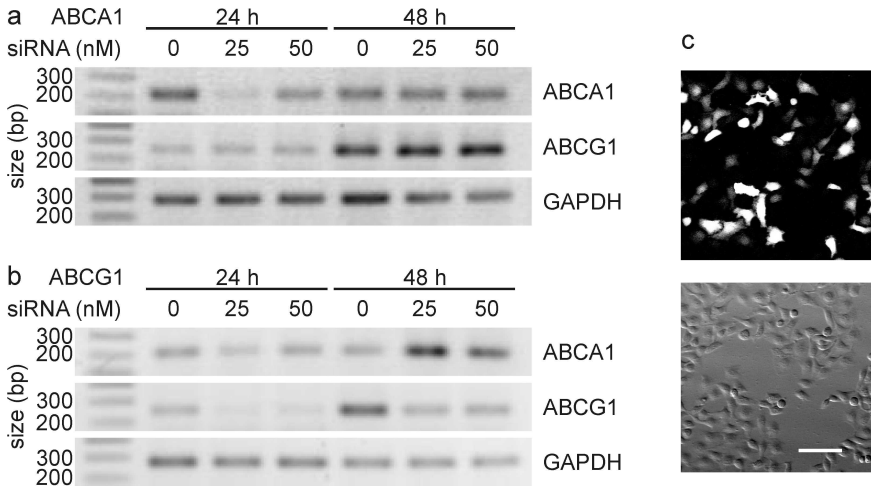

Supplementary figure 5: siRNA-mediated knockdown of ABCA1 and ABCG1 in HaCaT cells. HaCaT were transfected with siRNA against ABCA1 (a) and ABCG1 (b). 24 or 48 h after transfection, total RNA was isolated and mRNA of ABCA1, ABCG1 and GAPDH, as loading control, were reversely transcribed, and amplified with specific primers. ABCA1 and ABCG1 mRNA was most efficiently downregulated after 24 h using 25 nM siRNA. c: Transfection effciency was tested by cotransfecting HaCaT with cytosolic GFP, revealing a transfection efficiency of about 30–50 % (scale bar: 100 µm).

Eigener Beitrag

HaCaT keratinocytes exhibit a cholesterol and plasma membrane viscosity gradient during directed migration

- Zellkultur
- Durchführung der TIR/FRAP Versuche (Vorarbeit: Astrid Tannert)
- Durchführung der Fluoreszenzlebenszeitmessungen unter TIR-Belichtung (Vorarbeit: Astrid Tannert)
- Durchführung der bildgebenden Fluoreszenzlebenszeitmessungen (in Zusammenarbeit mit Astrid Tannert, Thomas Korte und Andreas Herrmann)
- Durchführung der konfokalen Laser-Scanning-Mikroskopie
- Etablierung und Durchführung der Migrationsversuche (scratch assays)
- Durchführung der quantitativen Cholesterolmessung
- Etablierung des siRNA-Knockdowns (Transfektion, Reverse Transkriptase-PCR)
- Auswertung aller Versuche
- Schreiben des Manuskriptes: Erstellen der Abbildungen und des Textes (in Zusammenarbeit mit Astrid Tannert und Michael Schaefer)

Michael Schaefer

Thomas Korte

Andreas Herrmann

Astrid Tannert

Cholesterol sensitises the transient receptor potential channel TRPV3 to lower temperatures and activator concentrations

- Eingrenzung des Themas
- Zellkultur (beinhaltete die Herstellung der stabilen Zelllinie)
- Durchführung der Calciummessungen (Plattenlesegerät und Einzelzellmessungen)
- Durchführung der konfokalen Laser-Scanning-Mikroskopie
- Durchführung der Patch-Clamp-Experimente
- Auswertung aller Versuche
- Schreiben des Manuskriptes: Erstellen der Abbildungen und des Textes (in Zusammenarbeit mit Astrid Tannert und Michael Schaefer)

Astrid Tannert

Astrid Tannert

M. Schaefer

Michael Schaefer

Eigenständigkeitserklärung

Erklärung über die eigenständige Abfassung der Arbeit

Hiermit erkläre ich, dass ich die vorliegende Arbeit selbstständig und ohne unzulässige Hilfe oder Benutzung anderer als der angegebenen Hilfsmittel angefertigt habe. Ich versichere, dass Dritte von mir weder unmittelbar noch mittelbar eine Vergütung oder geldwerte Leistungen für Arbeiten erhalten haben, die im Zusammenhang mit dem Inhalt der vorgelegten Dissertation stehen, und dass die vorgelegte Arbeit weder im Inland noch im Ausland in gleicher oder ähnlicher Form einer anderen Prüfungsbehörde zum Zweck einer Promotion oder eines anderen Prüfungsverfahrens vorgelegt wurde. Alles aus anderen Quellen und von anderen Personen übernommene Material, das in der Arbeit verwendet wurde oder auf das direkt Bezug genommen wird, wurde als solches kenntlich gemacht. Insbesondere wurden alle Personen genannt, die direkt an der Entstehung der vorliegenden Arbeit beteiligt waren. Die aktuellen gesetzlichen Vorgaben in Bezug auf die Zulassung der klinischen Studien, die Bestimmungen des Tierschutzgesetzes, die Bestimmungen des Gentechnikgesetzes und die allgemeinen Datenschutzbestimmungen wurden eingehalten. Ich versichere, dass ich die Regelungen der Satzung der Universität Leipzig zur Sicherung guter wissenschaftlicher Praxis kenne und eingehalten habe.

Publikationen

Wittenbrink N, Weber TS, Klein AS, Weiser AA, Zuschratter W, Sibila M, Schuchhardt J, Or-Guil M. Broad volume distributions indicate nonsynchronized growth and suggest sudden collapses of germinal center B cell populations. *J Immunol*, 2010, 184:1339–47.

Wittenbrink N, Klein AS, Weiser A, Schuchhardt J, Or-Guil M. Is there a typical germinal center? A large-scale immunohistological study on the cellular composition of germinal centers during the hapten-carrier-driven primary immune response in mice. *J Immunol*, 2011, 187:6185–6196.

Klein AS, Schaefer M, Korte T, Herrmann A, Tannert A. HaCaT keratinocytes exhibit a cholesterol and plasma membrane viscosity gradient during directed migration. *Exp Cell Res*, 2012, 318:809–818.

Jezierski S, Klein AS, Benz C, Schaefer M, Nagl S, Belder D. Towards an integrated device combining separation and biosensing capabilities utilizing adherent cells in a micro-free-flow-electrophoresis chip. *Anal Bioanal Chem*, 2013, 405:5381–5386.

Klein AS, Tannert A, Schaefer M. Cholesterol sensitises the transient receptor potential channel TRPV3 to lower temperatures and activator concentrations. *Cell Calcium*, 2014, 55:59-68.

Danksagung

Ich bedanke mich bei allen Mitgliedern der Arbeitsgruppe, Freunden und Familie, die mich während der Entstehung der Arbeit unterstützt haben und mir mit Rat und Tat zur Seite standen.

Mein ganz besonderer Dank gilt jedoch Michael Schaefer und Astrid Tannert, die mir als Betreuer und Ansprechpartner die Dissertation erst ermöglichten, sowie Isabelle Straub und Melanie Kaiser, die mit konstruktiver Kritik zur Verbesserung dieser Arbeit beitrugen.